

University of Alberta

**Design, Synthesis, and Evaluation of Peptide-based Hepatitis C Virus
Entry Inhibitors**

by

Reem Beleid



A thesis submitted to the Faculty of Graduate Studies and Research
in partial fulfillment of the requirements for the degree of

Master of Science

In

Pharmaceutical Sciences

Faculty of Pharmacy and Pharmaceutical Sciences

Edmonton, Alberta

Spring 2008



Library and
Archives Canada

Published Heritage
Branch

395 Wellington Street
Ottawa ON K1A 0N4
Canada

Bibliothèque et
Archives Canada

Direction du
Patrimoine de l'édition

395, rue Wellington
Ottawa ON K1A 0N4
Canada

Your file *Votre référence*
ISBN: 978-0-494-45776-4
Our file *Notre référence*
ISBN: 978-0-494-45776-4

NOTICE:

The author has granted a non-exclusive license allowing Library and Archives Canada to reproduce, publish, archive, preserve, conserve, communicate to the public by telecommunication or on the Internet, loan, distribute and sell theses worldwide, for commercial or non-commercial purposes, in microform, paper, electronic and/or any other formats.

The author retains copyright ownership and moral rights in this thesis. Neither the thesis nor substantial extracts from it may be printed or otherwise reproduced without the author's permission.

AVIS:

L'auteur a accordé une licence non exclusive permettant à la Bibliothèque et Archives Canada de reproduire, publier, archiver, sauvegarder, conserver, transmettre au public par télécommunication ou par l'Internet, prêter, distribuer et vendre des thèses partout dans le monde, à des fins commerciales ou autres, sur support microforme, papier, électronique et/ou autres formats.

L'auteur conserve la propriété du droit d'auteur et des droits moraux qui protègent cette thèse. Ni la thèse ni des extraits substantiels de celle-ci ne doivent être imprimés ou autrement reproduits sans son autorisation.

In compliance with the Canadian Privacy Act some supporting forms may have been removed from this thesis.

Conformément à la loi canadienne sur la protection de la vie privée, quelques formulaires secondaires ont été enlevés de cette thèse.

While these forms may be included in the document page count, their removal does not represent any loss of content from the thesis.

Bien que ces formulaires aient inclus dans la pagination, il n'y aura aucun contenu manquant.


Canada

Abstract

Inhibition of viral entry using entry inhibitors is a promising target for new antiviral therapy. Peptides that bind regions of HCV-envelope 2 (E2) protein which interact with cell entry receptors may provide an interesting approach to prevent HCV infectivity. Five α -peptides derived from human lactoferrin were synthesized, characterized, and evaluated for E2 binding. E2 from HCV genotype 1b was expressed in mammalian cells and purified using affinity chromatography. An ELISA-based binding assay was developed to determine the binding affinity of peptides for E2 protein. Two of the peptides bound E2 specifically with submicromolar to low micromolar affinity. These two peptides had the highest helical content in solution as observed by CD spectroscopy, suggesting that binding affinity increases with increase in helicity. In addition, a facile synthetic strategy was developed to synthesize a new class of peptidomimetic β^3 -peptides using natural α -amino acid. A representative β^3 -hexapeptide was synthesized from L-aspartic acid monomers that adopted a right-handed helical conformation in TFE solution. These results will assist in the identification of peptide and peptidomimetic lead compounds that will facilitate the development of novel therapeutic agents for HCV.

For My Parents

Amghalia Azzouz and Abdellah Algryani

*I start with you when I count my blessings; your love and faith are a
light that guides me though life.*

With all my love

Reem

Acknowledgements

Throughout my Master's program, there has been lot of people who helped me in many different ways. Without their help, it would not have been possible for me to finish my project.

First of all, I would like to thank my supervisor Dr. Kamaljit Kaur for giving me an opportunity to work in her lab. Kamaljit's enormous knowledge and expertise were the most valuable resources for me, which helped me during my Master's. Her tremendous support, leadership, and affection helped me being focused on my research. Thanks to her patience, guidance, and encouragement which made the completion of this thesis possible.

Next, I am greatly indebted to Dr. Donna Douglas for her extensive help. She spent her valuable time teaching me all the techniques in great detail. In addition, I would like to thank Dr. Norman Kneteman; I am grateful to him for allowing me to use his lab equipment as well as the cell lines.

I would also like to show my gratitude to my lab members, Sahar Ahmed and, Weal Soliman. Their help and support always have been a great inspiration.

I would also like to thank IRBM (Merck, Italy) for kindly providing me with plasmid vectors. I am grateful to the Libyan Education Program, Libya for the financial support during the first 2 years, and to my supervisor Dr. Kamaljit Kaur and the Faculty of Pharmacy and Pharmaceutical Sciences, Alberta, Canada, for the financial support during the last year.

Most importantly, I would like to thank my family for all the love and support they have given over the years. I would like to thank my mother for all the patience, love, and encouragement; my father for inspiring my interest in science and always holding me to a higher standard; and my sister and my brothers for their support. Without their support and encouragement, this work would not have been fulfilled.

Table of Content

Chapter 1 Introduction.....	1
1.1 Hepatitis C virus.....	1
1.2 HCV Envelope 2 Glycoprotein.....	4
1.3 Lactoferrin.....	5
1.4 HCV Entry Inhibitors.....	7
1.5 Peptidomimetic Entry Inhibitors.....	12
1.6 References.....	13
Chapter 2 Synthesis and Evaluation of HCV Entry Inhibitors...17	
2.1 Background.....	17
2.2 Objective.....	20
2.3 Results and Discussion.....	21
2.3.1 Synthesis of α -Peptide Ligands.....	21
2.3.2 Circular Dichroism of α -Peptides.....	24
2.3.3 Expression and Purification of HCV-E2.....	25
2.3.4 Binding of Lactoferrin-derived Peptides to E2 Protein.....	31
2.4 Summary.....	36
2.5 Experimental Section.....	36
2.5.1 General.....	36
2.5.2 Synthesis of Peptides 1-5.....	39
2.5.3 Circular Dichroism of Peptides 1-5.....	42
2.5.4 Bacterial Transformation and Plasmid Purification.....	42

2.5.5 Cell Culture and Transfection.....	45
2.5.6 Purification of the Expressed E2 Glycoprotein	47
2.5.7 ELISA-based Binding Assay	49
2.6 References.....	52
Chapter 3 Synthesis of Peptidomimetic β^3-Peptides.....	54
3.1 Background	54
3.1.1 β -Peptides.....	55
3.1.2 Synthesis of β^3 -Peptides.....	56
3.1.3 Conformation of β -Peptides.....	57
3.1.4 Biological Activity of β -Peptides.....	59
3.2 Objective	60
3.3 Result and Discussion	60
3.3.1 β^3 -Peptides from L-Aspartic Acid Monomers.....	60
3.3.2 Synthesis of β^3 -Hexapeptide 6 using Orthogonally Protected L-Asp .	64
3.3.3 Solution Conformation of β^3 -Hexapeptide 6	67
3.3.4 Synthesis of β^3 -Hexapeptide 7 at Ambient and Elevated Temp.	73
3.3.5 Synthesis of β^3 -Peptide 8 using Fmoc-Asp-OAll or Fmoc-Asp-OtBu	76
3.4 Summary	79
3.5 Experimental Section	80
3.5.1 General	80
3.5.2 Synthesis of β^3 -Hexapeptide 6	81
3.5.3 Synthesis of Heterooligomeric β^3 -Peptide 7	86
3.5.4 Synthesis of Homooligomeric β^3 -Peptide 8	87

3.6 References	90
Chapter 4 General Conclusions and Future Directions	93
Bibliography	96
Appendix A	105
Dynafit Files and Plasmid Map.....	105
Appendix B.....	108
NMR Data for Structure Elucidation of 6	108

List of Figures

- Figure 1.1** HCV genome organization and polyprotein processing..... 2
- Figure.1.2** Model of hepatocellular HCV binding and entry. In the beginning, HCV may be captured by L-SIGN of liver sinusoidal endothelial cells (LSEC). Captured HCV may then be transferred to hepatocytes by binding to liver complex receptor 5
- Figure 1.3** HCV life cycle can be targeted by specific class of antiviral drugs... 7
- Figure 1.4** Small molecule HCV entry inhibitors. (A) bis-imidazole scaffold as CD81 mimic , (B) 1-boraadamantane, and (C) Arbidol. 10
- Figure 2.1** Crystal structure of recombinant human lactoferrin (pdb 1CB6) (11). Residues 600-632 (33-residue Nozaki peptide) are shown in color. 18
- Figure 2.2** (A) Three-dimensional structure of 33-residue lactoferrin-derived peptide (600-632 amino acids) obtained from the crystal structure of recombinant human lactoferrin (pdb 1CB6). Structure is shown as a ribbon diagram highlighting the helical (red) secondary structure. (B) Amino acid sequence of the 33-residue lactoferrin-derived peptide. Helical residues are underlined. 19
- Figure 2.3** Sequence of five lactoferrin-derived peptides synthesized and studied herein. Residues that are underlined indicate a change from the native lactoferrin sequence. L_N stands for norleucine and b denotes biotin covalently linked to the N-terminus of the peptides..... 21
- Figure 2.4** RP-HPLC chromatographs for the α -peptides **1-5**. 23
- Figure 2.5** CD spectra of peptides **1-5** in PB (10 mM, pH 7.4) at 25 °C. The ellipticity was expressed as the mean residue molar ellipticity (θ) in deg cm² dmol⁻¹. 24
- Figure 2.6** Agarose gel electrophoresis for purified vector DNA samples. The lanes 1, 3, 5, and 7 are the *Hind*III digested samples, where as the lanes 2, 4, 6, and 8 are the samples before digestion. 27
- Figure 2.7** Western blot analysis of E2N and E2H proteins, probed with mouse anti-His6 mAb (1:1000) 1° antibody and goat anti-mouse (1:10000) 2° antibody. Columns M, C, N2, N5, H2, and H5 stand for marker, control (without plasmid),

2 µg N2 plasmid, 5 µg N2 plasmid, 2 µg H plasmid, and 5 µg H plasmid, respectively. 28

Figure 2.8 Western blot analysis of E2N and E2H proteins, probed with mouse anti-His6 mAb (1:1000) 1° antibody and goat anti-mouse (1:10000) 2° antibody. Columns M, C, N10, N20, and H20 stand for marker, control, 10 µg N2 plasmid, 20 µg N2 plasmid, and 20 µg H plasmid, respectively..... 29

Figure 2.9 Western blot analysis of the fractions obtained from the IMAC probed with mouse anti-His6 mAb (1:1000) 1° antibody and goat anti-mouse (1:10000) 2° antibody. column during purification of the E2H and E2N proteins. CL: crude lysate; FT: flow through; 1-7: fractions 1-7 obtained using the elution buffer..... 30

Figure 2.10 Western blot analysis of the fractions obtained from the IMAC column during E2N purification, probed with mouse anti-E2 mAb (1:20) (top) and anti-His6 mAb (1:1000) (bottom) 1° antibody. C: control; CL: crude lysate; FT: flow through; W3: wash # 3; E2-E10: fractions 2-10 obtained using the elution buffer; EL: E2 protein sample from previous expression. 31

Figure 2.11 Binding of E2 protein to peptides **3** (top) and **5** (bottom). Shown is absorbance of TMB substrate at 650 nm as a function of different peptide concentration. 33

Figure 2.12 Binding of E2 protein to peptides **1** (Δ), **2** (□), and **4** (o). Shown is absorbance of TMB substrate at 650 nm as a function of different peptide concentration..... 34

Figure 3.1 Examples of monomeric units of peptidomimetics. 55

Figure 3.2 Nomenclature for β-peptides depending upon the substitution of the backbone carbon. 56

Figure 3.3 Nomenclature for β-peptide helices based on hydrogen-bonding patterns..... 58

Figure 3.4 Synthesis of mono-substituted β³-peptides from L-aspartic acid monomers..... 61

Figure 3.5 The chemical structures of β³-hexapeptides **6,7**, and **8**. 62

Figure 3.6 RP-HPLC chromatogram of β³-hexapeptide **6**. (C8 VYDAC HPLC column, 0.46 x 25 cm, 5 µm, flow rate = 1 ml/min, gradient of 10-40 % CH₃CN in 0.05% aqueous TFA over a period of 40 min)..... 66

Figure 3.7 Electrospray spectrum of pure β^3 -hexapeptide 6	66
Figure 3.8 $^1\text{H-NMR}$ (500 MHz) spectrum of β^3 -peptide 6 in $\text{CF}_3\text{CD}_2\text{OH}$	67
Figure 3.9 Circular dichroism spectra of 6 in water, phosphate buffer (1 mM, pH 7.4), methanol, and TFE at 25 °C.	68
Figure 3.10 1D NMR of β^3 -peptide 6 showing the amide H-atoms in 100% TFE- d_2 (top) and 90% $\text{H}_2\text{O}/10\%$ D_2O (bottom). HN refers to the backbone amide proton and HS refers to the one in the side chain. The number in the parentheses is for the number of overlapping peaks and impurities are marked with *.....	70
Figure 3.11 Chemical structure of β^3 -peptide from L-aspartic acid monomers (left) and β^3 -peptides from β^3 -amino acids derived from natural L-amino acids (right).	71
Figure 3.12 Solution structure of β^3 -hexapeptide 6 in TFE obtained by NMR spectroscopy.....	72
Figure 3.13 Backbone conformation of right-handed α -helix in an α -peptide and 14-helix in a β -peptide from L-aspartic acid monomers.....	73

List of Tables

Table 2.1: The HPLC purification details for peptides 1-5	22
Table 2.2: CD Analysis of the secondary structure fractions of peptides 1-5 in PB at 25 °C.	25
Table 2.3: ELISA-based binding data for peptide 1 when 30 nM/well (200 ng/well) E2N was used (Figure 2.12).	50
Table 2.4: ELISA-based binding data for peptide 2 when 40 nM/well (200 ng/well) E2N was used (Figure 2.12).	50
Table 2.5: ELISA-based binding data for peptide 3 when 30 nM/well (150 ng/well) E2N was used (Figure 2.11).	51
Table 2.6: ELISA-based binding data for peptide 4 when 30 nM/well (150 ng/well) E2N was used (Figure 2.12).	51
Table 2.7: ELISA-based binding data for peptide 5 when 40 nM/well (200 ng/well) E2N was used (Figure 2.11).	51
Table 3.1: Deallylation of the allyl group from side chain carboxylic acid.....	65
Table 3.2: Coupling and deprotection times for the synthesis of β^3 -hexapeptide 6	83
Table 3.3: Coupling, capping, and deprotection times for the synthesis of 8	88
Table 3.4: Coupling and deprotection times for the synthesis of β^3 -peptide 8	89

List of Schemes

- Scheme 3.1** Arndt Eistert homologation affords β^3 -substituted amino acid..... 57
- Scheme 3.2** General pathway of solid phase synthesis of β^3 -peptides from L-aspartic acid..... 63
- Scheme 3.3** Synthesis of heterooligomeric β^3 -hexapeptide **7** at room temp.. 75
- Scheme 3.4** Synthesis of homooligomer β^3 -peptide **8** using Fmoc-Asp-OAll... 77
- Scheme 3.5** Synthesis of homooligomer β^3 -peptide **8** using Fmoc-Asp-OtBu. .. 78

List of Abbreviations

aa	Amino acid
BOP	Benzotriazol-1-yloxy-tris(dimethylamino)-phosphonium hexafluorophosphate
BSA	Bovine serum albumin
cDNA	Complementary deoxyribonucleic acid
d	Doublet
DCM	Dichloromethane
dd	Doublet of double
ddH ₂ O	Double distilled water
DIC	1,3-diisopropylcarbodiimide
DMF	<i>N,N</i> -dimethylformamide
DMSO	Dimethylsulfoxide
DNA	Deoxyribonucleic acid
ECL	Enhanced chemiluminescence
EDTA	Ethylene diamine tetraacetic acid
Fmoc	9-Fluorenylmethoxycarbonyl
HBTU	<i>O</i> -Benzotriazole- <i>N,N,N,N</i> -tetramethyl-uronium hexafluorophosphate
HCC	Hepatocellular carcinoma
HCV	Hepatitis C virus
HEK	Human Embryonic kidney
HIV	Human Immunodeficiency Virus
HOBt	<i>N</i> -Hydroxybenzotriazole
HPLC	High Performance Liquid Chromatography
HRPO	Horseradish peroxidase
HSV-1	Herpes Simplex Virus 1
HVR	Hyper variable region
IMAC	Immobilized metal affinity chromatography
IPA	Isopropyl alcohol
IRES	Internal ribosome entry site
LB	Luria broth
m	Multiplet
mAb	Monoclonal antibody
mRNA	Messenger ribonucleic acid
MS	Mass spectrometry
Ni-NTA	nickel-nitrilotriacetic acid
NMM	<i>N</i> -methylmorpholine
NMP	1-Methyl-2-pyrrolidinone
NMR	Nuclear magnetic resonance
PDB	Protein Data Bank
q	Quartet
quint	Quintet
RNA	Ribonucleic acid

s	Singlet
SDS-PAGE	Sodium dodecyl sulfate-polyacrylamide gel electrophoresis
SIGN	Specific intercellular adhesion molecule-3-grabbing nonintegrin
t	Triplet
TFA	Trifluoroacetic acid
TMB	3,3',5,5'-Tetramethylbenzidine
WHO	World Health Organization

Amino acids

Ala (A)	Alanine
Arg (R)	Arginine
Asn (N)	Asparagine
Asp (D)	Aspartic acid
Cys (C)	Cysteine
Gln (Q)	Glutamine
Glu (E)	Glutamic acid
Gly (G)	Glycine
His (H)	Histidine
Leu (L)	Leucine
Lys (K)	Lysine
Phe (F)	Phenylalanine
Pro (P)	Proline
Ser (S)	Serine
Val (V)	Valine
NorLeu (Nle)	Norleucine

Chapter 1 Introduction

1.1 Hepatitis C Virus

Background. Hepatitis C virus (HCV) infection was first recognized in 1975, when the majority of transfusion-associated infections were found to be unrelated to hepatitis A and B, the two hepatitis viruses recognized at that time. This transmissible disease was then simply called “non-A, non-B” hepatitis. Sequencing of the HCV genome was accomplished in 1989, and the term hepatitis C was subsequently applied to infection with this single strand ribonucleic acid (RNA) virus (1).

The propensity of HCV to cause chronic infection is explained by the extraordinary ability of this virus to avoid destruction by the body’s immune system. Once established, HCV infection causes an inflammation of the liver called chronic hepatitis. This condition can progress to scarring of the liver, called fibrosis, or more advanced scarring, called cirrhosis. Some individuals with cirrhosis go on to develop liver failure or complications of cirrhosis including hepatocellular carcinoma (HCC).

HCV infection, transmitted primarily by the parenteral route, is now recognized as a serious national problem. WHO estimates that about 180 million individuals in the world (3% worldwide) have been infected with HCV. It is estimated that three to four million persons are newly infected each year, 70 percent of whom will develop chronic hepatitis. HCV is responsible for 50–76 percent of all liver cancer cases, and two thirds of all liver transplants in the developed world (2).

HCV Genome and Proteins. Hepatitis C virus (HCV) is a small, enveloped RNA virus belonging to the family *Flaviviridae*, genus *Hepacivirus*. HCV genome is composed of a single-stranded positive sense RNA of approximately 9600 nucleotides which codes for a polyprotein of about 3,000 amino acids. The polyprotein precursor is processed by host and viral proteases to yield structural and non-structural proteins, which are essential for assembly of new viral particles and replication (Figure 1.1). The three structural proteins, namely, core and envelope glycoproteins E1 and E2, are located within the N terminus of the polyprotein, whereas the non-structural (NS) proteins reside within the C-terminal part (4).

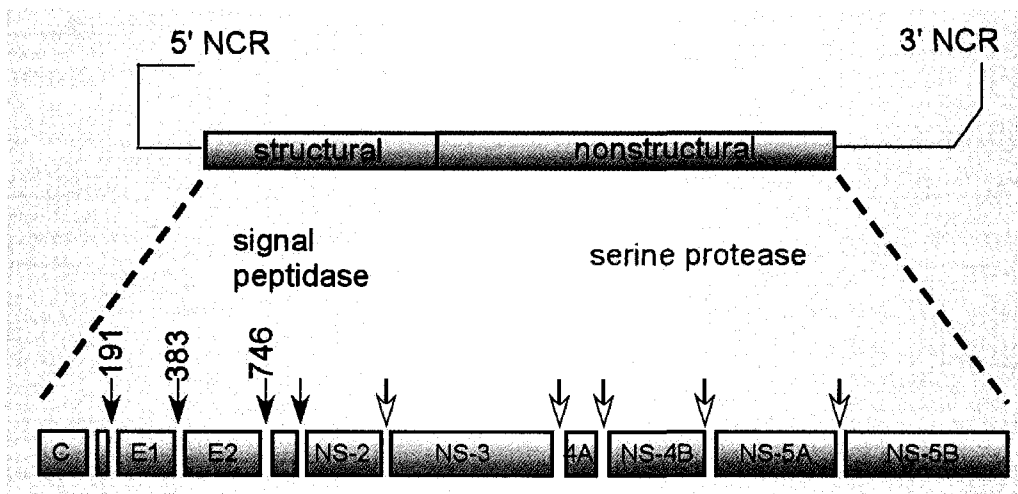


Figure 1.1 HCV genome organization and polyprotein processing (4).

HCV Genotypes. HCV is classified into at least six genotypes and more than 50 subtypes (3). These genotypes differ by as much as 30-35% in their nucleotide sequences, whereas subtypes differ by 15-20% based on full-length genomic sequence comparisons. The extensive genetic heterogeneity of HCV has important diagnostic and clinical implications, perhaps explaining difficulties in

vaccine development and the lack of response to therapy (4). Moreover, HCV genotypes distribution varies by region (5). Genotype 1 is most common in North America and Europe, and is considered the most difficult to treat with current medication (~50% response rate) (4).

Interferon-ribavirin Therapy. Interferon alfa (IFN- α)-ribavirin combination therapy is the standard treatment for chronic hepatitis C since late 1990s (6). The therapeutic efficacy of the combination therapy has been subsequently improved by pegylation of IFN α in order to improve pharmacokinetic and pharmacodynamic (allowing weekly injections) properties. The PEG-IFNs display enhanced virological response both as monotherapy and in combination with ribavirin. Other modifications of IFN, such as a fused form of IFN- α 2b with human serum albumin (in phase II clinical), for better bioavailability and optimized pharmacokinetics have also been explored. Ribavirin, a synthetic guanosine analog is administered at a dose of 0.8 to 1.2 g/day according to body weight and the HCV genotype. Efforts have been devoted to develop ribavirin analogs to reduce dosage and improve the safety profiles associated with hemolytic anemia (7).

PEG-IFN α with ribavirin is the current treatment option for all HCV-infected patients. Although this combination therapy has led to a dramatic improvement in the treatment outcome, the low efficacy of the therapy along with resistance problems, poor tolerability, and high cost necessitates exploration of new and more effective therapies (8, 9). Recently, Law *et al.* have reported specific human monoclonal antibodies that neutralize genetically diverse HCV

isolates (10). These antibodies hold promise for the development of a prophylactic vaccine against HCV.

1.2 HCV Envelope 2 Glycoprotein

The HCV envelope 2 (E2) glycoprotein extends from aa 384 to 746 of the polyprotein and carries regions of extreme variability (11). E2 is a heavily glycosylated protein (~65 kDa) with N-terminal ectodomains and C-terminal hydrophobic anchors (12). The most variable region, known as hypervariable region 1 (HVR-1), is located within the N-terminal 27 residues (aa 384–411) of E2. HVR-1, exposed at the outside of the virus, contains linear B-cell epitopes, which create positive escape mutants. These mutants lead to persistent viral infection and are resistance to treatment (11). Other hypervariable regions in E2 that might also play a role in viral entry are HVR2 (aa 474–482) and HVR3 (aa 431–466) (13).

E2 has highly conserved glycosylation sites, four O-linked and eleven N-linked, which play an important role in its function (14). It has been shown that the removal of O and N glycosylation sites leads to significant inhibition of viral entry (14). Furthermore, E2 is considered responsible for HCV binding to host cells. Antibodies specific for epitopes within HVR-1 have been reported to inhibit the binding of E2 to cells, and block HCV infectivity (15). E2 mediates attachment to target cells and binds to several receptor candidates for the HCV. Several candidate receptors (Figure 1.2), such as, large extracellular loop of tetraspanin CD81, scavenger receptor class B type 1 (SR-B1), mannose binding

lectins DC-SIGN and L-SIGN, heparan sulfate proteoglycans (HSPG), and low-density lipoprotein, at the surface of target cells have been proposed which play an important role in HCV entry (16-21). All of these together have been proposed

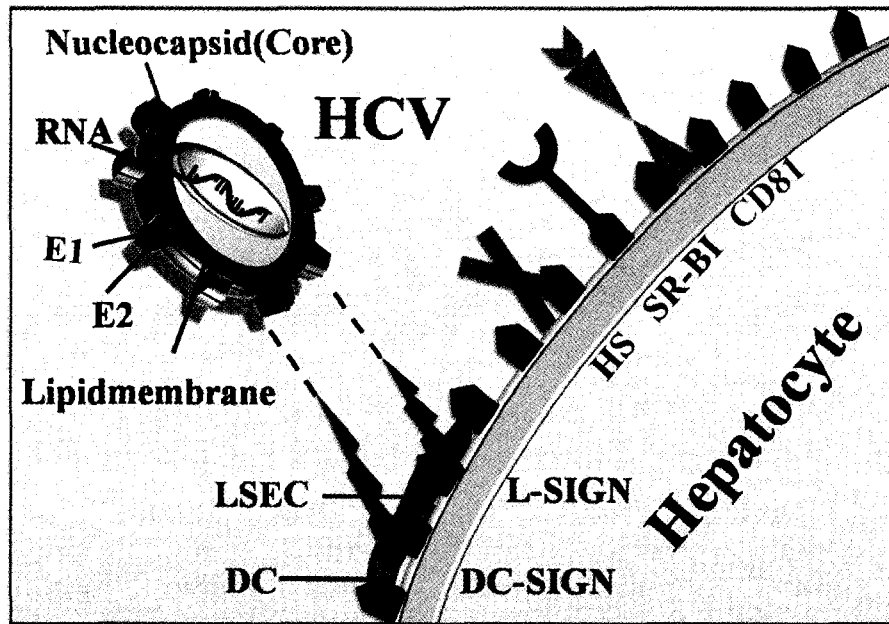


Figure 1.2 Model of hepatocellular HCV binding and entry. In the beginning, HCV may be captured by L-SIGN of liver sinusoidal endothelial cells (LSEC). Captured HCV may then be transferred to hepatocytes by binding to liver complex receptor (22).

as components of a putative HCV-receptor complex. These studies suggest that E2 is the primary binding site on HCV that allows initial docking of HCV on the target cells.

1.3 Lactoferrin

Lactoferrin (LF) is an 80 kDa iron-binding milk glycoprotein consisting of 692 amino acids that belongs to the transferrin family (23). The protein consists of a single polypeptide chain, folded in 2 symmetric globular lobes, representing its N and C-terminal halves (residues 1–334 and 346–692 in human LF). Apart from its potent antibacterial and antiviral activity, LF is an antioxidant because of

its iron binding ability that inhibits the iron catalyzed formation of free radicals (24).

LF displays antiviral activity against both DNA and RNA viruses, including human cytomegalovirus, respiratory syncytial virus, herpes viruses, hepatitis B virus, and HIV. The antiviral effect of LF lies in the early phase of infection. Lactoferrin prevents entry of virus in the host cell, either by blocking cellular receptors, or by direct binding to the virus particles (25). LF is known to bind cell surface glycosaminoglycans and low-density lipoprotein receptors, which in turn act as binding sites for HSV1 and HIV (26). Camel lactoferrin which is similar to human and bovine LF, leads to a complete HCV (genotype 4) entry inhibition into human leukocytes through direct interaction with virus molecules rather than interaction with cells (27). Bovine LF was able to prevent early phase of adenovirus replication (28).

LF is the first physiological substance other than interferon that shows anti-HCV activity. LF is believed to reduce serum HCV RNA levels in patients with chronic hepatitis. It binds and neutralizes the activity of HCV virions, thereby inhibiting viral adsorption to hepatocytes (29). Clinical studies reported that LF monotherapy is associated with a decrease in serum HCV RNA and alanine aminotransferases (ALT) in some patients with chronic hepatitis. Although the effects are limited (30, 31), 25% of hepatitis C patients with high viral load of genotype 1b were responders to bovine LF treatment using a dose of 3.6 g/day, for 12 months (31).

1.4 HCV Entry Inhibitors

Virtually, all steps of the HCV life cycle can be targeted by specific inhibitors, including inhibitors of (i) viral entry, (ii) replication of the viral genome by polymerases, and (iii) proteolytic processing of viral polyproteins (Figure 1.3). Currently, the principal targets of new antivirals are the HCV NS3 protease and the RNA-dependent RNA polymerase (RdRp)(32). More recently, cyclophilin inhibitors that target host-virus interactions have also gained attention (33). Several molecules inhibiting these targets are currently in either preclinical or clinical stages.

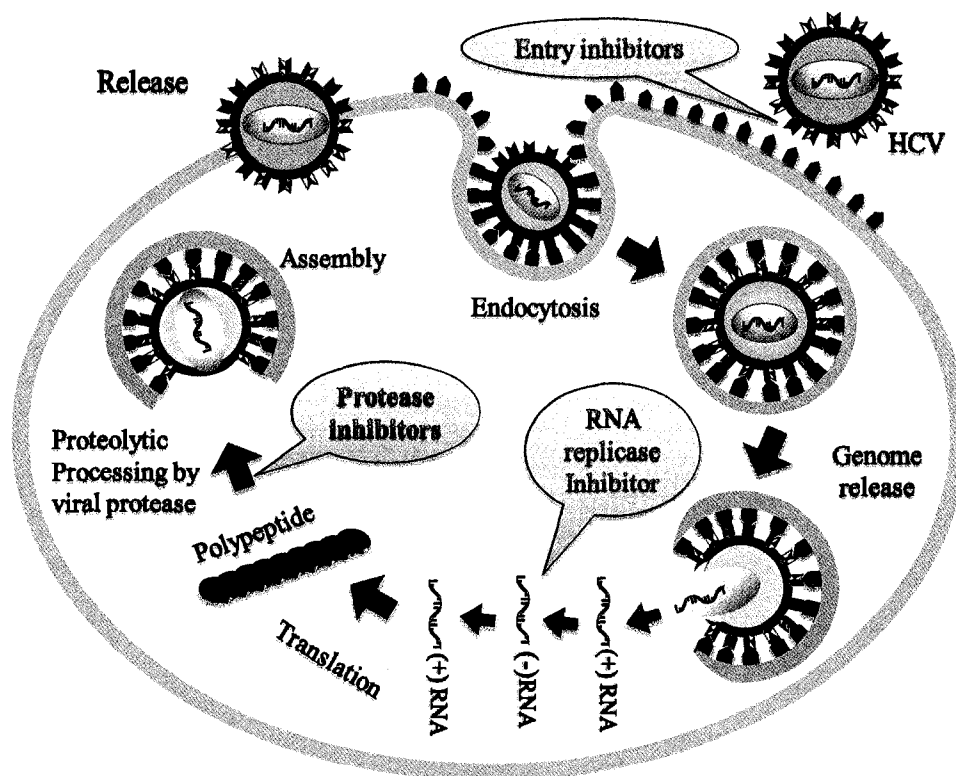


Figure 1.3 HCV life cycle can be targeted by specific class of antiviral drugs (32).

Competitive inhibitors of the NS3 serine protease that form a covalent and reversible complex with NS3 have been reported (34). Telaprevir (VX-950) and Boceprevir (SCH 503034), peptidomimetic NS3/4A serine protease inhibitors, are two such molecules with promising profiles that have now advanced to phase II clinical trials. Valopicitabine (NM283), a nucleoside analogue and an orally bioavailable pro-drug, inhibits HCV NS5B (or RdRp) polymerase. At higher doses, NM283 displayed superior rapid response rates but was associated with gastrointestinal and hematological disorders(35). However, combination therapy of Valopicitabine and boceprevir showed enhanced anti-replicon activity against HCV(36). The above mentioned drugs which target replication cycle are susceptible to cross-resistance due to the high mutation rate of the virus (33).

Another attractive mechanism that targets the cellular host proteins required for HCV RNA replication is the cyclophilin inhibitors (CsA) (33). These inhibitors have been reported to block the binding of cyclophilin B to NS5B leading to inhibition of HCV RNA replication. Debio 025 has been shown to exert anti-HCV activity that is independent of the HCV genotype (33). These agents do not affect the viral escape achieved through mutations. However, strategies that target cellular proteins risk interfering with important cellular processes (35).

The early steps of the HCV life cycle are also attractive targets for novel therapies, such as virus attachment to host cells, internalization of the virus-

receptor complex, and the fusion that releases the nucleocapsid into the cytoplasm. However, the later targets have been less explored.

Virus entry inhibitors act extracellularly by blocking the binding of the virus to the host cell and this process of shielding the virus from attachment to the target cells seems more facile compared to targeting other intracellular sites that require exacting precision. HCV entry inhibitors prevent HCV from binding to the host cell receptor(s). Compounds that block HCV envelope protein E2 from binding to cellular receptors by binding to the receptor itself may also inhibit important cellular functions. However, molecules that target the viral envelope protein or bind to the viral envelope protein exclude themselves from interfering with cellular processes, providing additional opportunities for the discovery of novel drugs.

The entry of virus into host cells is an obligatory step in virus replication that presents a multi-faceted opportunity for drug discovery (37-39). Although the entry mechanism of HCV remains unclear, it has become evident that the initiation of the infection takes place by association of the viral envelope protein E2 with specific cell-surface receptor(s). Many groups have demonstrated that the truncated soluble versions of E2 bind specifically to human cells. This glycoprotein is used to identify interaction with CD81, SR-B1, LDL, DC-SIGN and L-SIGN. Inhibition of this interaction between E2 and the cell-surface receptors has therefore been identified as a possible target for designing anti-HCV molecules. This approach, still at its inception, holds a promise as evidenced by the recent success of FDA approved HIV entry inhibitor, Fuzeon.

Fuzeon, T20, or enfuvirtide is the first virus entry inhibitor, approved in 2003 for the treatment of HIV infection. Fuzeon is a synthetic 36 amino acid peptide that mimics the sequence of heptad repeat 2 (HR2) domain (aa 127–162) of HIV's gp41 protein preventing the formation of 6-helix bundle and thus arresting the HIV entry process (40).

Small Molecules Inhibitors. Several groups have designed small molecules that inhibit binding of HCV-E2 to CD81 (41, 42). Molecules with bis-imidazole scaffold, as mimics of helix D of CD81 (Figure 1.4A), were found to inhibit binding of HCV-E2 to CD81 (41). A variety of amine complexes with 1-boraadamantane, namely, amantidine analogues (Figure 1.4B) showed antiproliferative effect on CD81-enriched cell lines (43). Recently, an oral antiviral Arbidol (ARB, Figure 1.4C), an indole derivative has been shown to inhibit HCV entry via HCV pseudoparticles (HCVpp). Arbidol inhibited HCVpp-mediated membrane fusion in a dose-dependent manner in different HCV genotypes, namely, 1a, 1b, and 2a (44).

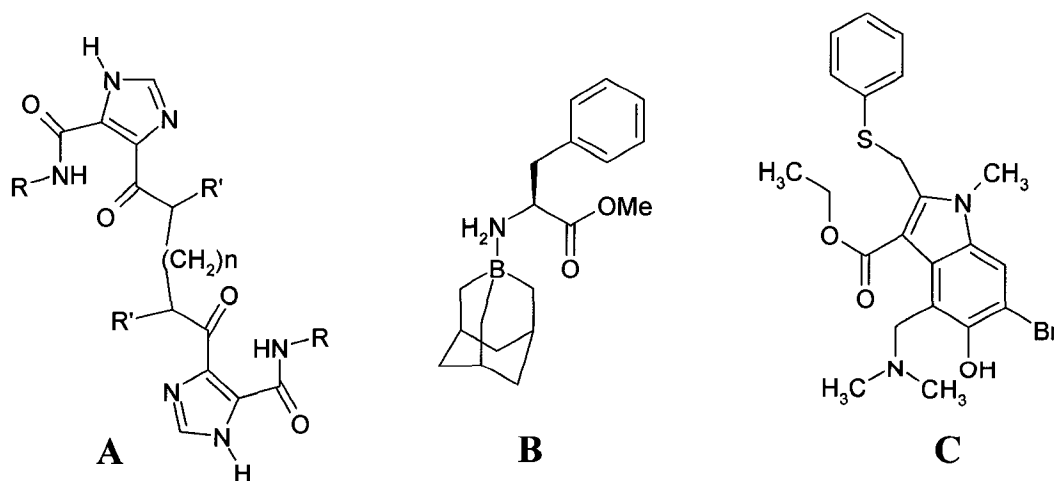


Figure 1.4 Small molecule HCV entry inhibitors. (A) bis-imidazole scaffold as CD81 mimic (41), (B) 1-boraadamantane (43), and (C) Arbidol (44).

Furthermore, carbohydrate-binding agents (CBAs) derived from different prokaryotic and plant lectins have antiviral activity due to their carbohydrate-binding properties. These agents interact with the viral envelope glycoprotein and efficiently prevent the HCV entry process. Pradimicin-A, a non-peptidic (CBAs) plant lectin, is a small molecule produced by actinomycete strain (*Actinomadura hibisca*) that inhibits entry of HCV to target cell. It interferes with the virus capture via DC-SIGN by binding to the glycan in the envelope protein (45).

Peptide-based Entry Inhibitors. Two peptides derived from cyanobacterium and human lactoferrin (LF) have been reported as HCV entry inhibitors (46, 47).

Cyanovirin-N, a 101-residue peptide (11 kDa), from cyanobacterium *Nostoc ellipsosporum* has been shown to inhibit HCV entry by binding to the envelope protein. Cyanovirin-N shows broad inhibitory effect against various genotypes in nanomolar concentrations. The mode of action is thought to be through interaction with N-glycans of the E2 protein preventing E2 binding to the CD81, consequently blocking HCV entry to the target cell (46).

Another peptide derived from the C-terminal region of human LF showed binding activity to HCV-E2, leading to the inhibition of HCV infection in the target cells (47, 48). Using a cell-based assay, it was shown that 33-residue LF fragment or *Nozaki peptide* specifically prevented HCV infection in human hepatocytes. Furthermore, the Nozaki peptide did not bind the hyper variable region (HVR-1) located at the N-terminal of E2 protein (384-415). The authors demonstrated that the mechanism of action of this peptide fragment is by binding

to the E2 protein of HCV, thereby blocking its entry into the host cell, rather than binding to the host cell-surface receptors (47).

1.5 Peptidomimetic Entry Inhibitors

Peptidomimetics, such as β -peptides that fold into predicted secondary structures, that can be prepared via straight forward modular chemistry, and that enable display of a wide range of functional groups are attractive as a basis for creating biologically active agents (49, 50). These molecules are interesting from a pharmaceutical stand-point as mimics of α -peptides as they do not have disadvantageous peptide characteristics, and therefore may generate viable pharmaceuticals. Peptidomimetics are mostly protease-resistant, resistant to metabolism, and may have reduced immunogenicity relative to α -peptide analogues (51).

Several β -peptides that inhibit protein-protein interactions have been recently reported (37). For instance, English *et al.* have developed β -peptides that mimic the glycoproteins heptad repeat of human cytomegalovirus (HCMV) and block virus entry. The most potent β -peptide inhibits HCMV infection in a cell based-assay with an IC_{50} of $\sim 30 \mu\text{M}$ and is more potent than the native α -peptide (52). Also, peptidomimetic terphenyl derivatives have been used to mimic the helical HR2 domain of the HIV protein. The most potent molecule with hydrophobic side chains at the *ortho* position of the three phenyl rings efficiently inhibits HIV-1 infection in a cell fusion assay (IC_{50} 15.7 $\mu\text{g/ml}$) (53).

Our efforts toward the design and synthesis of helical α -peptides as HCV entry inhibitors are described in Chapter 2. Potent α -peptides can be mimicked using more stable β -peptide analogues. Strategies for synthesizing helical β -peptides are described in Chapter 3.

1.6 References

1. Purcell R. 1997. *Hepatology* 26: 11S-4S
2. Organization WHH.
3. Lyra AC, Fan X, Di Bisceglie AM. 2004. *Braz J Med Biol Res* 37: 691-5
4. Margraf RL, Erali M, Liew M, Wittwer CT. 2004. *J Clin Microbiol* 42: 4545-51
5. Nousbaum JB. 1998. *Bull Soc Pathol Exot* 91: 29-33
6. Pawlotsky JM. 2006. *Hepatology* 43: S207-20
7. Huang Z, Murray MG, Secrist JA, 3rd. 2006. *Antiviral Res* 71: 351-62
8. Chevaliez S, Pawlotsky JM. 2007. *World J Gastroenterol* 13: 2461-6
9. Manns MP, Wedemeyer H, Cornberg M. 2006. *Gut* 55: 1350-9
10. Law M, Maruyama T, Lewis J, Giang E, Tarr AW, et al. 2008. *Nat Med* 14: 25-7
11. van Doorn LJ, Capriles I, Maertens G, DeLeys R, Murray K, et al. 1995. *J Virol* 69: 773-8
12. Yagnik AT, Lahm A, Meola A, Roccasacca RM, Ercole BB, et al. 2000. *Proteins* 40: 355-66
13. Helle F, Dubuisson J. 2007. *Cell Mol Life Sci*

14. Falkowska E, Kajumo F, Garcia E, Reinus J, Dragic T. 2007. *J Virol* 81: 8072-9
15. Rosa D, Campagnoli S, Moretto C, Guenzi E, Cousens L, et al. 1996. *Proc Natl Acad Sci U S A* 93: 1759-63
16. Pileri P, Uematsu Y, Campagnoli S, Galli G, Falugi F, et al. 1998. *Science* 282: 938-41
17. Petracca R, Falugi F, Galli G, Norais N, Rosa D, et al. 2000. *J Virol* 74: 4824-30
18. Scarselli E, Ansuini H, Cerino R, Roccasecca RM, Acali S, et al. 2002. *Embo J* 21: 5017-25
19. Barth H, Schafer C, Adah MI, Zhang F, Linhardt RJ, et al. 2003. *J Biol Chem* 278: 41003-12
20. Agnello V, Abel G, Elfahal M, Knight GB, Zhang QX. 1999. *Proc Natl Acad Sci U S A* 96: 12766-71
21. Lozach PY, Lortat-Jacob H, de Lacroix de Lavalette A, Staropoli I, Foung S, et al. 2003. *J Biol Chem* 278: 20358-66
22. Barth H, Liang TJ, Baumert TF. 2006. *Hepatology* 44: 527-35
23. Rey MW, Woloshuk SL, deBoer HA, Pieper FR. 1990. *Nucleic Acids Res* 18: 5288
24. Baker HM, Baker EN. 2004. *Biomaterials* 17: 209-16
25. Ammendolia MG, Pietrantoni A, Tinari A, Valenti P, Superti F. 2007. *Antiviral Res* 73: 151-60

26. Roderiquez G, Oravec T, Yanagishita M, Bou-Habib DC, Mostowski H, Norcross MA. 1995. *J Virol* 69: 2233-9
27. Redwan el RM, Tabll A. 2007. *J Immunoassay Immunochem* 28: 267-77
28. Arnold D, Di Biase AM, Marchetti M, Pietrantonio A, Valenti P, et al. 2002. *Antiviral Res* 53: 153-8
29. Yi M, Kaneko S, Yu DY, Murakami S. 1997. *J Virol* 71: 5997-6002
30. Tanaka K, Ikeda M, Nozaki A, Kato N, Tsuda H, et al. 1999. *Jpn J Cancer Res* 90: 367-71
31. Iwasa M, Kaito M, Ikoma J, Takeo M, Imoto I, et al. 2002. *Am J Gastroenterol* 97: 766-7
32. De Clercq E. 2007. *Nat Rev Drug Discov* 6: 1001-18
33. Pawlotsky JM, Chevaliez S, McHutchison JG. 2007. *Gastroenterology* 132: 1979-98
34. Pawlotsky JM. 2007. *Gastroenterology* 132: 1611-5
35. Parfieniuk A, Jaroszewicz J, Flisiak R. 2007. *World J Gastroenterol* 13: 5673-81
36. Ralston R, Bichko V, Chase R, LaColla M, Lalloo L, et al. 2007. *J Hepatol* 46: S298
37. Kaur K, Das D, Suresh M. 2007. in press
38. Meanwell NA. 2006. *Curr Opin Investig Drugs* 7: 727-32
39. Dimitrov DS. 2004. *Nat Rev Microbiol* 2: 109-22
40. Este JA, Telenti A. 2007. *Lancet* 370: 81-8

41. VanCompernelle SE, Wiznycia AV, Rush JR, Dhanasekaran M, Baures PW, Todd SC. 2003. *Virology* 314: 371-80
42. Cao J, Zhao P, Miao XH, Zhao LJ, Xue LJ, Qi Zt Z. 2003. *Cell Res* 13: 473-9
43. Wagner CE, Mohler ML, Kang GS, Miller DD, Geisert EE, et al. 2003. *J Med Chem* 46: 2823-33
44. Pecheur EI, Lavillette D, Alcaras F, Molle J, Boriskin YS, et al. 2007. *Biochemistry* 46: 6050-9
45. Bertaux C, Daelemans D, Meertens L, Cormier EG, Reinus JF, et al. 2007. *Virology* 366: 40-50
46. Helle F, Wychowski C, Vu-Dac N, Gustafson KR, Voisset C, Dubuisson J. 2006. *J Biol Chem* 281: 25177-83
47. Nozaki A, Ikeda M, Naganuma A, Nakamura T, Inudoh M, et al. 2003. *J Biol Chem* 278: 10162-73
48. Abe K, Nozaki A, Tamura K, Ikeda M, Naka K, et al. 2007. *Microbiol Immunol* 51: 117-25
49. Kritzer JA, Stephens OM, Guarracino DA, Reznik SK, Schepartz A. 2005. *Bioorg Med Chem* 13: 11-6
50. Cheng RP, Gellman SH, DeGrado WF. 2001. *Chem Rev* 101: 3219-32
51. Seebach D, Beck AK, Bierbaum DJ. 2004. *Chem Biodivers* 1: 1111-239
52. English EP, Chumanov RS, Gellman SH, Compton T. 2006. *J Biol Chem* 281: 2661-7
53. Ernst JT, Kutzki O, Debnath AK, Jiang S, Lu H, Hamilton AD. 2002. *Angew Chem Int Ed Engl* 41: 278 – 81

Chapter 2 Synthesis and Evaluation of HCV Entry Inhibitors

2.1 Background

Human and bovine LF inhibit HCV infection in cultured human hepatocytes (PH5CH8), which demonstrated that the anti-HCV activity of LF was due to the direct interaction between LF and HCV. The interaction of LF and HCV occurs faster than HCV entry to the cells, suggesting that the rapid interaction with HCV is due to a neutralizing activity which prevents the entry of HCV virion in to cultured PH5CH8 human hepatocytes and MT-2C human lymphocyte cells (1). Furthermore, it was found that a basic N-terminal loop of bovine LF did not exhibit any anti-HCV activity, suggesting that some other region is involved in anti-HCV activity (2).

LF can prevent adsorption to target cells by the fact that it binds to the E1 and E2 envelope proteins of HCV (3). Studies with LF also show that some of its antiviral activity is due to peptides released by proteolysis (4). By inhibiting viral infection of host cells, LF possesses antiviral activity toward HCV. LF is an 80-kDa milk glycoprotein consisting of two homologous iron-binding lobes (N- and C-lobe). It is considered to be a primary defense protein possessing potent bacteriostatic and bactericidal activities against pathogenic bacteria, as well as inhibitory activity against pathogenic viruses (5-9). In an elegant work by Nozaki *et al.*, a small peptide fragment of 33 residues was identified starting from 692-residue full length LF. It was shown that 33-residue LF fragment (Nozaki peptide, Np) from the C-terminal of LF specifically binds HCV-E2 and prevents HCV infection in PH5CH8 hepatocyte cells (10). Figure 2.1 highlights the 33-

residue LF fragment in colour and shows that these amino acids are present on the surface of LF in the C-terminal domain.

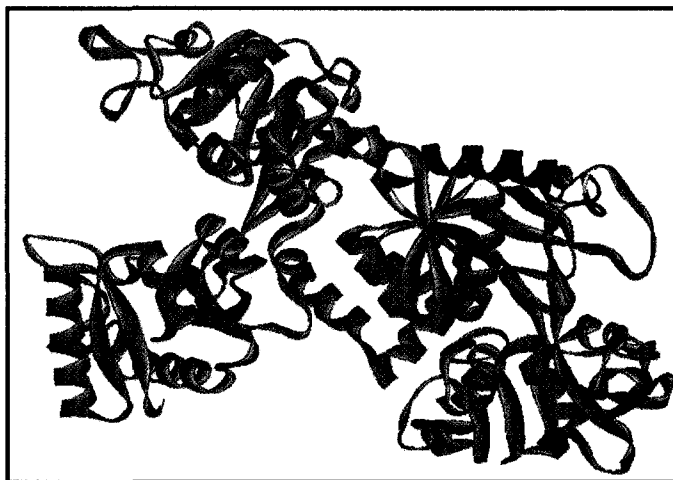


Figure 2.1 Crystal structure of recombinant human lactoferrin (pdb 1CB6) (11). Residues 600-632 (33-residue Nozaki peptide) are shown in color.

The Nozaki peptide, however, was found to possess weaker E2-protein binding activity and anti-HCV activity to that of human LF (10). Next, the authors made tandem repeats of the 33-fragment LF in order to enhance binding activity leading to better anti-HCV activity. The results show that the binding activity of the three-repeats [(33-Np)₃] was stronger than two-repeats [(33-Np)₂] which in turn was stronger than the 33-residue Nozaki peptide (12). However, the activity of these tandem repeat peptides was still less than the full length LF.

Our group decided to study the 33-residue LF fragment more closely to synthesize and evaluate peptide libraries based on its sequence. Our goal is to identify peptide sequences smaller than 33 amino acids that can latter serve as lead peptides for the design of proteolytically and metabolically stable

2.2 Objective

Binding of the HCV to the cell surface followed by viral entry is the first step required for the initiation of infection. Because this step represents a critical determinant of tissue tropism and pathogenesis, it is a major target for host cell responses and a promising target for new antiviral therapy. Although the entry mechanism of HCV is still unclear, several HCV receptor proteins have been identified. Most of the receptor have been shown to interact with the soluble and truncated form of HCV-envelope protein 2 (E2). Lactoferrin and a 33-residue peptide derived from LF have been identified as potent binders of E2 that prevent HCV infection in hepatocytes. The objective of my research was to synthesize and evaluate binding activity of five LF-derived peptides (1-5) to E2 protein. Peptides 1-5 were synthesized manually using solid-phase peptide synthesis (SPPS). His tagged E2 protein (E2H and E2N) was expressed in mammalian cells and purified using Immobilized Metal Ion Affinity Chromatography (IMAC). Finally, an ELISA-based binding assay was developed to assess binding affinity of the synthesized peptides for E2 protein. Two potent binders, peptides 3 and 5, of E2N were identified. The results from this study will allow design and evaluation of next generation peptide libraries, and may allow identification of a lead molecule for the development of HCV entry inhibitor based therapeutics.

2.3 Results and Discussion

2.3.1 Synthesis of α -Peptide Ligands

Five α -peptides **1-5** (Figure 2.3) derived from the C-terminal region of human lactoferrin were synthesized manually on Wang resin using standard Fmoc solid-phase peptide synthesis (SPPS). HBTU or BOP and HOBt were used as coupling agents. For peptides **1** and **4**, methionine (Met) was replaced by norleucine (Nle) in order to avoid any oxidation problems. After addition of all the amino acids on solid phase, the peptides were biotinylated at the N-terminus. The biotinylated peptides were used to develop an ELISA-based binding assay for the evaluation of binding affinity of these peptides toward HCV-E2 envelope protein.

Peptide	Amino acid sequence	Number of residues
1	b-VVSR <u>L_N</u> DKVERLKQVLLHQQAKFGRNGSDCPDKF	33
2	b-KVERLKQVLLHQQAKFGRNGSDCPDKF	27
3	b-KVERLKQVLLHQQAKFG	17
4	b-VVSR <u>L_N</u> DKVERLKQVLLHQQAKFGRNG <u>A</u> DC <u>P</u> AKF	33
5	b-KVERLKQVLLHQQAKFGRNG <u>A</u> DC <u>P</u> AKF	27

Figure 2.3 Sequence of five lactoferrin-derived peptides synthesized and studied herein. Residues that are underlined indicate a change from the native lactoferrin sequence. L_N stands for norleucine and b denotes biotin covalently linked to the N-terminus of the peptides.

The details of all the synthesized peptides are listed in Table 2.1. The mass of the crude and pure peptides were confirmed by MALDI-TOF mass spectrometry. Peptides were purified on a semi-preparative reverse-phase HPLC column using either isocratic or a gradient elution method as listed in Table 2.1. Purity of the peptides was confirmed by analytical HPLC (0.46 x 250 mm, 5 μ m, flow rate 1 ml/min) and mass spectrometric analysis. The RP-HPLC chromatographs for the purified peptides are shown in Figure 2.4. The yield of the purified peptides ranged between 50-65%.

Table 2.1: The HPLC purification details for peptides **1-5**.

Peptide	Mass [M+H]⁺ Observed (Calcd.)	Solvent used for HPLC purification	Elution time (min)	Pure Yield
1	4040 (4039)	10-45% ACN/H ₂ O	22.3	50%
2	3370 (3369)	30% ACN/H ₂ O	12.8	55%
3	2249 (2249)	30% ACN/H ₂ O	3.2	65%
4	3980 (3979)	20-65% ACN/H ₂ O	33.1	56%
5	3309 (3309)	20-65% ACN/H ₂ O	29.8	52%

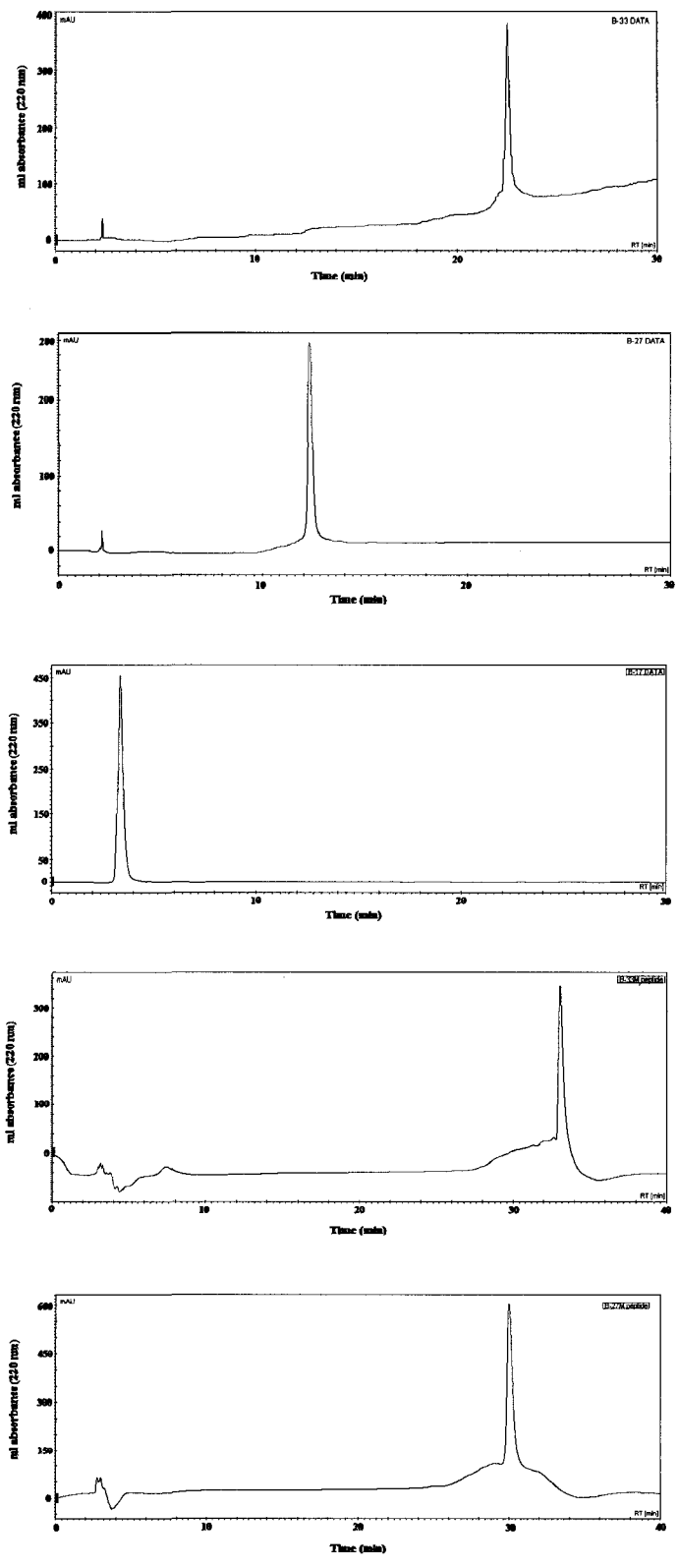


Figure 2.4 RP-HPLC chromatographs for the α -peptides 1-5.

2.3.2 Circular Dichroism of α -Peptides

Circular dichroism (CD) spectroscopy was used to evaluate the secondary structure of the synthetic peptides in solution. CD samples were prepared in PB (pH 7.4) at three different concentrations, namely, 25, 50, and 100 μM . The CD spectra obtained for peptide 1-5 are shown in Figure 2.5. The spectra were found to be independent of concentration suggesting no aggregation in this concentration range. The CD data were normalized and expressed in terms of mean residue ellipticity ($\text{deg cm}^2 \text{dmol}^{-1}$).

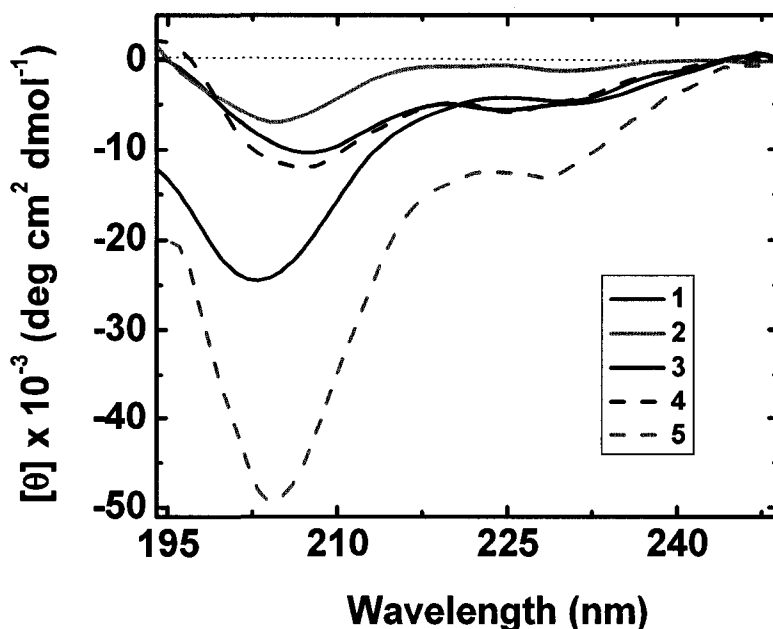


Figure 2.5 CD spectra of peptides 1-5 in PB (10 mM, pH 7.4) at 25 °C. The ellipticity was expressed as the mean residue molar ellipticity (θ) in $\text{deg cm}^2 \text{dmol}^{-1}$.

In all peptides, helical structure was induced as indicated by the appearance of distinct negative bands at 206-207 nm and negative shoulders near 220 nm (Figure 2.5). Initial inspection of the CD spectra suggested maximum

secondary structure in peptide **5** followed by peptide **3**. This was further confirmed by quantitative analysis of the secondary structure using CDPro software (Table 2.2) (13). Quantitative analysis of the distribution of secondary structure showed that peptides **3** and **5** have high helical content of 38 and 71%, respectively. Both the 33-residue peptides, **1** and **4**, displayed similar secondary structure with about 32-34% α -helix. Surprisingly, peptide **2** with 27 amino acids, same as peptide **5**, showed substantial loss of α -helical structure, however, displayed more of the β -sheet conformation (35%).

Table 2.2: CD Analysis of the secondary structure fractions of peptides **1-5** in PB at 25 °C.

Peptide ^a	Number of residues	α -helix	β -sheet	coil
1	33	0.32	0.20	0.48
2	27	0.12	0.35	0.53
3	17	0.38	0.15	0.47
4	33	0.34	0.16	0.51
5	27	0.71	0.05	0.23

^a The final concentration of all the peptides was 50 μ M in 10 mM PB (pH 7.4).

2.3.3 Expression and Purification of HCV-E2

The first contact between a virus and its host cell occurs via binding of the virus envelope to cell-surface receptors. Neutralization of this interaction is expected to be one of the major infection neutralization modes (14). The HCV major envelope E2 glycoprotein, exposed on the surface of virions, is likely to be involved in the interactions with the host and has been identified as responsible

for binding of HCV to target cells (15). HCV-E2 binds with high affinity to target cells only when expressed in mammalian cells, which is most likely due to the N-glycosylation and conformational changes it undergoes when expressed specifically in mammalian cells.

A large number of peptide-based entry inhibitors can be synthesized based on the preliminary experiments of Nozaki *et al.*(10) . However, an in vitro assay is essential for initial high-through put screening of such HCV entry inhibitors. Therefore, an ELISA-based binding assay for evaluating binding affinity of the peptide ligands for E2 protein was developed. For the ELISA assay, E2 proteins from two HCV genotypes (Ectodomains of E2 proteins, aa 334-661, with an additional tag of six histidine residues at the C-terminus) were expressed in mammalian cells. Plasmids for expressing E2 protein from two different genotypes of HCV, namely 1a (isolate H77) and 1b (isolate N2) were obtained from IRBM, Italy. The protein were expressed in Kneteman laboratory and the results of the protein expression are discussed below.

2.3.3.1 Bacterial Transformation

The uptake of exogenous DNA by cells that alters the phenotype or genetic trait of a cell is called transformation. For cells to uptake exogenous DNA they must first be made permeable so the DNA can enter the cells. This state is referred to as competency.

Plasmid vectors E2H661 (genotype 1a isolate H77) and E2N2661 (genotype 1b isolate N2) were transformed into competent *E. coli* DH5 α and the

kanamycin resistant clones were selected. Two different colonies from each strain, namely HC₁, HC₂, NC₁, and NC₂ were grown in LB medium, and the plasmid DNA were purified. The plasmid DNA were digested with *Hind*III and analyzed in 5% agarose gel electrophoresis (Figure 2.6).

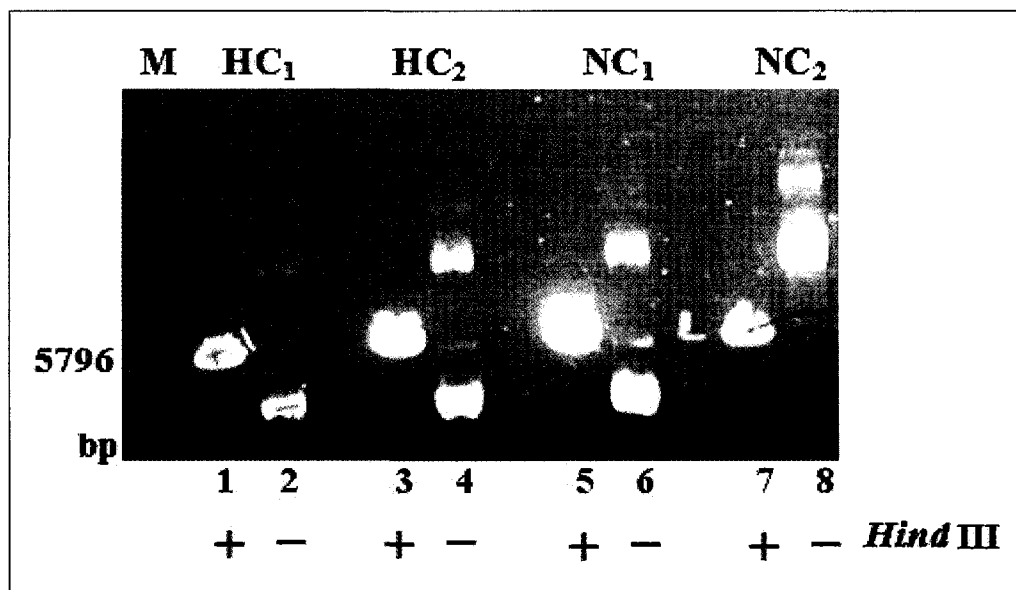


Figure 2.6 Agarose gel electrophoresis for purified vector DNA samples. The lanes 1, 3, 5, and 7 are the *Hind*III digested samples, where as the lanes 2, 4, 6, and 8 are the samples before digestion.

+ : Single fragment corresponding to 5796 bp.

- : Anomylous migration of closed circular plasmid DNA.

As shown in Figure 2.6, the even number lanes are the control samples before digestion, and the odd numbers represent the samples obtained after *Hind*III DNA digestion. The predicted 5796 bp migration of the digested plasmid confirms that the transformation of the DNA has ocured and the plasmid DNA is present in the transformed cells. The resulting plasmid DNA were grown and purified in large scale for expression of the E2 protein.

2.3.3.2 Transfection of HCV-E2 in Mammalian Cells

293 Human Embryonic Kidney (HEK) cells were transfected with either the E2 plasmid of N (genotype 1b) or H (genotype 1a) strain using Lipofectamine 2000, and the two proteins E2N and E2H were harvested after 48 hr as described in the Experimental Section (Section 2.5.5). The expected molecular weight of the glycosylated E2 protein is in the range of 62-66 kDa depend on glycosylation sites (20). Western blot analysis of the expressed proteins suggested the expression of E2 protein from both strains with MW ~63 kDa (Figure 2.7). However, the expression of E2H seemed to be less compared to E2N when the same amounts of plasmids (2 or 5 µg) were used for transfection.

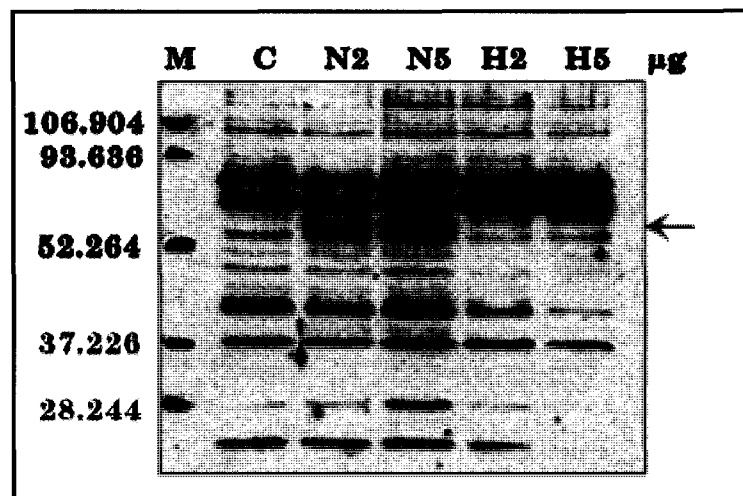


Figure 2.7 Western blot analysis of E2N and E2H proteins, probed with mouse anti-His6 mAb (1:1000) 1° antibody and goat anti-mouse (1:10000) 2° antibody. Columns M, C, N2, N5, H2, and H5 stand for marker, control (without plasmid), 2 µg N2 plasmid, 5 µg N2 plasmid, 2 µg H plasmid, and 5 µg H plasmid, respectively.

Accordingly using the same conditions, the transfection was repeated with increased amount of DNA. For both strains, 10 or 20 µg of the DNA was

transfected. As a result, expression of E2 was readily observed for both E2N and E2H as shown by the Western blot analysis using anti-His6 mAb (Figure 2.8).

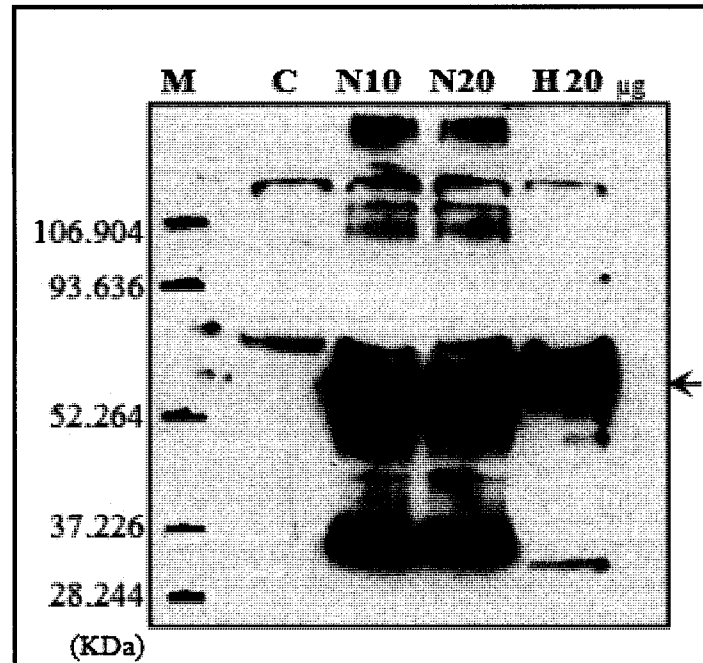


Figure 2.8 Western blot analysis of E2N and E2H proteins, probed with mouse anti-His6 mAb (1:1000) 1° antibody and goat anti-mouse (1:10000) 2° antibody. Columns M, C, N10, N20, and H20 stand for marker, control, 10 µg N2 plasmid, 20 µg N2 plasmid, and 20 µg H plasmid, respectively.

These results suggest that increase in the DNA concentration in the transfected cells, allows expression of both strains in the mammalian cells. After successful transfection of both strains, a large scale transfection of the HEK cells for the isolation and purification of the expressed E2 proteins was attempted.

2.3.3.3 Purification of the Expressed E2 Glycoprotein

The expressed E2H and E2N proteins contain a His tag at the C terminus which facilitates purification using a nickel nitrilotriacetic acid resin (Ni-NTA)

column. The crude cell lysate containing the His-tagged E2 protein was incubated with the Ni-NTA resin allowing non-covalent binding of the protein to the resin. The resin was then washed thoroughly to remove any unbound impurities and the pure protein was eluted with high concentration of imidazole (300 mM, elution buffer). All the fractions were analyzed by Western blot and the fractions containing pure protein were combined and subjected to dialysis. The Western blot analysis showed that the fractions collected with the elution buffer contained pure protein (Figure 2.9).

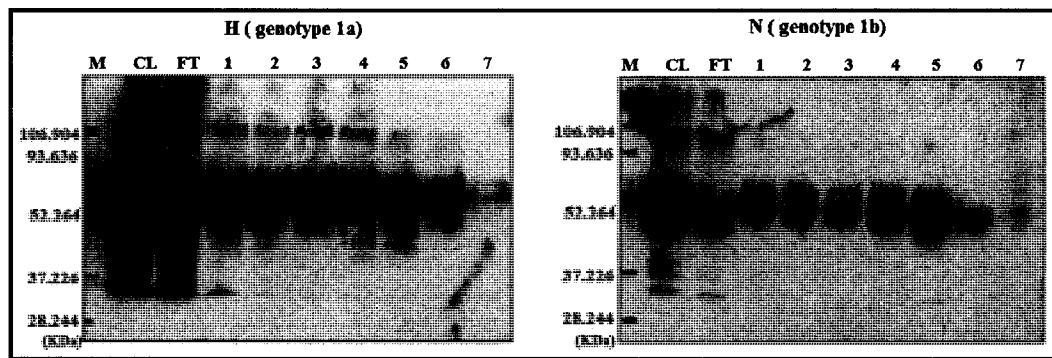


Figure 2.9 Western blot analysis of the fractions obtained from the IMAC probed with mouse anti-His6 mAb (1:1000) 1° antibody and goat anti-mouse (1:10000) 2° antibody. column during purification of the E2H and E2N proteins. CL: crude lysate; FT: flow through; 1-7: fractions 1-7 obtained using the elution buffer.

At this stage, attention was directed solely toward the production of E2N protein. The transfection and purification steps were repeated for the E2N protein. The identity of E2N was further confirmed by Western blot analysis using anti-E2-mAb against 1b genotype. Figure 2.10 shows the presence of E2N protein in fractions 3-7 (or E3-E7) using both the anti-E2-mAb and anti-His6-mAb.

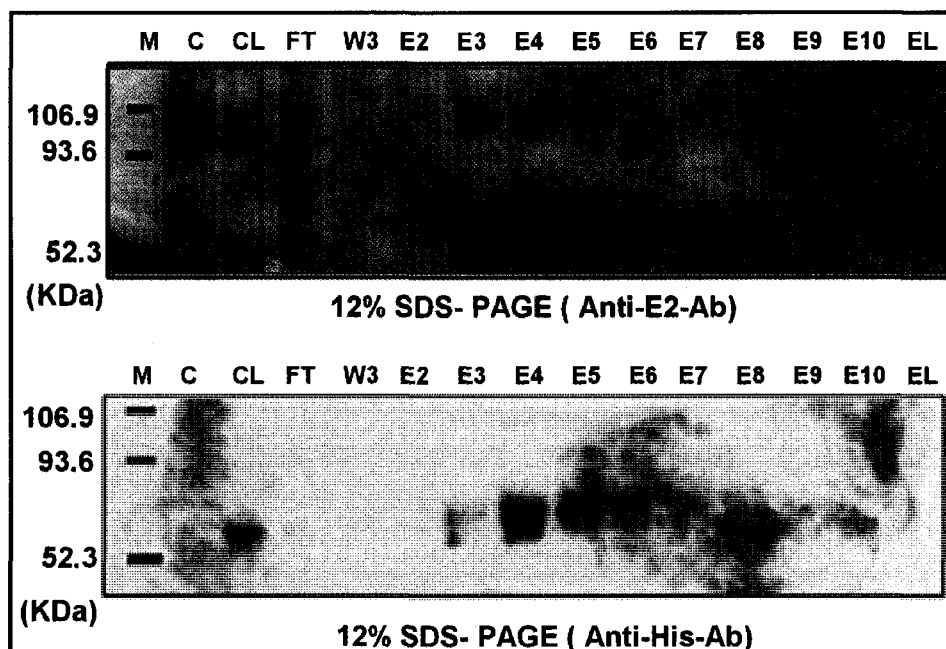


Figure 2.10 Western blot analysis of the fractions obtained from the IMAC column during E2N purification, probed with mouse anti-E2 mAb (1:20) (top) and anti-His6 mAb (1:1000) (bottom) 1^o antibody. C: control; CL: crude lysate; FT: flow through; W3: wash # 3; E2-E10: fractions 2-10 obtained using the elution buffer; EL: E2 protein sample from previous expression.

Five fractions, E3-E7, containing the highest concentrations of the pure protein were combined and dialyzed against PBS. Protein concentration was determined by the method of *Lowry assay* using bovine serum albumin (BSA) as a standard. The concentration of the pure E2N was 16.6 $\mu\text{g/ml}$ with a total volume of 7.8 ml.

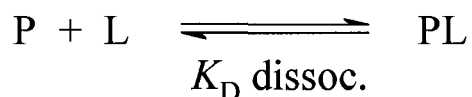
2.3.4 Binding of Lactoferrin-derived Peptides to E2 Protein

An ELISA-based binding assay was developed to access the binding affinity of the lactoferrin-derived synthetic peptides for E2N glycoprotein. In this assay, biotin-labeled peptides bind to E2 protein allowing detection of the E2-bound peptides using a strepavidin-horseradish peroxidase (Strep-HRPO) conjugate. At the end of the assay, absorbance of the TMB substrate for Strep-

HRPO is observed at 650 nm. All the five peptides (1-5) tested here displayed dose-dependent response of peptide binding to E2 protein. Several attempts were made for optimizing the conditions for the binding assay in order to obtain the binding constant of the synthesized peptides. The results of the final five binding assays for the five peptides are presented here. During the assays, biotin without the peptide was used as a control. For each peptide, the binding assay was repeated at least 3-4 times.

It was suggested by Nozaki *et al.* that the lactoferrin-derived peptides bind to a single site on the surface of the E2 protein (10). Based on this hypothesis, it was assumed that all the peptides will display binding curves following the Scheme 1,

Scheme 1



where P = E2 protein, L = ligand or peptide, and PL = noncovalent protein-peptide adduct. Initial glance at the binding curves showed that peptides 3 and 5 displayed an exponential rise in absorbance with increasing peptide concentration (Figure 2.11). However, peptides 1, 2, and 4 displayed a more complex mechanism of binding. These peptides show an initial lag in the binding curve suggesting non-specific binding or multiple binding sites for the peptide ligands on E2 protein (Figure 2.12).

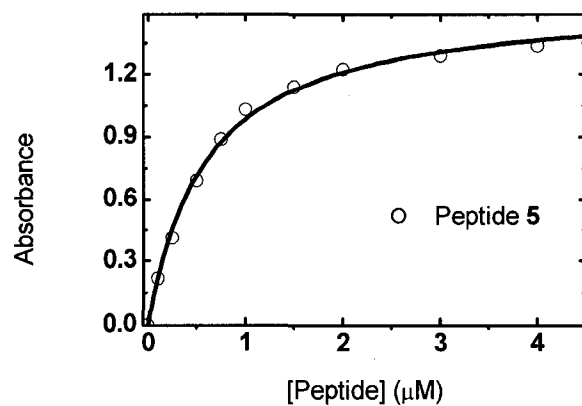
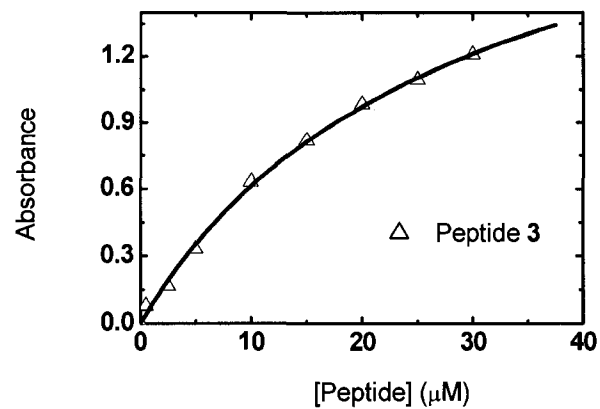


Figure 2.11 Binding of E2 protein to peptides **3** (top) and **5** (bottom). Shown is absorbance of TMB substrate at 650 nm as a function of different peptide concentration. The symbols are experimental data points whereas the line was calculated by fitting the data to Scheme 1 as described in the text.

Accordingly, the data for peptides **3** and **5** were fitted to Scheme 1 using DynaFit program (16) as described in the Experimental Section. DynaFit is a software that allows nonlinear least-squares regression of the equilibrium or kinetic data to obtain binding constants (K_D). Using this program, K_D values of 28.8 ± 2.9 and $0.569 \pm 0.04 \mu\text{M}$ were obtained for peptides **3** and **5**, respectively.

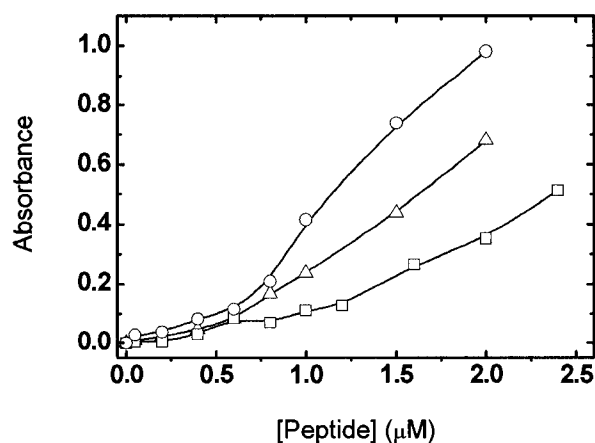


Figure 2.12 Binding of E2 protein to peptides **1** (Δ), **2** (\square), and **4** (\circ). Shown is absorbance of TMB substrate at 650 nm as a function of different peptide concentration. The symbols are experimental data points whereas the line is drawn to guide the eye.

The results of the binding assays suggest that 27-residue peptide **5** and 17-residue peptide **3** are the most potent binders of E2 protein and suitable candidates for further investigation using cell-based anti-HCV assay. These peptides will also serve as the lead molecule for the design of future peptide-based libraries. Interestingly, both the peptides are smaller than 33-residue Nozaki peptide. Previously, Nozaki *et al* proposed that 33-residue peptide was the minimum

length needed for binding E2 and anti-HCV activity. They proposed that the two loop regions on both sides of the helix of 33-residue peptides are critical for E2 binding. Having said that anti-HCV activity of peptides **3** and **5** remains to be tested. Finally, our designed peptide **5** with two mutations (S626A and D630A), which individually showed enhanced binding affinity during alanine scan (by Nozaki *et al.*) of the Nozaki peptide, displayed better binding profile compared to 33 residue Nozaki peptide (or peptide **1**). Our results further confirm that these mutations augment binding activity.

The 17-residue peptide **3** (607-622aa) is the smallest peptide sequence that was found to bind E2 specifically. This peptide does not contain the C-terminal loop present in the Nozaki peptide. The cysteine residue (aa 628) in the C-terminal loop was identified as a critical residue for E2 binding via a disulphide bridge interaction (10). However, **3** bound E2 with low micromolar affinity suggesting the possibility of other interactions, such as, electrostatic or hydrogen bonding interactions, to be predominant.

It is also noteworthy that peptides **3** and **5** have the highest helical content as observed by CD spectroscopy (Table 2.8). The helical region may be crucial for binding as also pointed out by Nozaki and coworkers (10). The 33-residue Nozaki peptide derived from lactoferrin is located on the surface of the C-terminal domain in the three-dimensional structure of human LF and is thought to be important for E2 binding activity.

2.4 Summary

HCV infection is a major worldwide public health concern for which novel therapies are in urgent demand. In this chapter, we summarize our efforts toward the design and synthesis of peptides that binds tightly and specifically to the HCV-E2 envelope glycoprotein. These peptides may prove to be the next generation entry inhibitors that may help in preventing the spread of HCV infection. Five peptides (**1-5**), derived from lactoferrin sequence, were synthesized and tested *in vitro* for binding activity to E2 from N strain. All the peptides bound to E2 in a dose-dependent manner as found by an ELISA-based binding assay. Two of the peptides, **3** and **5**, bound to E2 specifically at a single binding site with low micromolar affinity. Further investigation of these peptides using a cell-based assay or an *in vivo* animal model will confirm their ability to block HCV entry into the target cells and suppress viral infectivity.

2.5 Experimental Section

2.5.1 General

Solvents and reagents: all commercially available solvents and reagents were used without further purification. DMF, DCM, methanol, IPA, ACN, diethyl ether, pyridine, and piperidine were purchased from Caledon Laboratories LTD (Canada). D-Biotin was purchased from Sigma Chemical Co. (St. Louis, MO, USA). Wang resin and BOP were obtained from Novabiochem (San Diego, USA). HOBt, HBTU, and Fmoc-protected amino acids were purchased Peptides international (Louisville, USA). The side chains of the amino acids used in the

synthesis were protected as follows: Boc (Lys), But (Ser, Thr), OBut (Asp, Glu), Trt (Asn, Cys, Gln, His), and Pbf (Arg).

All peptides were manually synthesized using the HBTU / BOP activation protocol for Fmoc solid-phase peptide synthesis. Peptide syntheses were performed in plastic columns with plastic sinters at their base for solvent removal under suction. RP-HPLC purification and analysis were carried out on a Waters (625 LC system) HPLC system using Vydac semi-preparative C18 (1 x 25 cm, 5 μ m) and analytical C8 (0.46 x 25 cm, 5 μ m) columns. Compounds were detected by UV absorption at 220 nm. Mass spectra were recorded on a MALDI Voyager time-of-flight (TOF) spectrometer, (VoyagerTM Elite) Department of Chemistry, University of Alberta, Edmonton, Alberta, or on a Waters micromass ZQ, Faculty of Pharmacy and Pharmaceutical Sciences, University of Alberta, Edmonton, Alberta. The CD measurement was made on an Olis CD spectrometer (Georgia, USA) at 25 °C in a thermally controlled quartz cell over 190-260 nm, Department of Chemistry, University of Alberta, Edmonton, Alberta.

Plasmid vectors E2H661 (genotype 1a isolate H77) and E2N2661 (genotype 1b isolate N2) were kindly provided by IRBM (Merck, Italy) (17). The concentration of E2H661 and E2N2661 was 710 and 10 μ g/ μ l, respectively. *E. coli* strain DH5 α , ethidium bromide, lipofectamine 2000, 0.05% Trypsin / EDTA, OptiMEM-I, nitrocellulose membrane Dulbecco's Modified Eagle's Medium (DMEM) and fetal bovine serum (FBS) were purchased from Invitrogen (Carlsbad, Canada). Human Embryonic kidney (HEK) 293 cells were obtained from American Type Tissue Culture (Bethesda, MD, USA). Kanamycin, bovine

serum albumin (BSA), agarose, 2-mercaptoethanol, imidazole and Folin-phenol were purchased from Sigma Chemical Co. (St. Louis, MO, USA). Equipment and reagents for sodium dodecyl sulfate-polyacrylamide gel electrophoresis (SDS-PAGE) and Western blotting were from Bio-Rad (Mississauga, Canada). The anti-His₆ mAb was purchased from Novagen (Madison, USA). Restriction endonucleases *Hind*III was obtained from Life Technologies (Burlington, Canada). Plasmid Mega Kit, plasmid mini-preparation kit and Ni-NTA-agarose resin was obtained from Qiagen (Mississauga, Canada). Enhanced chemiluminescence (ECL) immunodetection kits, antimouse horseradish peroxidase-linked secondary antibodies and DNA molecular weight markers were purchased from Amersham Biosciences (Oakville, Canada). Anti-HCV-E2 mouse monoclonal antibody was purchased from ViroStat (Portland, ME).

96-well microtiter immunoplates for ELISA were obtained from Maxisorb Immunoplates, Nunc, (Roskilde, Denmark). Recombinant Hepatitis C Virus E2 antigen for the initial ELISA was obtained from AUSTRAL Biologicals (San Ramon, CA USA). For subsequent ELISAs, E2 antigen was expressed in the mammalian cells. Streptavidin-horseradish peroxidase (SA-HRPO) and BSA (bovine serum albumin) were obtained from Sigma Chemical Co. (St. Louis, MO, USA). Substrate solution TMB (3,3',5,5'-tetramethylbenzidine) including Peroxidase substrate & Peroxidase substrate solution B was obtained from KLP Laboratories, (Gaithersburg, USA).

2.5.2 Synthesis of Peptides 1-5

b-VVSR _N DKVERLKQVLLHQQAKFGRNGSDCPDKF-OH	1
b-KVERLKQVLLHQQAKFGRNGSDCPDKF-OH	2
b-KVERLKQVLLHQQAKFG-OH	3
b-VVSR _N DKVERLKQVLLHQQAKFGRNG <u>AD</u> CP <u>AK</u> F-OH	4
b-KVERLKQVLLHQQAKFGRNG <u>AD</u> CP <u>AK</u> F-OH	5

2.5.2.1 Preparation of Peptides through Fmoc-amino Acid Coupling Method

Stepwise synthesis of the peptides was done manually on a 0.3-mmol scale of Wang resin following the standard Fmoc solid-phase peptide chemistry (18). Wang resin was swelled in dry DCM for 30 minutes, followed by washing with DCM, IPA, and DMF twice each, and the resin was suspended in dry DMF.

In a separate vial, Fmoc amino acid (0.6 mmol) was activated by the addition of HBTU (0.6 mmol), HOBt (0.6 mmol), NMM (1.2 mmol), and 1 ml DMF and the mixture was vortexed for 5 minutes. The pre-activated amino acid was added to the resin suspended in DMF, and the reaction mixture was shaken at room temperature for 30 minutes. After coupling the resultant suspension was drained and washed with DMF, IPA, and DCM four times each. The completion of each coupling step was confirmed by Ninhydrin test (Kaiser test) allowing determination of any residual free amine. Fmoc group was removed by suspending the resin with 20% piperidine in DMF twice for 7 minutes each. Solvents were drained for 5 minutes followed by wash with DMF, IPA, and DCM

four times each. The resin was then suspended in DMF and was allowed to swell for 10 min for the next coupling.

The synthesis cycles (coupling, washing, deprotection, and washing) were continued up to the addition of 27 amino acids. At this stage, a portion of the resin was saved to obtain peptide **2** and the remaining resin was used to carry out the synthesis of peptide **1**. Similarly for peptides **4** and **5**, the resin was split after the addition of 27 amino acids. Peptide **3** which contains 17 amino acids was synthesized separately. With the increase in chain length, the coupling time and the deprotection time were increased to a maximum of 3 hours for each coupling step and 10 minutes for each deprotection step. Also, coupling of the amino acids was repeated where necessary and the deprotection with piperidine was done three times for 10, 7, and 5 minutes for the last 10 amino acids.

2.5.2.2 Biotinylation of the Peptides

After complete assembly of the peptide on the resin, the N-terminus was used for covalent modification with biotin. The resin with complete peptide sequence was suspended in DMF. Biotinylation was achieved by addition of biotin (0.5 mmol), DIC (0.5 mmol), and HOBT (0.5 mmol) dissolved in 5 ml DMF to the resin. The suspension was allowed to stir for 27 hours at room temperature. The resin was washed extensively with DMF (10 times). Kaiser test was carried out to ensure the completion of the biotinylation reaction.

2.5.2.3 Cleavage of the Peptides from the Resin

A test cleavage was performed after each five residues were coupled, and the desired product was confirmed by MALDI-TOF mass spectrometry. Each test peptide was cleaved from the resin with a mixture of 87.5% TFA, 5% phenol, 5% water, and 2.5% ethanedithiol for 90 min at room temperature with mechanical shaking.

The biotinylated peptide chain was released from solid support, with concomitant removal of acid labile side-chain protecting groups using the same procedure as used for the test cleavages. The filtrate from the cleavage reactions was collected, combined with TFA washes (3 X 2 min, 1 ml), and concentrated in vacuo. Cold diethyl ether (~ 15 ml) was added to precipitate the crude cleaved peptide. After trituration for 2 min, the peptide was collected upon centrifugation and decantation of the ether. The crude peptide precipitate was dried under vacuum and stored at -20 °C.

2.5.2.4 HPLC Purification of the Peptides

The crude material was dissolved in 10-20% aqueous ACN and purified on a semi-preparative VYDAC C18-reversed phase HPLC column (10 x 250 mm, 5 µm) using an acetonitrile/water (in the presence of 0.05% TFA, v/v) gradient (flow rate = 2 ml/min, monitored at 220 nm) over a period of 40 minutes. The details of the gradient elution method used for each peptide purification are listed in the Table 2.1. The identity and purity of the peptides were assessed by analytical VYDAC C8 (0.46 x 25 cm, 5 µm) HPLC columns and mass

spectrometric analysis. Mass spectrometric analysis of the crude as well as the pure peptides was confirmed using matrix-assisted laser desorption ionization time-of-flight (MALDI-TOF) mass spectrometry and was performed on a VoyagerTM Elite instrument using α -cyano-4'-hydroxycinnamic acid as the matrix.

2.5.3 Circular Dichroism of Peptides 1-5

The CD measurement was made on an Olis CD spectrometer (Georgia, USA) at 25 °C in a thermally controlled quartz cell over 190-260 nm, Department of Chemistry, University of Alberta, Edmonton, Alberta, Canada. The sample was dissolved in appropriate amount of phosphate buffer (1 mM, pH 7.4). The final concentrations for CD measurements were 25, 50, and 100 μ M. The length of the cuvette was 0.02 cm and number of scans was set to 10. The CD data are normalized and are expressed in terms of mean residue ellipticity ($\text{deg cm}^2 \text{dmol}^{-1}$).

2.5.4 Bacterial Transformation and Plasmid Purification

Protein expression experiments were done in collaboration with Kneteman laboratory under the supervision of Dr. Donna Douglas (Department of Surgery, Faculty of Medicine and Dentistry, University of Alberta, Edmonton, Alberta, T6G 2B7 Canada).

2.5.4.1 Bacterial Transformation

DH5 α *E. coli* (50 μ l) was thawed on ice and 2 μ l of E2H661 or 2 μ l of E2N2661 plasmid was gently mixed with *E. coli*. After incubation on ice for 10 minutes, *E. coli* was incubated at 42 °C for 45 seconds and then kept on ice for another 2 minutes. After heat shock treatment, *E. coli* was recovered by culturing in LB broth (200 μ l) for 1 hr. The resulting *E. coli* suspension was spread on the LB agar plate containing 30 μ g/ml kanamycin and the plate was incubated at 37 °C overnight for the colony formation. Fresh individual colonies (2-per strain) of the transformed *E. coli* (HC₁, HC₂, NC₁, and NC₂) were picked from the plates and were inoculated individually in 12 ml LB medium containing 30 μ g/ml kanamycin and allowed to grow over night at 37 °C in an incubator shaker to generate the starter culture.

The overnight starter culture (2 ml) from the two different colonies of each strain (HC₁, HC₂, NC₁, and NC₂) was purified using the QIAprep Spin Miniprep Kit following the manufacturer's instructions. The plasmid DNA was digested with *Hind*III and analyzed by 5% agarose gel electrophoresis.

2.5.4.2 Restriction Digestion and Gel Electrophoresis

Purified vector DNA samples of each strain (HC₁, HC₂, NC₁, and NC₂) were digested with *Hind*III. Restriction digests were set up using 5 μ l aliquots of purified plasmid DNA along with 2 μ l of the appropriate restriction enzyme buffer, 2 μ l of the restriction enzyme, and 12 μ l of sterile water. After incubating

the reaction mixture at 37°C for one hour, 2 µl of sample was loaded on 5% agarose gel.

Gel electrophoresis experiment was run for the four plasmid DNA samples (HC₁, HC₂, NC₁, and NC₂) and the corresponding controls, where the control samples were not digested with *Hind*III. A 5% agarose gel containing 0.5 µg/ml ethidium bromide was run in a horizontal gel electrophoresis unit along with 1 Kb ladder DNA molecular weight marker. The running buffer was TAE (40 mM Tris, 20 mM acetic acid, 1 mM EDTA, pH 8.0). Electrophoresis was carried out at 100 V for 40 minutes.

2.5.4.3 Large Scale Plasmid Purification

The overnight starter culture, 10 ml each NC₁ and HC₂, was diluted to 500 ml fresh LB medium containing 30 µg/ml of kanamycin and was grown at 37 °C with vigorous shaking overnight. The resulting plasmid DNA was purified using the Qiagen Plasmid Mega Kit following the manufacturer's instructions. The concentration was estimated by spectrophotometry at 260 nm. The plasmids were purified from the culture in two batches. From a 50 ml culture of NC₁ and HC₂, pure plasmids (100 µl) were obtained with a concentration of 1.5 µg/µl and 1.1 µg/µl for the N and H strains, respectively. In a second attempt, 250 ml of the culture produced 100 µl of pure plasmids with a concentration of 4.2 µg/µl and 0.85 µg/µl for N and H, respectively.

2.5.5 Cell Culture and Transfection

2.5.5.1 Cell Culture

Human Embryonic kidney (HEK) 293 cells were grown in 75 cm² flasks and maintained in high-glucose Dulbecco's modified Eagle's medium (DMEM) supplemented with 10 % (v/v) fetal bovine serum at 37 °C in a humidified 5% CO₂ atmosphere. The cells were sub-cultured weekly, and the attached cells were treated with trypsin-EDTA followed by counting of the cells.

2.5.5.2 Transient Transfection

One day before transfection, cells were trypsinized and resuspended in DMEM, and plated into two 6-well plates, one plate for the N strain (genotype 1b) and the other for H strain (genotype 1a). The cells were transfected at a density of 1.5×10^5 cells per 0.6 ml per well. Transfections were performed using Lipofectamine 2000. In separate vials, 2 µg and 5 µg of the vector DNA for the N strain (genotype-1b) was transferred and allowed to stand for 5 minutes. To each of these vials was added 2 µl of lipofectamine 2000 suspended in 50 µl of OptiMEM-I medium. The contents of the vial were gently mixed and were incubated at room temperature for 20 minutes. After 20 minutes the mixture was diluted to 400 µl with OptiMEM-I and the contents of the vial were transferred to a single well of the plate. Prior to the addition of the plasmid, cells were washed with the OptiMEM-I medium. The cells were incubated with the lipid/DNA complex mixture for 4 hours followed by addition of fresh, pre-warmed to 37°C, DMEM medium (2 ml) to each well. Cells were allowed to transfect for 48 hours.

Lipofectamine 2000 without the vector DNA was used as a transfection negative control.

Transfection of the vector DNA for the H strain (genotype-1a) was performed similarly using 2 and 5 μg of the DNA vector. For each strain, cells were harvested two days after transfection at about 90% confluence. Cells were washed with cold PBS, harvested in ice-cold lysis buffer [50 mM Tris pH 7.4, 1 M NaCl and 1 mM phenylmethylsulfonyl fluoride (PMSF) as protease inhibitor], lysed on ice for 30 minutes followed by sonication (twice) for 10 seconds. Finally, cells were pre-cleared by centrifugation at 10,000 g for 10 minutes. The supernatant was carefully transferred into 15 ml Falcon tubes and stored at $-20\text{ }^{\circ}\text{C}$ until further use.

Transfection of HEK-293 cells with N and H DNA vectors was repeated with increased amount of DNA (10-20 μg) to improve the amount to protein expressed.

2.5.5.3 SDS-PAGE and Western Blot

The supernatant containing protein lysate was loaded onto 12% SDS-PAGE gel. Prior to loading on the gels, the samples were treated by heating at $95\text{ }^{\circ}\text{C}$ for 5 minutes in sample loading buffer (80 mM Tris-HCl, pH 6.8, 2% SDS, 10% glycerol, 2% β -mercaptoethanol, 0.02% bromophenol blue). Gel-separated proteins were electroblotted onto nitrocellulose membrane in blotting buffer containing Tris (48 mmol/L), glycine (39 mmol/L), SDS (0.037%), and methanol (20% vol/vol) for 1 h at 100 V in the cold room. The membrane was blocked

overnight at 4 °C in 5% skim milk in a buffer containing Tris-buffered saline (TBST, 0.05 M Tris, 0.15 M NaCl, 0.05% Tween, pH 7.4). The membrane was washed with TBST (10 ml x 1 min followed by 10 ml x 10 min) followed by incubation for 1 h with the anti-His₆ mAb (1:1000 dilution). Subsequently the membrane was washed with TBST (as before) and incubated with antimouse horseradish peroxidase-linked secondary antibodies GAM-HRPO (1:10,000 dilution) for 1 h. Following a final washing step, the binding of mAbs to antigen was detected using the enhanced chemiluminescence substrate (ECL).

2.5.6 Purification of the Expressed E2 Glycoprotein

Expression of proteins fused to a His tag allows purification using a nickel nitrilotriacetic acid resin (Ni-NTA) column under denaturing conditions according to the protocol provided by the manufacturer (Qiagen). Briefly, the crude cell lysate (CL) was incubated with Ni-NTA resin at a ratio of 1 ml of resin per 5 ml of the CL, and the suspension was incubated overnight at 4 °C with gentle rocking. 50 µl of the CL was saved for SDS-PAGE analysis. The resin was loaded on a plastic IMAC column (15 ml) and then equilibrated with 10 bed volumes of the lysis buffer (50 mM Tris-HCl, 1 M NaCl, pH 7.4). It was then washed with 20 bed volumes of washing buffer #1 (0 mM imidazole, 50 mM Tris-HCl, and 1 M NaCl, pH 7.4), followed by 10 bed volumes of washing buffer # 2 (20 mM imidazole, 50 mM Tris-HCl, and 1 M NaCl, pH 7.4), and finally with 20 bed volumes of washing buffer # 3 (40 mM imidazole, 50 mM Tris-HCl, 1 M NaCl, pH 7.4). His-tag protein was then eluted using elution buffer (50 mM Tris-

HCl, 1 M NaCl, and 300 mM imidazole, pH 7.4), and 7 fractions (~1 ml each) were collected. After elution with 300 mM imidazole, 50 μ l of each fraction was subjected to SDS-PAGE analysis and Western blot as described in Section 2.2.3 using anti-His₆ mAb (Figure 2.9).

In a second attempt to produce large amount of E2 protein, the transfection and purification for the N strain was repeated using 20 μ g of the DNA vector in five 6-well plates. After Ni-NTA column purification, 10 fractions of ~1.5 ml each were collected. All the fractions were analyzed by SDS-page and Western Blot using anti-His₆ mAb and anti-E2-mAb (Figure 2.10). Five fractions (E3 to E7) containing the highest concentrations of the pure protein were combined and dialyzed against phosphate buffered saline (PBS) pH 7.4 overnight at 4 °C. The purified protein was aliquoted into five vials and stored at -80 °C.

The protein concentration was determined by the method of Lowry *et al.* (1951) using bovine serum albumin (BSA) as standard. Duplicates were prepared for both the standards and the experimental samples. Experimental samples consisted of 50 μ L of the purified E2N or E2H protein. Protein concentrations were determined using the standard curve obtained for BSA and was found to be 38.1 μ g/ml for E2N and 65.0 μ g/ml for E2H. The protein concentration of E2N obtained in the second attempt (20 μ g DNA used) was 16.6 μ g/ml for a total volume of 7.8 ml and in a third attempt (15 μ g DNA used) protein concentration was 25.07 μ g/ml for a total of 3.7 ml pure protein.

2.5.7 ELISA-based Binding Assay

An Enzyme-linked Immunosorbent Assay (ELISA)-based binding assay was developed to examine the binding affinity between the E2 protein and peptide ligands. E2 (N strain) antigen (100 μ L, 150 or 200 ng/well) in PBS (1 mM, pH 7.4) was added to the wells of a 96-well microtiter immunoplate and incubated overnight at 4 $^{\circ}$ C to allow the antigen to adsorb to the surface. Excess antigen was removed from the plate by rinsing each well with 300 μ l PBS (1 mM, pH 7.4) containing 0.05% Tween-20. Subsequently the wells were blocked by incubating with 200 μ l of 2% BSA in PBS. After discarding the supernatant, each well was washed with 0.05% Tween-20 in PBS (300 μ l). Stock solutions of peptides **1-5** were diluted with PBS in small aliquots (300 μ l) in eppendorf tubes to obtain different peptide concentrations. Concentration of the stock solutions of peptides **1-5** was obtained by Lowry assay. Biotin samples with different concentrations were prepared and used as a control without the peptide. Peptide solution or biotin (100 μ l/well) was added to each well in duplicates and the plate was incubated at room temperature on a shaker (200 rpm) for 3 h. The supernatant was discarded and the wells were rinsed with 0.05% Tween-20 in PBS (300 μ l). To each well was then added a solution (100 μ l) of Strep-HRPO (0.1 μ g) in 1% BSA and the plate was incubated at room temperature for 1h while gently agitating on a shaker. After discarding the Strep-HRPO solution, plate was rinsed with 0.05 % Tween-20 in PBS (300 μ l x 3) and substrate solution (100 μ l, TMB Peroxidase:Peroxidase solution B, 1:1, v/v) was added to each well. The plate was then incubated at room temperature for about 15 minutes until the absorbance

levels reached an appropriate level (0.7-0.8). The absorbance in each well was measured using ELISA V_{max} kinetic microplate reader at 650 nm (Molecular Devices Corp., California, USA). (Tables 2.3-2.7).

Table 2.3: ELISA-based binding data for peptide 1 when 30 nM/well (200 ng/well) E2N was used (Figure 2.12).

Peptide concentration (μM)	Absorbance at 650 nm	Final Absorbance
0 (PBS)	0.0893	-
50	0.0975	0.0082
200	0.1115	0.0222
400	0.1352	0.0459
600	0.1715	0.0822
800	0.2583	0.1690
1000	0.3267	0.2374
1500	0.5277	0.4384
2000	0.7690	0.6797

Table 2.4: ELISA-based binding data for peptide 2 when 40 nM/well (200 ng/well) E2N was used (Figure 2.12).

Peptide concentration (μM)	Absorbance at 650 nm	Final Absorbance
0 (PBS)	0.0597	-
50	0.0639	0.0042
200	0.0637	0.004
400	0.0892	0.0295
600	0.1447	0.085
800	0.1302	0.0705
1000	0.1722	0.1125
1200	0.1882	0.1285
1600	0.3262	0.2665
2000	0.4122	0.3525
2400	0.5722	0.5125

Table 2.5: ELISA-based binding data for peptide 3 when 30 nM/well (150 ng/well) E2N was used (Figure 2.11).

Peptide concentration (μM)	Absorbance at 650 nm	Final Absorbance
0 (PBS)	0.092	-
500	0.1705	0.0785
2500	0.258	0.166
5000	0.4217	0.3297
10000	0.7226	0.6306
15000	0.9094	0.8174
20000	1.0768	0.9848
25000	1.1857	1.0937
30000	1.3015	1.2095

Table 2.6: ELISA-based binding data for peptide 4 when 30 nM/well (150 ng/well) E2N was used (Figure 2.12).

Peptide concentration (μM)	Absorbance at 650 nm	Final Absorbance
0 (PBS)	0.0657	-
50	0.1187	0.028
200	0.1035	0.0379
400	0.1482	0.0825
600	0.182	0.1164
800	0.2756	0.2100
1000	0.4813	0.4157
1500	0.8043	0.7387
2000	1.0473	0.9816

Table 2.7: ELISA-based binding data for peptide 5 when 40 nM/well (200 ng/well) E2N was used (Figure 2.11).

Peptide concentration (μM)	Absorbance at 650 nm	Final Absorbance
0 (PBS)	0.1719	-
100	0.3918	0.2199
250	0.5855	0.4136
500	0.8638	0.6919
750	1.061	0.8892
1000	1.205	1.0331
1500	1.312	1.1401
2000	1.397	1.2250
3000	1.463	1.2914
4000	1.511	1.3390

Absorbance values for the duplicate wells were averaged and blank (PBS) was subtracted from each well to give the final absorbance. The final absorbance and the corresponding peptide concentration were plotted for all the peptides (Figures 2.11 and 2.12). The data was fitted to Scheme 1 for peptides **3** and **5** (P = E2 protein and L = ligand or peptide). Nonlinear least-squares regression of the data was performed using DynaFit (19) to obtain K_D values for **3** and **5**. The binding constants were estimated by fitting the equilibrium data to the single site protein-ligand complex formation model as shown in Scheme 1. The input script files for peptides **3** and **5** and some of the pertinent results (output files) from Dynafit are shown in Figures A.1 and A.2 (Appendix A), respectively.

2.6 References

1. Ikeda M, Sugiyama K, Tanaka T, Tanaka K, Sekihara H, et al. 1998. *Biochem Biophys Res Commun* 245: 549-53
2. Ikeda M, Nozaki A, Sugiyama K, Tanaka T, Naganuma A, et al. 2000. *Virus Res* 66: 51-63
3. Yi M, Kaneko S, Yu DY, Murakami S. 1997. *J Virol* 71: 5997-6002
4. Siciliano R, Rega B, Marchetti M, Seganti L, Antonini G, Valenti P. 1999. *Biochem Biophys Res Commun* 264: 19-23
5. Arnold D, Di Biase AM, Marchetti M, Pietrantoni A, Valenti P, et al. 2002. *Antiviral Res* 53: 153-8
6. Ammendolia MG, Pietrantoni A, Tinari A, Valenti P, Superti F. 2007. *Antiviral Res* 73: 151-60

7. Redwan el RM, Tabll A. 2007. *J Immunoassay Immunochem* 28: 267-77
8. Wakabayashi H, Abe S, Teraguchi S, Hayasawa H, Yamaguchi H. 1998. *Antimicrob Agents Chemother* 42: 1587-91
9. Bellamy W, Takase M, Yamauchi K, Wakabayashi H, Kawase K, Tomita M. 1992. *Biochim Biophys Acta* 1121: 130-6
10. Nozaki A, Ikeda M, Naganuma A, Nakamura T, Inudoh M, et al. 2003. *J Biol Chem* 278: 10162-73
11. Jameson GB, Anderson BF, Norris GE, Thomas DH, Baker EN. 1998. *Acta Crystallogr D Biol Crystallogr* 54: 1319-35
12. Abe K, Nozaki A, Tamura K, Ikeda M, Naka K, et al. 2007. *Microbiol Immunol* 51: 117-25
13. Sreerama N, Venyaminov SY, Woody RW. 2001. *Anal Biochem* 299: 271-4
14. Lauer GM, Walker BD. 2001. *N Engl J Med* 345: 41-52
15. Rosa D, Campagnoli S, Moretto C, Guenzi E, Cousens L, et al. 1996. *Proc Natl Acad Sci U S A* 93: 1759-63
16. Kuzmic P. 1996. *Anal Biochem* 237: 260-73
17. Yagnik AT, Lahm A, Meola A, Roccasecca RM, Ercole BB, et al. 2000. *Proteins* 40: 355-66
18. Chan WC, White PD. 2000. *Oxford University Press, Oxford*. 2 Editions
19. Kuzmic P, Hill C, Janc JW. 2004. *Methods Enzymol* 383: 366-81.
20. Wakita T, Taya C, Katsume A, Kato J, Yonekawa H, et al. 1998. *J Biol Chem* 273: 9001-6

Chapter 3 Synthesis of Peptidomimetic β^3 -Peptides

3.1 Background

The number of native and modified peptides used as drugs is constantly increasing (1). However, the use of peptides as drugs is limited by the following factors: a) their low metabolic stability towards proteolysis in the gastrointestinal tract and in serum; and b) their rapid excretion through liver and kidneys. The unfavourable pharmacokinetic properties associated with peptides when used as orally administered drugs can, in principle, be avoided by development of peptidomimetics.

In recent years intensive efforts have been made to develop peptides or peptidomimetics that display more favorable pharmacological properties than their prototypes. Most of the research carried out concerns with the preparation of analogues with different chemical structure and possibly modified conformational preferences, in order to induce changes in the biological response. Such compounds that mimic or block the biological effects of a peptide or a protein motif, with the potential to act as a drug are known as peptidomimetics. Numerous structural modifications with peptidomimetic backbone have proved to be promising for the future drug development.

Peptidomimetic foldamers, such as azapeptides which are formed by replacing the $C\alpha$ of amino acid residues with nitrogen, the closely related azatides (2), peptoids which are N-substituted glycines (3), β -peptides, γ -peptide (4), and

δ -peptides (5) have attracted a lot of attention because of their unique conformations and interesting bioactivities (Figure 3.1).

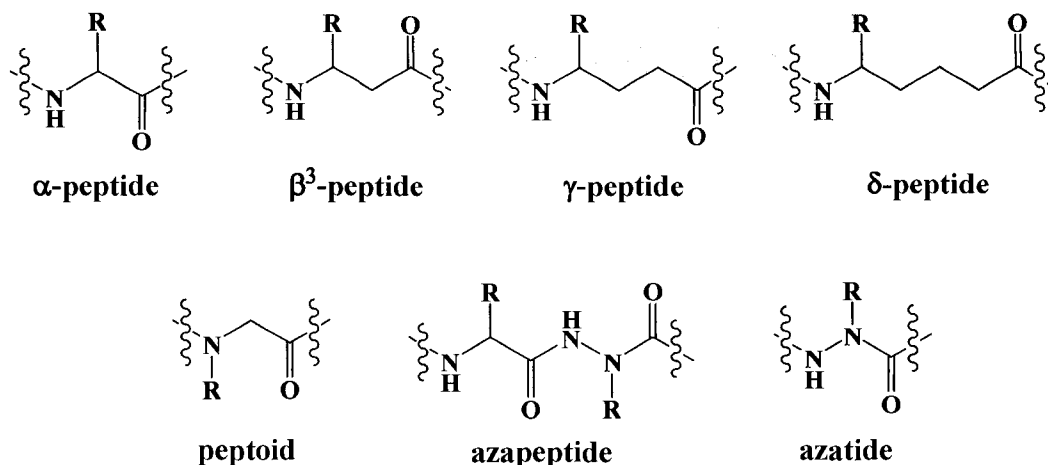


Figure 3.1 Examples of monomeric units of peptidomimetics.

β -Peptides are one of the most extensively studied peptidomimetic oligomers or foldamers (6, 7). β -peptides i) are stable toward proteolysis and metabolism, ii) can form helices, β -strands, and coil-like structures, iii) can be designed specifically for a target with a large surface area, and iv) are non toxic to humans. These characteristics make them attractive scaffolds for mimicking the α -peptides.

3.1.1 β -Peptides

β -Peptides are oligomers of β -amino acids that contain an additional methylene group compared to α -amino acids. β -Peptides are subdivided into

mainly three types β^2 -, β^3 -, and $\beta^{2,3}$ -peptides depending upon the substitution of side chain(s) on the 3-aminoalkanoic skeleton (Figure 3.2) (8).

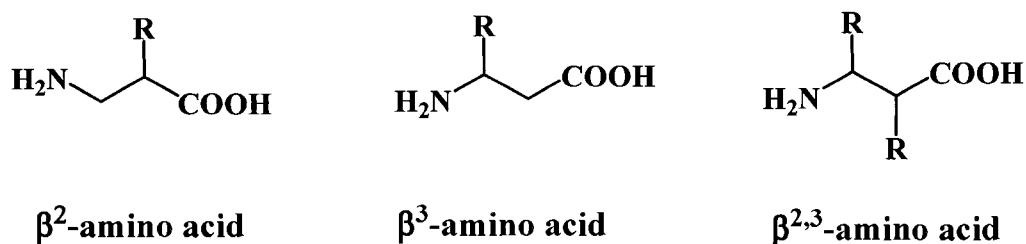
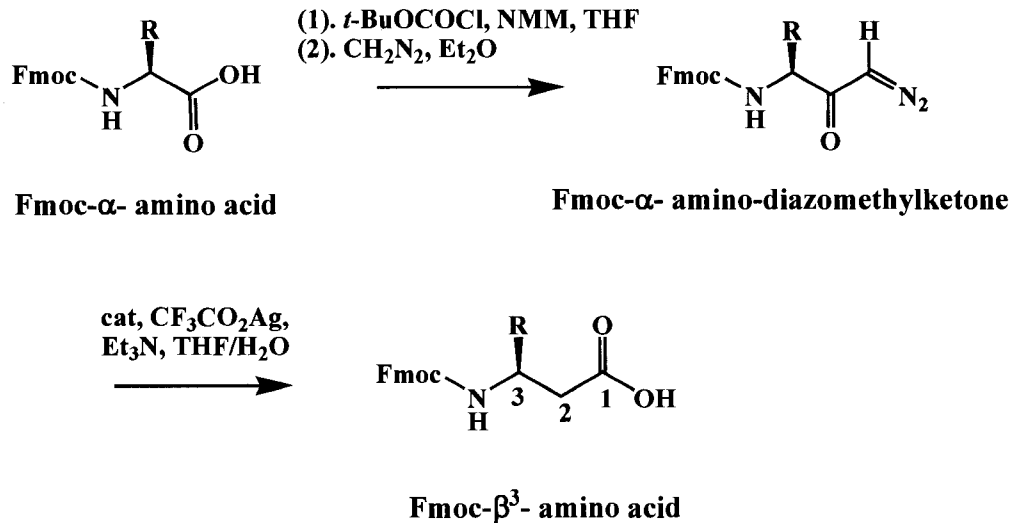


Figure 3.2 Nomenclature for β -peptides depending upon the substitution of the backbone carbon.

3.1.2 Synthesis of β^3 -Peptides

In 1996, β^3 -peptides consisting of β^3 -amino acid residues with proteinogenic side chains were synthesized and described for the first time by Seebach *et al.* (9), Seebach's method is the most widely used procedure for obtaining β^3 -homoamino acids. This method utilizes β -homoamino acids synthesized via Arndt-Eistert homologation for composing β^3 -peptides. Arndt-Eistert synthesis is a popular method for producing β^3 -amino acid from α -amino acid. Acid chlorides react with diazomethane to give diazoketones. In the presence of a nucleophile (water) and a metal catalyst (Ag_2O), diazoketones form the desired acid homologue (Scheme 3.1).

This procedure for obtaining β^3 -amino acids requires the use of diazomethane which is a highly toxic and explosive gas, making the synthetic procedure non trivial. In addition, it is based on direct conversion of α -amino acid to the corresponding β^3 -amino acid, making the synthesis limited to the natural α -



Scheme 3.1 Arndt Eistert homologation affords β^3 -substituted amino acid.

amino acids only. Novel methods for easy access of these oligomers with a wide variety of side chains are therefore sought for.

3.1.3 Conformation of β -Peptides

The biological activity of peptides is strongly dependent on their three-dimensional structures. Because bioactive peptides must adopt a specific conformation in order to bind to a receptor, the characterization of the binding conformation is important in order to obtain potent and selective therapeutic agents. β -Peptides have more conformational freedom than α -peptides, because of an additional methylene unit present in the polymer backbone. Consequently, whereas α -peptide helices most commonly adopt the α -helix conformation, β -peptide require relatively few residues to adopt several distinct secondary structures like turns, helices or sheets (6). Many types of helix structures

consisting of β -peptides have been reported. These conformation types are distinguished by the number of atoms in the hydrogen-bonded ring that is formed in solution; 8-helix, 10-helix, 12-helix, and 14-helix (10) (Figure 3.3).

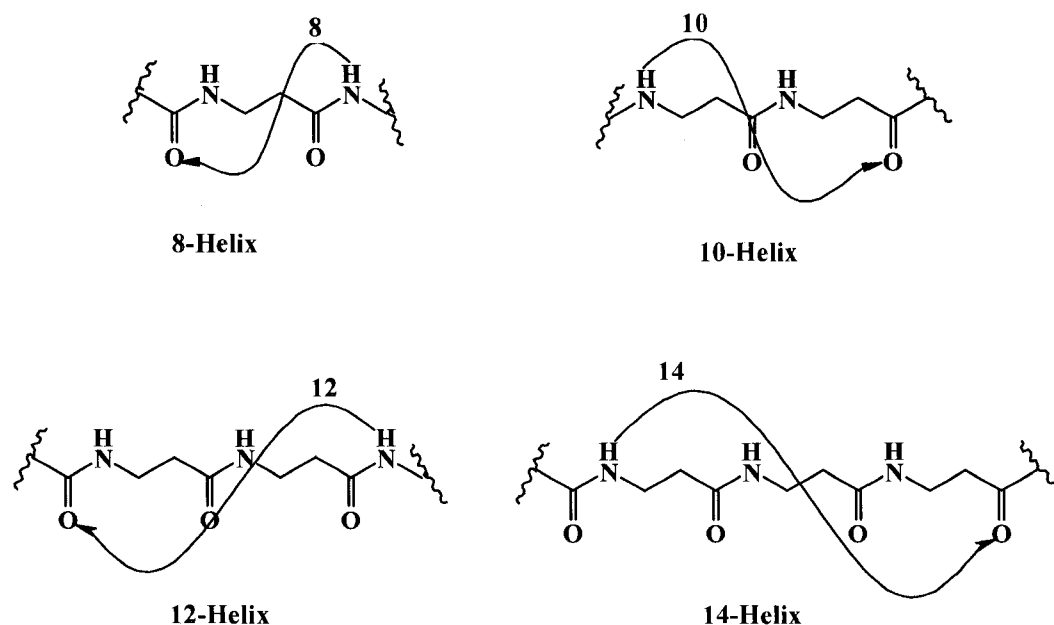


Figure 3.3 Nomenclature for β -peptide helices based on hydrogen-bonding patterns (6).

It has been shown that monosubstituted β^3 - or β^2 -peptides adopt 14-helical secondary structure and alternating β^2/β^3 -peptides prefer 10/12 helices (11). β^3 -peptides that fold into stable 14-helical conformations have received particular attention (9, 12-14) The helical secondary structure is enhanced by the presence of organic solvents, such as methanol and 2,2,2-trifluoroethanol (TFE), and efforts have been made to stabilize this conformation in aqueous solutions (15-19). Introduction of constraints like cyclic ring systems, salt-bridge formation, or neutralization of the helix macrodipole have been utilized to obtain stable helical structures in aqueous media (12, 15, 20). The finding that β -peptides are able to

adopt stable helical conformation in solution has provided a useful starting point for the design of functional mimics of natural peptides and proteins.

3.1.4 Biological Activity of β -Peptides

Natural peptides often make poor drugs and have therapeutically limited use due to their low cell permeability, high proteolytic sensitivity, and poor pharmacokinetics (21). β -peptides are more attractive than α -peptides for developing bioactive compounds because of several desirable characteristics, such as, metabolic stability against proteolytic enzymes (22) and long elimination half-lives (23). Several antibacterial β -peptides have been designed by incorporating the amphipathic helix with appropriate side chains (24, 25). Gellman's group has reported a 17-residue β -peptide (β -17) with 12-helix that possess potent antibacterial activity against a variety of Gram-positive and Gram-negative bacteria (26)

Seebach's group designed a β -peptide with β^2/β^3 motif to mimic the peptide hormone somatostatin (27). This oligomer binds to one of the somatostatin receptor subtype (hsst4) with K_D of 83 nM. Kritzer *et al.* designed a β^3 -peptide with 14-helix structure in water, that showed nanomolar activity ($K_D = 233$ nM) for hDM2 (human oncogene product double minute 2) protein, an important candidate in cancer therapy (28). More recently, English and coworkers have explored β -peptides as inhibitors of human cytomegalovirus entry (29). Finally, Gellman and colleagues have synthesized a highly cationic β^3 -decapeptide that bound TAR RNA with a K_D of 29 nM, competitively inhibiting

the Tat-TAR interaction (30). These studies and many more strongly corroborate the versatility of β -peptides as peptidomimetic therapeutic agents in diverse circumstances.

3.2 Objective

In this Chapter, we describe our efforts toward the synthesis of β^3 -peptides using a novel synthetic procedure. The synthetic strategy involves the use of easily available L-aspartic acid monomers for building up the β -peptide backbone. Using the new synthetic procedure, the syntheses of three model β^3 -hexapeptides (**6**, **7**, and **8**) was attempted. Synthesis of one of the β^3 -peptides, **6**, was accomplished successfully and sufficient peptide was purified for solution structure studies using CD and NMR spectroscopy.

3.3 Results and Discussion

3.3.1 β^3 -Peptides from L-Aspartic Acid Monomers

As mentioned above (Section 3.1.2), β^3 -peptides are typically synthesized using N-Fmoc-protected β^3 -amino acid monomers. These β^3 -amino acids are usually made from corresponding α -amino acids. The synthesis of Fmoc- β -amino acids from Fmoc- α -amino acids is non trivial and this synthetic procedure allows access to only a limited number of Fmoc- β^3 -amino acids. This also renders β^3 -amino acids extremely expensive starting materials.

To this end, our group has employed a novel synthetic strategy for the synthesis of mono-substituted β^3 -peptides using easily available L-aspartic acid

monomers that allow synthesis of β^3 -peptides with a wide variety of side chains (Figure 3.4)(31). The α -carboxy group of L-aspartic acid is left free for the

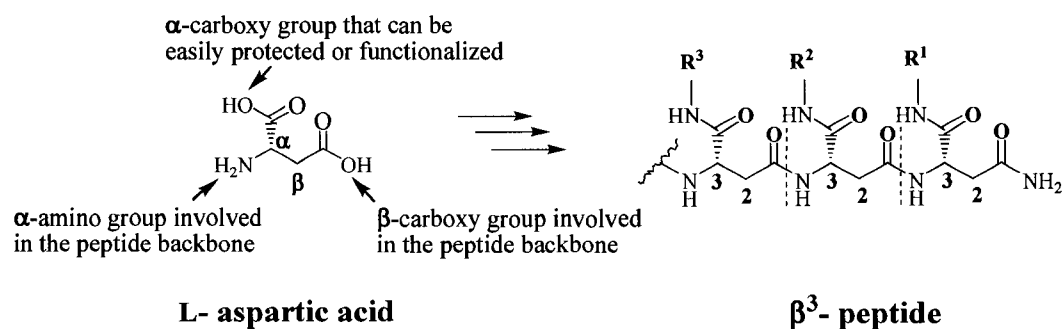


Figure 3.4 Synthesis of mono-substituted β^3 -peptides from L-aspartic acid monomers.

introduction of different substituents (to obtain heterooligomer) during the synthesis or same substituent as a final functionalization step (to obtain homooligomer), whereas, the β -carboxy group is used for building the peptide backbone. The independent buildup of the backbone and side-chain sequences leads to a very high level of synthetic versatility. Using this strategy, we attempted to synthesize three model β^3 -peptides (**6**, **7**, and **8**) with acyl-substituted side chains (Figure 3.5).

The model β^3 -hexapeptide **6** was designed to mimic a helical β^3 -hexapeptide reported by DeGrado *et al* (24). The reported β^3 -peptide adopts an amphiphilic helix with a 14-helical conformation in organic solvent (24). The presence of an additional amide bond in the side chains of **6** increases the opportunity for hydrogen bond interactions, and is speculated to provide stable secondary structure in solution for such peptides. In peptide **7**, two hydrophobic

side chains present in **6** were replaced with charged carboxylate side chains. Finally, peptide **8** was designed with side chains containing all free carboxylates. Peptides **7** and **8** were designed to study the influence of side chain substitution on the secondary structure compared to peptide **6**. While peptides **6**, **7**, and **8** were designed to establish the synthetic procedure for this novel class of β^3 -peptides, our goal is to synthesize mimics of helical α -peptides, such as peptide **5**, identified in chapter 2, using this pathway.

β^3 -hexapeptides were synthesized utilizing an Fmoc/Allyl or Fmoc/tBu combined solid-phase strategy (Scheme 3.1), where Fmoc protection was used to build the backbone of the peptide and Allyl or tBu protection was used to introduce the side chain functionalities. The same strategy allowed the synthesis

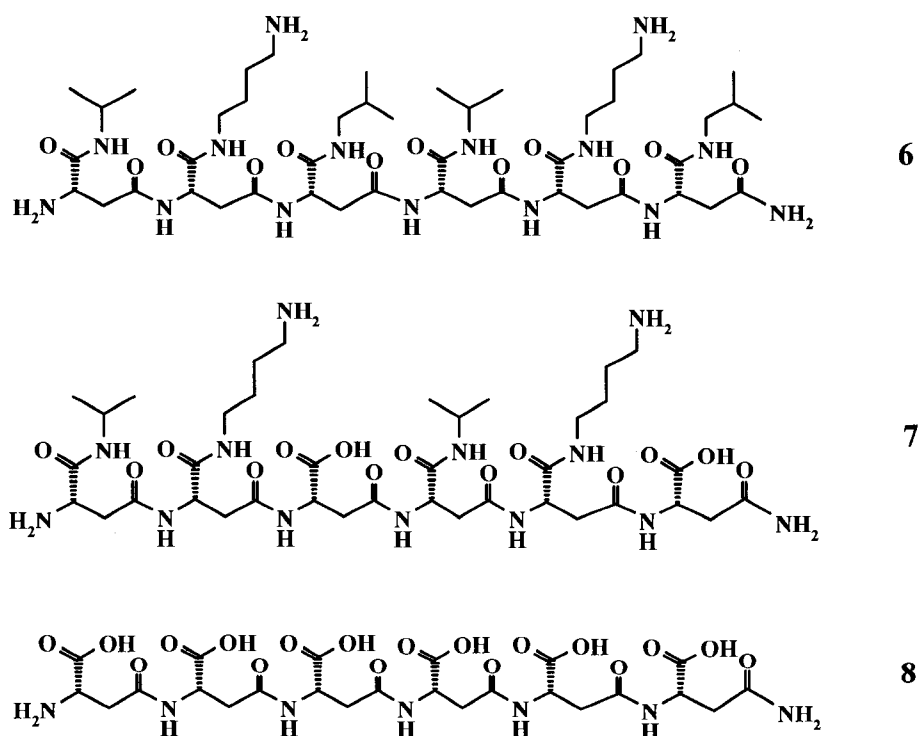
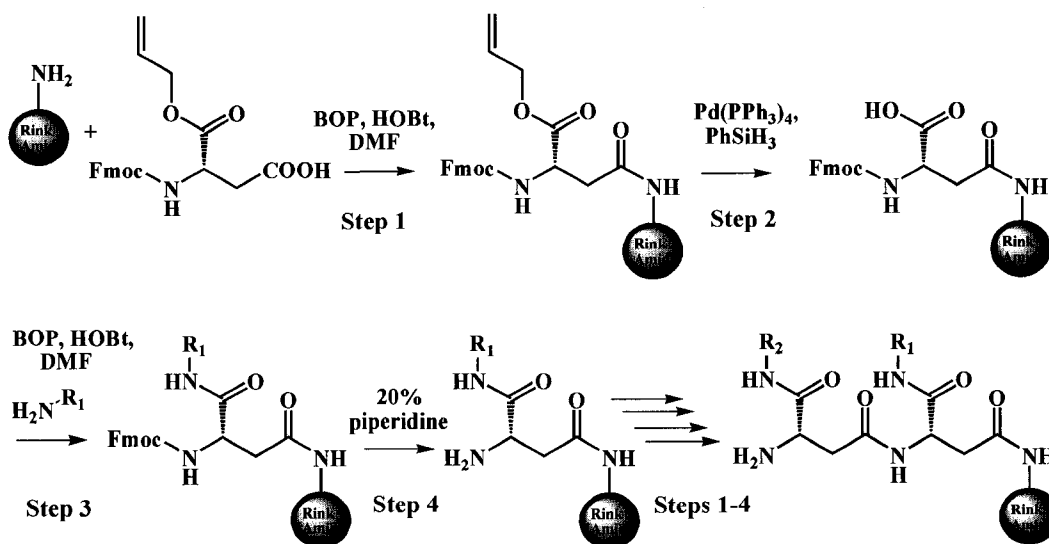


Figure 3.5 The chemical structures of β^3 -hexapeptides **6**, **7**, and **8**.

of either heterooligomeric β -peptides, such as **6** and **7** or homooligomeric β -peptides (e.g. **8**). In heterooligomeric β -peptides **6** and **7**, the different side chains were introduced after coupling of each monomer and deprotection of the side chain carboxy group. Two of the side chains were chosen with a free amino group (lysine side chain mimic) to keep a balance between both the hydrophobic and the charged groups and enhance solubility in aqueous medium. In the case of β -peptide homooligomer **8**, the backbone was synthesized first, and all the side chain protections (allyl or tBu) were removed in the end.

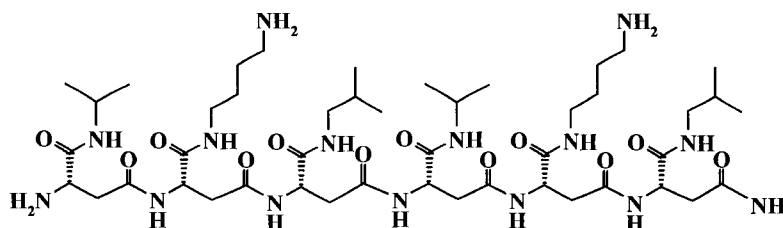
Using the above mentioned synthetic approach, the synthesis of β^3 -peptide **6** was completed and purified peptide was used for three-dimensional structure elucidation using NMR spectroscopy. Unfortunately, the synthesis of β^3 -peptides



Scheme 3.2 General pathway of solid phase synthesis of β^3 -peptides from L-aspartic acid.

7 and 8 was not accomplished. The details of the synthesis of each peptide are discussed below.

3.3.2 Synthesis of β^3 -Hexapeptide 6 using Orthogonally Protected L-Asp



6

The backbone of β^3 -peptide 6 was prepared from orthogonally protected L-aspartic acid, N^{α} -Fmoc-L-aspartic acid α -allyl ester using BOP with HOBT on Rink amide MBHA resin (Scheme 3.2). The reaction was monitored by the ninhydrin test. The side chain was deallylated followed by the introduction of the corresponding amine using the same coupling reagents as mentioned above. To achieve complete deallylation of the side chain carboxyl, the reaction was optimized by (i) varying the amount of palladium catalyst used, (ii) the length of the reaction time, and (iii) the number of times the reaction was repeated (Table 3.1). Treatment with 0.08 equivalents of $\text{Pd}(\text{PPh}_3)_4$ and 8 equivalents of PhSiH_3 for 35 minutes and repeating the reaction twice led to complete deallylation. During optimization, the reaction was monitored by test cleavage followed by mass spectrometric analysis.

The synthesis of β^3 -hexapeptide 6 on solid phase was completed by coupling L-aspartic acid six times along with the addition of appropriate side chain amine after every amino acid coupling. At the end of the synthesis, and

Table 3.1: Deallylation of the allyl group from side chain carboxylic acid.

Time (min) x the number of times the reaction was repeated	No of equiv. of (Pd(PPh₃)₄)	Deallylation (%)
35 x 1	0.08	20
60 x 1	0.16	95
15 x 2	0.16	45
20 x 2	0.16	65
30 x 2	0.08	30
15 x 3	0.08	30
35 x 3	0.08	>99

after the removal of the terminal Fmoc group, β -peptide **6** was cleaved from the resin using TFA/H₂O/silane at room temperature for 2 hours. Crude peptide was purified using semi-preparative reverse phase HPLC with an overall yield of 53%. The identity and purity of **6** were assessed by analytical HPLC (Figure 3.6) and electrospray ionization mass spectrometry (Figure 3.7). Pure peptide eluted as a single peak at 23 minutes on a C8 analytical HPLC column as shown in (Figure 3.6). The mass of this peak was found to be 1040.5 [M+H]⁺ (calcd ([M+H]⁺ 1040.0), as determined by using electrospray ionization mass spectrometry (Figure 3.7).

¹H-NMR of **6** further confirmed the purity and identity of the peptide. An NMR sample of **6** in trifluoroethanol (CF₃CD₂OH) displayed well dispersed peaks (Figure 3.8) and the chemical shifts for all the peaks were assigned (see Experimental Section).

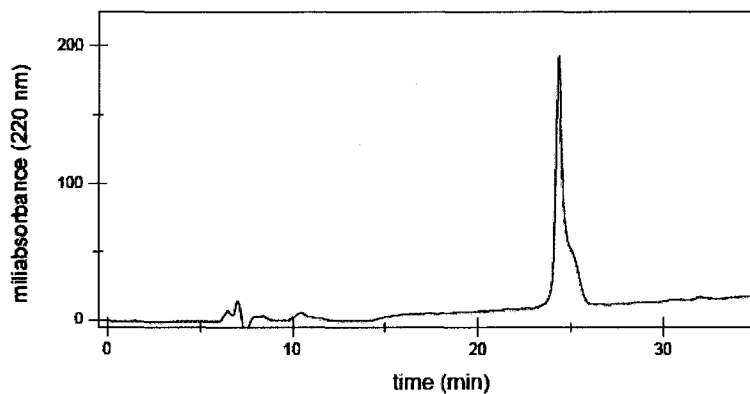


Figure 3.6 RP-HPLC chromatogram of β^3 -hexapeptide **6**. (C8 VYDAC HPLC column, 0.46 x 25 cm, 5 μ m, flow rate = 1 ml/min, gradient of 10-40 % CH₃CN in 0.05% aqueous TFA over a period of 40 min).

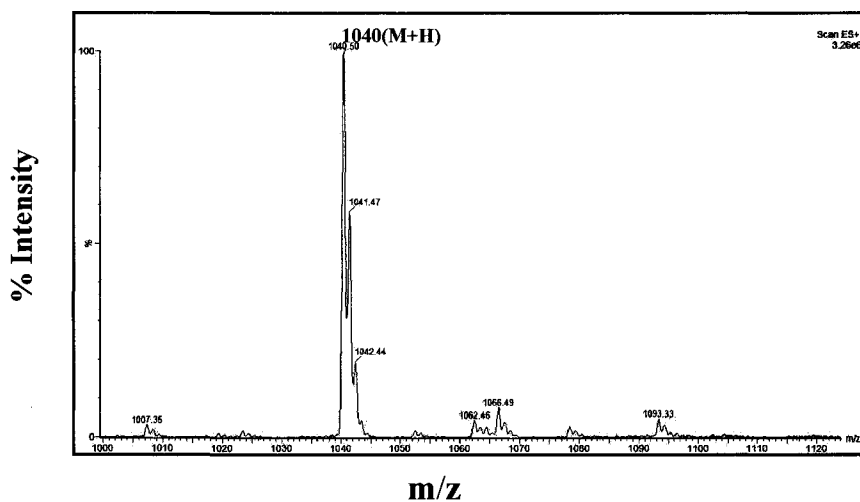


Figure 3.7 Electrospray mass spectrum of pure β^3 -hexapeptide **6**.

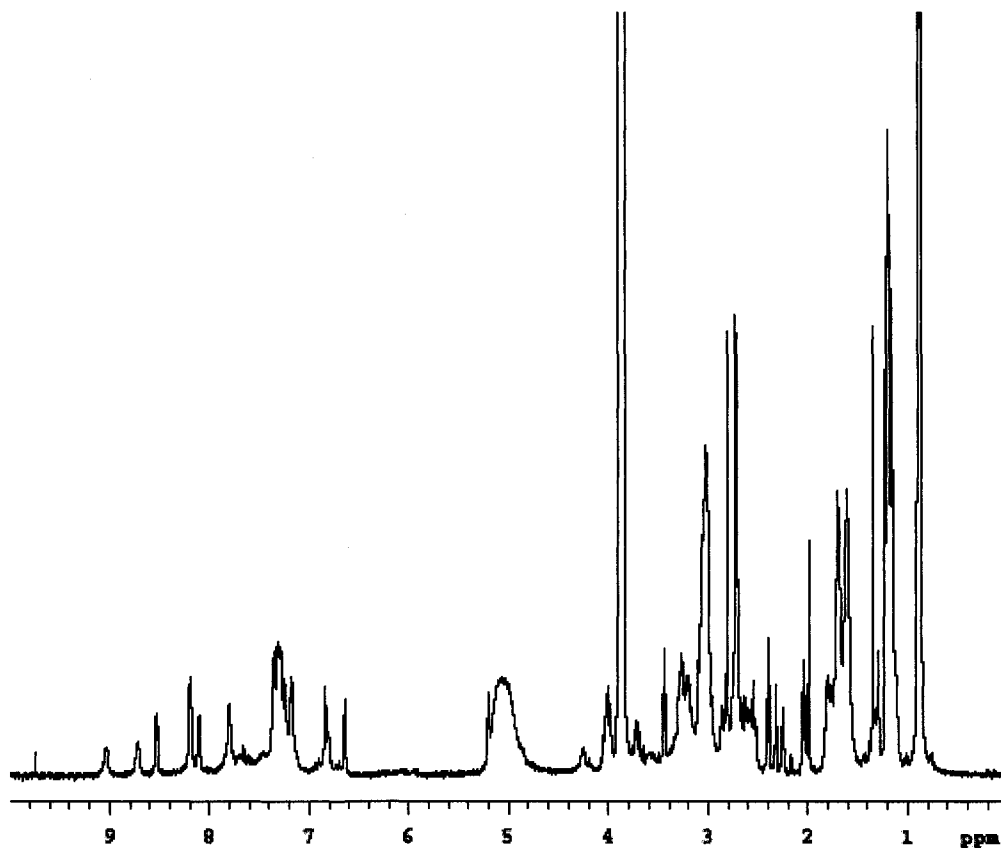


Figure 3.8 $^1\text{H-NMR}$ (500 MHz) spectrum of β^3 -peptide **6** in $\text{CF}_3\text{CD}_2\text{OH}$.

3.3.3 Solution Conformation of β^3 -Hexapeptide **6**

3.3.3.1 Circular Dichroism of **6**

The ability of the β^3 -peptide **6** to adopt an ordered secondary structure was evaluated by CD spectroscopy in four different solvents, namely, TFE, methanol, water, and phosphate buffer (pH 7.4). Peptide was studied at different concentrations (100-500 μM), and the CD spectra were found to be independent of concentration, suggesting that no changes in aggregation state occur in this concentration range. The CD spectra of **6** display a marked difference in organic

solvents (TFE and methanol) and aqueous solvents (water and phosphate buffer). In TFE, there is a minimum at 214 nm ($\Theta = -20 \times 10^3$) and a maximum at 204 nm (Figure 3.9). Similarly, in methanol there is a minimum at 214 nm; however, this peak is not present in aqueous solvents.

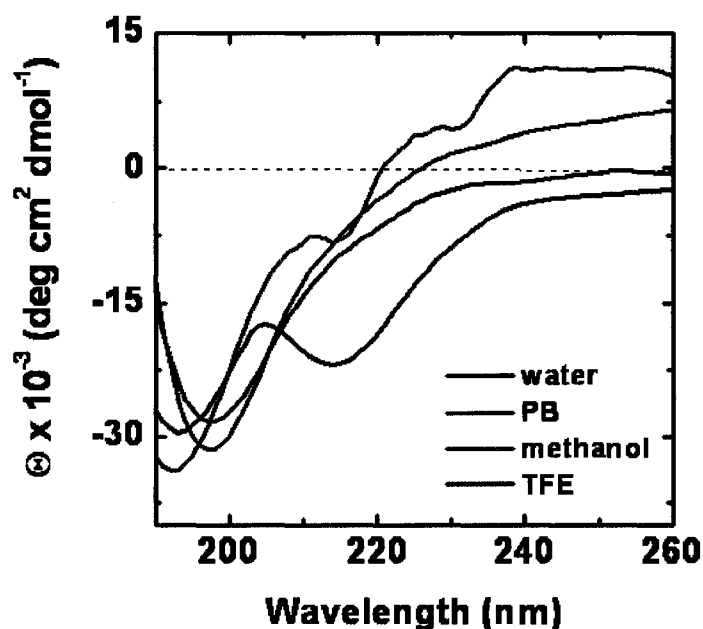


Figure 3.9 Circular dichroism spectra of **6** in water, phosphate buffer (1 mM, pH 7.4), methanol, and TFE at 25 °C.

Organic solvents like TFE and methanol have been suggested to be conducive to secondary structure formation (19, 32) and the CD spectra of **6** suggest gain of some structural feature in organic solvents. The CD spectra of monosubstituted β^3 -peptides typically display a negative minimum at 214-220 nm and a positive maximum near 200 nm that have been ascribed to 14-helical structure (12, 15, 20) β -peptide **6** is different from the reported β -peptide (6, 12, 15, 20), as it contains an extra amide group in the side chain and the CD of this

peptide measures the collective signal of all the amides, including those within the side chain making the spectrum difficult to interpret. Therefore, high resolution structure is required to fully interpret the CD results.

3.3.3.2 NMR Spectroscopy of **6**

The 1D NMR spectrum of **6** in TFE (Figure 3.10) and preliminary 2D NMR experiments suggested the presence of helical structure and one major conformational isomer. The well dispersed chemical shifts in the amide region allowed assignment of all the backbone and side chain protons (Figure 3.10 top). In this context, it is of particular interest to note that Fernandez-Santin *et al.* observed a helical structure for a β^3 -polypeptide, poly(α -isobutyl-L-aspartate), made by polymerization of α -isobutyl-L-aspartate based on X-ray diffraction and molecular modeling studies (33). This also supported our initial conjecture regarding the helical nature of β^3 -peptides from L-aspartic acid. However, for complete three dimensional structure elucidation of β^3 -peptides, such as **6**, detailed NMR studies are required.

6 lost all the secondary structure in water as evidenced by the limited dispersion of amide chemical shifts in NMR (Figure 3.10 bottom). Aspartic acid derived β^3 -peptides are expected to be more soluble than the “normal” β^3 -peptides. Therefore, **6** should be less prone to self-association in water compared to analogous sequences with similar distribution of hydrophobic side chains as shown by Gellman and coworkers (34).

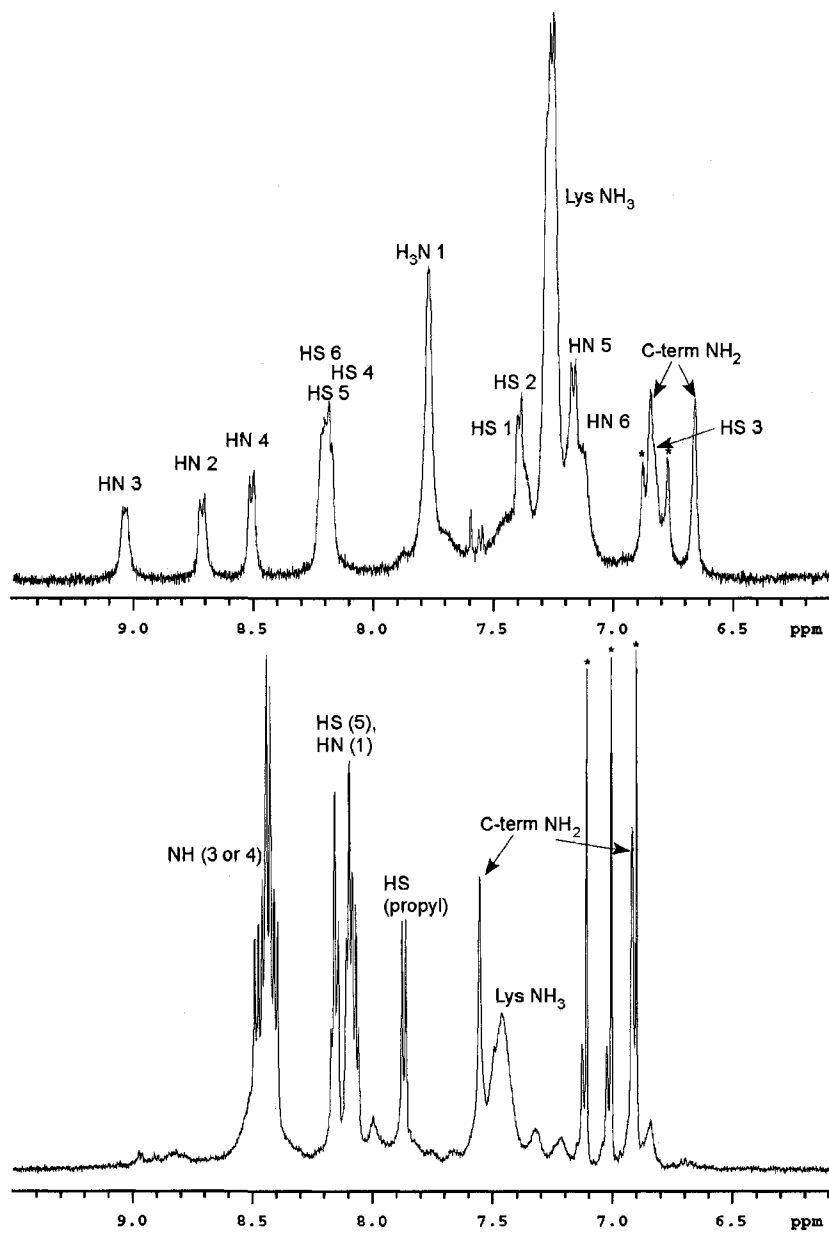


Figure 3.10 1D NMR of β^3 -peptide 6 showing the amide H-atoms in 100% TFE- d_2 (top) and 90% H₂O/10% D₂O (bottom). HN refers to the backbone amide proton and HS refers to the one in the side chain. The number in the parentheses is for the number of overlapping peaks and impurities are marked with *.

3.3.3.3 Solution Structure of **6**

β^3 -Peptides synthesized from L-aspartic acid monomers contain an extra amide bond in the side chain of the β -peptide scaffold making them more polar than the previously reported β -peptides (Figure 3.11). However, this extra amide bond provides opportunities for more hydrogen-bonding capabilities and is speculated to give unprecedented secondary structure in this class of β -peptides. Furthermore, the stereochemistry at the β^3 carbon is opposite in these two classes of β^3 -peptides (Figure 3.11).



Figure 3.11 Chemical structure of β^3 -peptide from L-aspartic acid monomers (left) and β^3 -peptides from β^3 -amino acids derived from natural L-amino acids (right).

A two-dimensional NOESY experiment of **6** performed at 10°C in CF_3CD_2OH showed multiple (five out of six possible) long-range $C_\alpha H(i) \rightarrow C_\beta H(i+3)$ NOEs (protons at β -carbon are not stereospecifically assigned) (see Appendix B, Figure B.1). These peaks are a hallmark of 14-helical secondary structure (14, 17). A three-dimensional structure of **6** was obtained using the NOE data (see Appendix B, Figure B.3) and the program CYANA (35) as described in the Experimental section. The pdb coordinates of the 10

structures (rmsd of all backbone atoms $0.47 \pm 0.11 \text{ \AA}$) obtained from CYANA were averaged to obtain final structure of **6** in TFE (Figure 3.12).

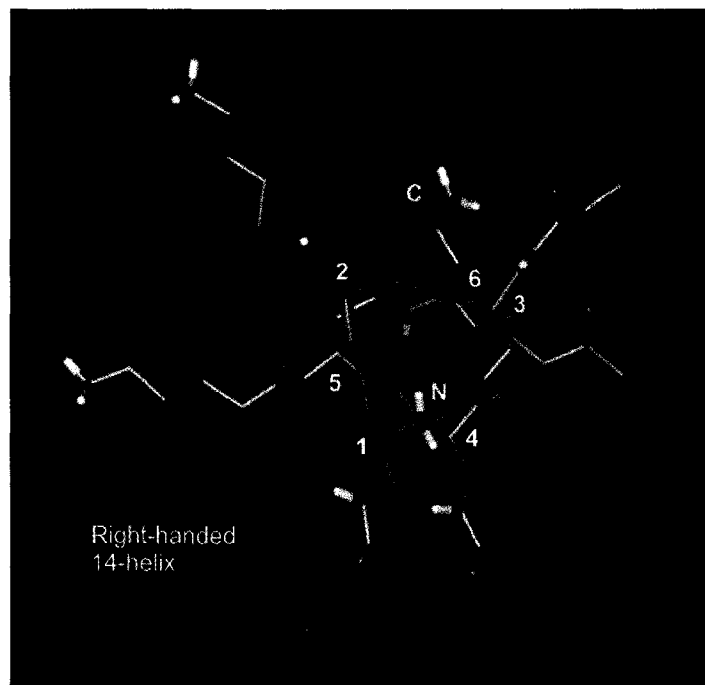


Figure 3.12 Solution structure of β^3 -hexapeptide **6** in TFE obtained by NMR spectroscopy.

β^3 -hexapeptide **6** forms a *right-handed* 14-helical structure with a radius of 2.6 \AA and 4.69 \AA rise/turn. In contrast, the reported β^3 -peptides formed from β^3 -amino acids derived from naturally occurring L-amino acids form left-handed 14 helices (6, 36). The difference in the conformation of the two helices (right-handed versus left-handed) could be due to the opposite stereochemistry at the β^3 carbon in the peptide backbone. The radius and the pitch for the two helices are found to be similar (6, 7). The right-handed 14-

helical conformation of **6** is a better mimic of right-handed α -helix of α -peptides (Figure 3.13).

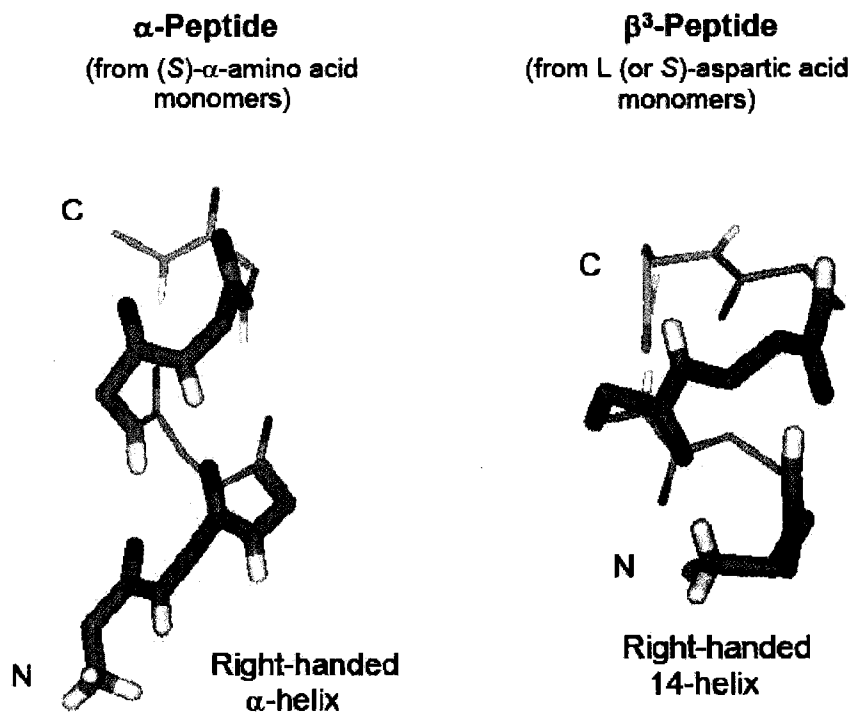
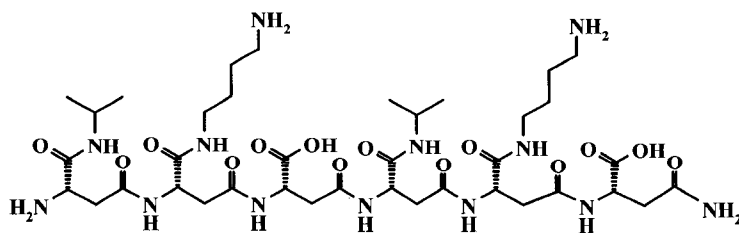


Figure 3.13 Backbone conformation of right-handed α -helix in an α -peptide and 14-helix in a β -peptide from L-aspartic acid monomers. N and C stand for N- and C-terminus of the peptides, respectively.

3.3.4 Synthesis of β^3 -Hexapeptide **7** at Ambient and Elevated Temperatures



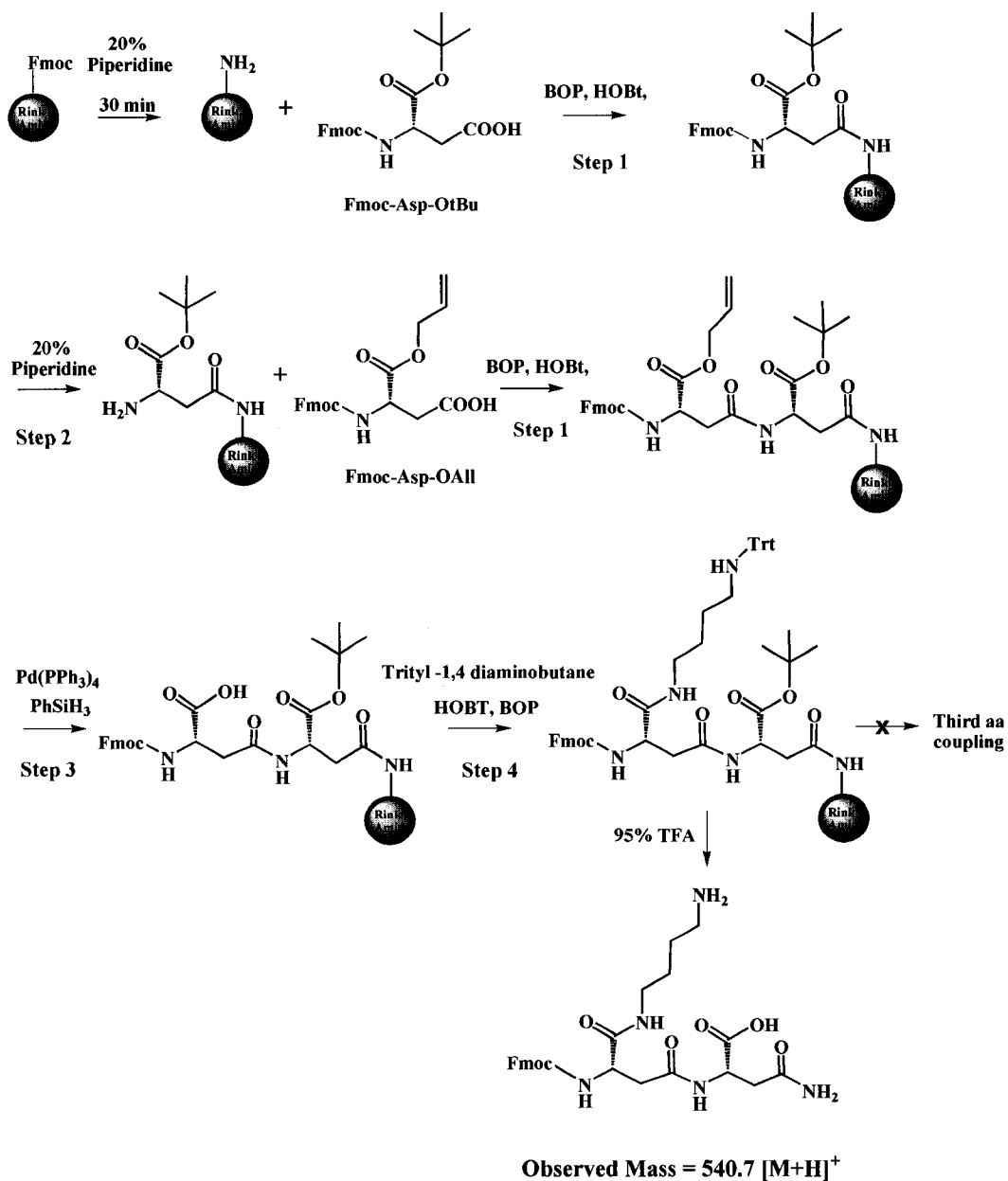
7

Another model peptide, β^3 -hexapeptide **7**, was designed to be synthesized using the same synthetic strategy as discussed above from L-aspartic acid monomers. The steps involved in the synthesis of **7** were essentially the same as for β^3 -peptide **6**, except for the addition of residues 1 and 4. For residues 1 and 4, the side chains were left as free carboxylates and can be introduced using N- α -Fmoc-L-aspartic acid α -t-butyl ester. The t-butyl protection can be removed at the end during acid cleavage of the peptide from the resin.

Synthesis of **7** was carried out on MBHA resin, and BOP with HOBT was used for coupling orthogonally protected L-aspartic acid (Scheme 3.3). A test cleavage was performed after the addition of each amino acid and coupling was confirmed by mass spectrometric analysis.

Mass analysis after the addition of second amino acid confirmed the presence of Fmoc-dipeptide (calcd. $[M+H]^+$ 540.0, observed $[M+H]^+$ 540.07) by electrospray ionization mass spectrometry. After the removal of Fmoc group, several attempts were made to couple the third amino acid. The test cleavage showed the presence of neither the starting material nor the product.

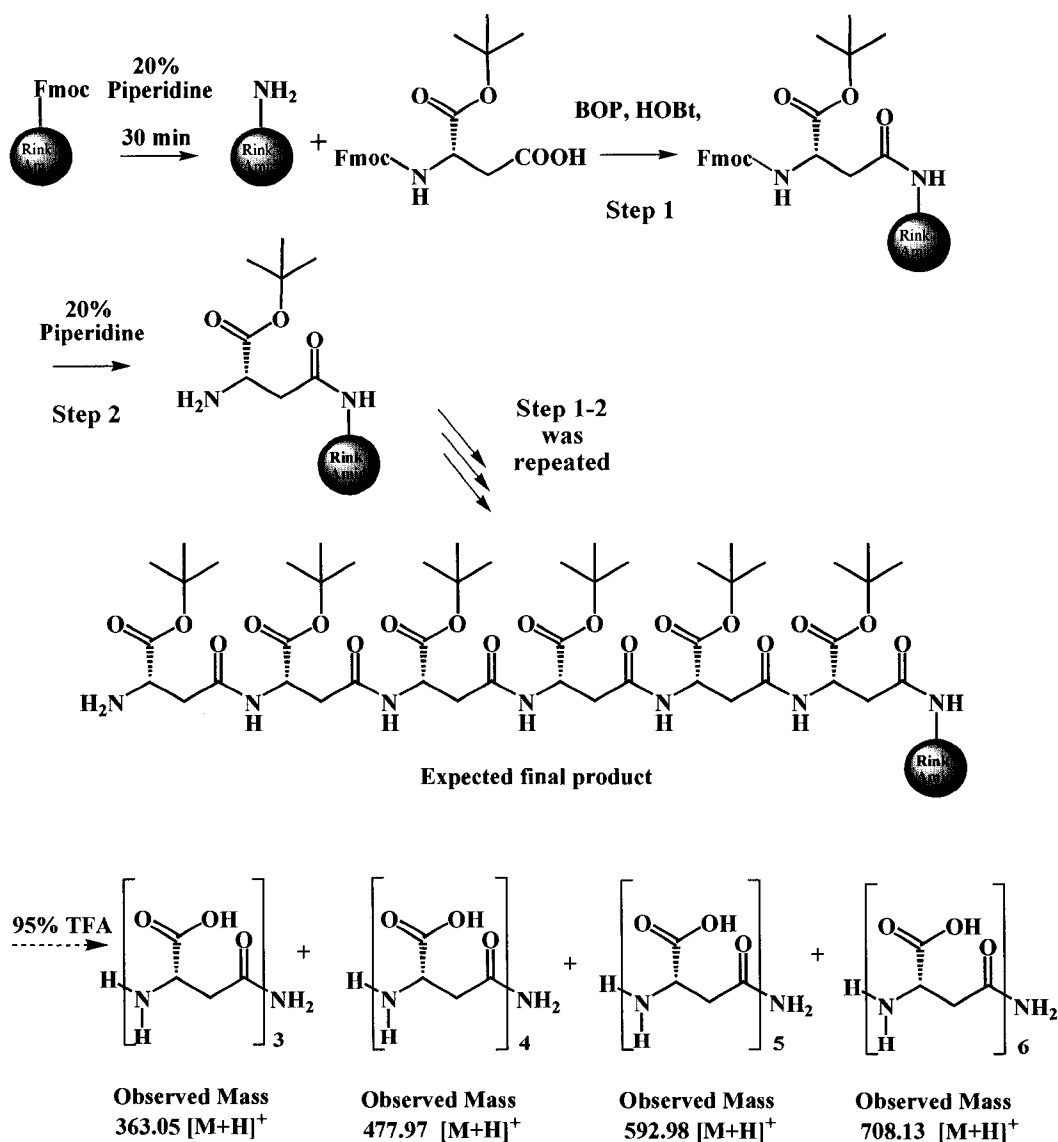
Gellman and co-workers reported that both microwave and conventional heating (oil bath at 60 °C) provided a method for rapid synthesis of β -peptides with high-purity. Moreover, they showed that the heat and LiCl worked synergistically during coupling and deprotection of the Fmoc-amino acids on the solid phase and provided a product up to 85% purity (37). Accordingly, the synthesis of peptide **7** using elevated temperatures was attempted. The coupling and deprotection steps involved in the buildup of the backbone were



Scheme 3.3 Synthesis of heterooligomeric β^3 -hexapeptide **7** at room temperature.

performed at 60 °C, whereas, the steps involved for the addition of the side chains were done at room temperature. Unfortunately, the synthesis at elevated temperature did not yield even the dipeptide. A test cleavage after the addition of side chain amine (trityl 1, 4 diaminobutane) for the second amino acid showed the

The mass spectrum of the complete sequence showed the presence of the final product with mass of 708.13 (calcd. 708.0, $[M+H]^+$), along with three truncated peptides, namely, tripeptide, tetrapeptide, and pentapeptide, with mass of 363.05 (calcd. 363.0, $[M+H]^+$), 477.97 (calcd. 478.0, $[M+H]^+$), and 592.98, $[M+H]^+$ (calcd. 593.0, $[M+H]^+$), respectively. The appearance of the truncated



Scheme 3.5 Synthesis of homooligomer β^3 -peptide **8** using Fmoc-Asp-OtBu.

peptides could be due to the incomplete coupling. More optimization of the coupling time along with a test cleavage after each amino acid coupling may lead to the completion of the sequence.

3.4 Summary

We report a solid phase synthesis method for the preparation of novel β^3 -peptides derived from L-aspartic acid monomers. The methodology allows independent buildup of the β -peptide backbone and the introduction of sequential side chain substitutions. Attempts were made to synthesize three representative peptides, namely, **6**, **7**, and **8** using this methodology. β^3 -hexapeptide **6** was synthesized, purified, and fully characterized. The synthesis of **7** and **8** was completed only up to the dipeptide and tripeptide, respectively, due to the unsuccessful coupling of the subsequent amino acids.

β^3 -peptides obtained from L-aspartic acid monomers contain an additional amide bond in the side chain that provides opportunities for additional hydrogen bonds and is speculated to give unprecedented secondary structures in this class of β -peptides. CD and NMR spectroscopy were used to study the solution conformation of **6** in TFE and water which suggested the presence of solvent-dependent secondary structure. Three dimensional NMR solution structure of **6** in TFE was obtained. **6** forms a right-handed 14-helical structure in TFE. This helical conformation is same as the 14-helical conformation for the β^3 -peptides which do not have an additional amide bond in the side chain. However, **6** forms a right-handed helix and the β^3 -peptides obtained from the β^3 -amino acids derived

from L-amino acids form left-handed helices, most likely due to the opposite stereochemistry at the β^3 carbon in the peptide backbone. These results will facilitate the design of β^3 -peptides that mimic biologically active α -peptides, such as the helical peptide (5) that binds HCV-E2 discussed in Chapter 2.

3.5 Experimental Section

3.5.1 General

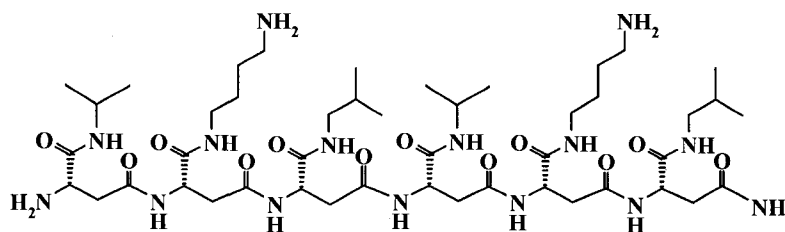
Solvents and reagents: Rink amide MBHA resin (0.58 mmol/g), N- α -Fmoc-L aspartic acid α -allyl ester, mono-trityl 1,4-diaminobutane acetic acid salt, BOP, and HOBt were purchased from NovaBiochem (San Diego, CA). Isobutyl amine, isopropyl amine, methylamine, phenylsilane, and triisopropylsilane were purchased from Sigma Chemical Co. (St. Louis, MO, USA). N-methyl morpholine (NMM) and trifluoroacetic acid (TFA) were purchased from Aldrich, while piperidine was purchased from Caledon (Canada). All other reagents were purchased from Sigma-Aldrich. All commercial reagents and solvents were used as received.

Peptide syntheses were performed manually in polypropylene peptide synthesis vessel with frit at the bottom and screw cap with a septum at the top for addition of reagents. Solvents and soluble reagents were removed by suction.

Equipment: RP-HPLC purification and analysis were carried out on a Waters (625 LC system) HPLC system using Vydac semi-preparative C18 (1 x 25 cm, 5 μ m) and analytical C8 (0.46 x 25 cm, 5 μ m) columns. Compounds were detected by UV absorption at 220 nm. Mass spectra were recorded on a MALDI

Voyager time-of-flight (TOF) spectrometer (Voyager™ Elite) or electrospray ionization mass spectrometry on a Waters micromass ZQ spectrometer, Faculty of Pharmacy and Pharmaceutical Sciences, University of Alberta, Edmonton. CD measurements were made on an Olis CD spectrometer (Georgia, USA) at 25 °C in a thermally controlled quartz cell over 190-260 nm. NMR experiments were recorded on a Varian INOVA 500 MHz NMR spectrometer equipped with a triple-resonance HCN Cold Probe with z-axis pulsed field gradients, at the Quebec/Eastern Canada High Field NMR Centre, McGill University, Montreal, Quebec. The CD measurement was made on an Olis CD spectrometer (Georgia, USA) at 25 °C in a thermally controlled quartz cell over 190-260 nm, Department of Chemistry, University of Alberta, Edmonton, Alberta, Canada.

3.5.2 Synthesis of β^3 -Hexapeptide 6



6

Rink amide resin (145 mg, 0.1 mmol), washed with DCM, DMF, and IPA twice each, was swelled in DMF for 30 min at room temperature. After addition of 20% piperidine in NMP (3 ml), the mixture was stirred for 30 min. The resin was washed with DCM twice, drained for 5 min, again washed with DCM, DMF, and IPA twice each, and was swelled in DMF for 10 min. N- α -Fmoc-L-aspartic

acid α -allyl ester (79 mg, 0.2 mmol) was activated by addition of BOP (86 mg, 0.2 mmol), HOBt (27 mg, 0.2 mmol), and NMM (50 μ l, 0.45 mmol) in DMF (1 ml) and the mixture was allowed to stand for 5 min. The preactivated amino acid was added to the resin and the amino acid was allowed to couple to the resin for 2.5 hr at room temperature. Following extensive washing of the resin with DCM, DMF, and IPA (twice each), it was swelled in DMF for 10 min under nitrogen.

Palladium catalyzed deprotection of the side chain allyl from carboxyl group (All) was done under nitrogen. PhSiH₃ (99 μ l, 0.8 mmol) in NMP (1 ml) was added to Pd(PPh₃)₄ (9.2 mg, 0.08 mmol) preweighed in a vial and the solution was flushed with nitrogen. Palladium solution was transferred to the resin using a steel cannula, and the resulting resin suspension was stirred under nitrogen for 30 minutes. The resin was washed and the deprotection step was repeated two more times. Following deprotection of the side chain allyl, coupling of the carboxyl was carried out using corresponding amine (RNH₂, 5 equiv) and the same coupling agents as above for 6-8 h at 25 °C. The resin was washed with DMF and DCM followed by removal of the N ^{α} -Fmoc group and the sequence of reactions was repeated to complete the synthesis of **6**. The details for the reactions times for coupling and deprotection of the side chain as well as the peptide backbone are listed in Table 3.2.

β^3 -hexapeptide **6** was cleaved from the resin using cleavage reagent (5 ml, 95:2:3, TFA/H₂O/triisopropylsilane) at room temperature for 2 hours and then washing the resin with the cleavage reagent (2 x 2 min, 3 ml). The cleaved peptide was collected, combined with TFA washes, and concentrated by rotary

Table 3.2: Coupling and deprotection times for the synthesis of β^3 -hexapeptide **6**.

aa	Fmoc-Asp-OAll coupling	Allyl deprotection	RNH ₂ coupling	Time (hr)	Fmoc- deprotection
	Time (hr)	Time (min)	Amine		Time (min)
First	2.5	30 x 3	Isobutylamine	4 x 3	15 x 2
Second	3.5	30 x 3	Trityl 1, 4 diaminobutane	4 x 3	16 x 2
Third	3.5	30 x 4	Isopropylamine	5 x 3	16 x 2
Fourth	3.5	30 x 4	Isobutylamine	5 x 3	15 x 3
Fifth	4	30 x 5	Trityl 1, 4 diaminobutane	5 x 3	15 x 3
Sixth	3 x 2	30 x 5 40 x 2	Isopropylamine	5 x 3	15 x 3

evaporation. Cold diethyl ether (~ 10 ml) was added to precipitate the crude cleaved peptide. The cleaved peptide was collected, combined with TFA washes, and concentrated by rotary evaporation. Cold diethyl ether (~ 10 ml) was added to precipitate the crude cleaved peptide. The peptide was collected upon centrifugation and decantation of the ether. The crude peptide was reconstituted in 30% CH₃CN and purified on a semipreparative Vydac C18 HPLC column (10 x 250 mm, flow rate = 2 ml/min, monitored at 220 nm) using a gradient of 10-40 % CH₃CN in 0.05% aqueous TFA over a period of 40 min. The identity and purity of the hexapeptide **6** were assessed by analytical HPLC (Figure 3.6) and electrospray ionization mass spectrometry (Figure 3.7). ¹H NMR [CF₃CD₂OH, 500 MHz]: δ 0.83-0.96 (m, 12H, isovaleric methyls), 1.12-1.28 (m, 12H, isopropyl methyls), 1.56-1.69 (m, 8H, two side chain CH₂ linkages to amine, CH₂CH₂CH₂CH₂NH₂), 1.7-1.85 (m, 2H, two isovaleric CH), 2.5-2.85 (m, 12H,

backbone CH₂), 2.9-3.1 (m, 4H, two isovaleric CH₂), 2.95-3.05 (m, 4H, two side chain methylenes CH₂CH₂CH₂CH₂NH₂), 3.15-3.32 (m, 4H, two side chain methylenes CH₂CH₂CH₂CH₂NH₂), 3.95-4.1 (m, 2H, two isopropyl CH), 4.2-4.28 (m, 1H, backbone CH N-terminal), 4.85-5.25 (m, 5H, backbone CH), 6.67 (s, 1H, carboxamide), 6.84-6.92 (m, 1H, side chain isovaleric NH), 7.22 (d, 1H, J= 7.4 Hz, backbone amide), 7.27-7.42 (m, 3H, one backbone NH, one side chain NH, and one carboxamide NH), 7.45 (d, 1H, J=7.3 Hz, isopropyl side chain NH), 7.8-7.88 (m, 1H, backbone amide), 8.18 (d, 1H, J=7.4 Hz, isopropyl side chain NH), 8.21-8.32 (m, 2H, side chain amides), 8.57 (d, 1H, J= 8.78 Hz, backbone amide), 8.78 (d, 1H, J= 7.7 Hz, backbone amide), 9.06-9.14 (m, 1H, backbone amide) (Figure 3.8). . MALDI-TOF calcd for C₄₆H₈₅N₁₅O₁₂, [M + H]⁺ 1040.00; found [M + H]⁺ 1040.50 and [M + Na]⁺ 1062.46; overall yield 53%.

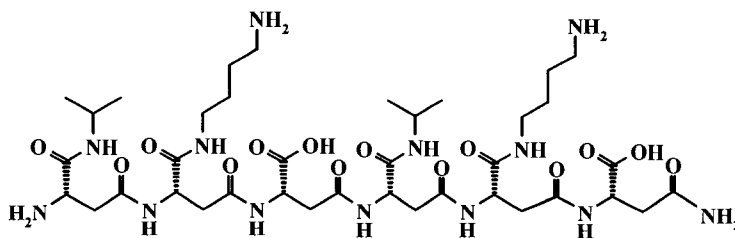
3.5.2.1 Circular Dichroism of β³-Hexapeptide 6

The stock solution of the β-peptide was diluted with different solvents, namely, water, phosphate buffer (1 mM, pH 7.4), methanol, and TFE to obtain final concentrations of 100, 250, and 500 μM for CD measurements (Figure 3.9). The length of the cuvette used was 0.02 cm and number of scans was set to 10. All CD scans were performed at 25 °C and the blank reading was subtracted from the sample data at the end. The CD data were normalized and expressed in terms of mean residue ellipticity (deg cm² dmol⁻¹).

3.5.2.2 2D NMR and Structure Elucidation of β^3 -Hexapeptide 6

Two-dimensional NMR measurements and structure elucidation was done in collaboration with Dr. Tara Sprules (Quebec/Eastern Canada High Field NMR Centre, McGill University, Montreal, Quebec). A 1.5 mM sample of **6** in 100% TFE-d₂ (CF₃CD₂OH) (Cambridge Isotope Laboratories, Inc.) was prepared for 2D NMR experiments. Sequence specific assignments were established by following the procedures used for α -amino acid peptides (38). 2D TOCSY (60 ms mixing time), COSY and NOESY (mixing time 100, 200 and 300 ms) spectra were recorded at 10°C on a Varian INOVA 500 MHz spectrometer at McGill University. 153 upper distance restraints for structure calculations were obtained from a 300 ms mixing time 2D-[¹H,¹H]-NOESY recorded at 10°C on a Varian INOVA 800 MHz NMR spectrometer, equipped with an HCN cold probe and pulsed-field gradients. Calculation of the complete three-dimensional structure was performed with the program CYANA v 2.1(35). Input data and structure calculation statistics are summarized in Tables B.2 and B.3 (Appendix B). The final calculation was started with 200 randomized conformers all of which converged to the helical conformation (average backbone RMSD to mean for 200 structures: 0.61 ± 0.21 Å). A bundle of the 10 lowest energy CYANA conformers were used to represent the NMR structure (Figure 3.12).

3.5.3 Synthesis of Heterooligomeric β^3 -Peptide 7



7

3.5.3.1 Solid Phase Synthesis of 7 at Room Temperature

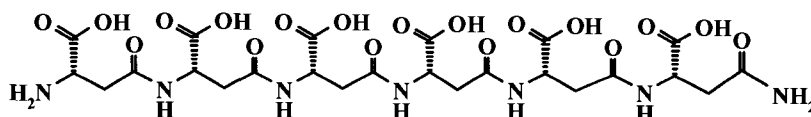
Rink amide resin (172.4 mg, 1 mmol) was washed and deprotected as before. N- α -Fmoc-L-aspartic acid α -allyl ester or Fmoc-Asp-OtBu (82.3 mg, 0.2 mmol) was activated by addition of BOP (86 mg, 0.2 mmol), HOBT (27 mg, 0.2 mmol), and NMM (50 μ l, 0.45 mmol) in NMP (1 ml). The amino acid mixture was allowed to stand for 5 minutes and was then added to the resin. The amino acid was allowed to couple for 2.5 hr. After washing the resin, Fmoc group was deprotected. The second amino acid was coupled by addition of Fmoc-Asp-OAll (79 mg, 0.2 mmol) activated with BOP (86 mg, 0.2 mmol), HOBT (27 mg, 0.2 mmol), and NMM (50 μ l, 0.45 mmol) in NMP (1 ml). The mixture was stirred for 2.5 hr, followed by washing and deprotection of the side chain allyl group. Palladium catalyzed deprotection was repeated three times to ensure complete deallylation. The resin was washed, and BOP (44.2mg, 0.1 mmol), HOBT (14 mg, 0.1 mmol), and NMM (33 μ l, 0.3mmol) in NMP (1 ml) were added to activate the free side chain carboxyl. To this mixture, trityl 1, 4 diaminobutane (100 mg, 0.3 mmol) was added and allowed to stir for 4 hr at room temperature. Resin was washed and the amine was coupled twice again (4 hr each). A test cleavage

confirmed the presence of the di-peptide of mass found to be (540.07, $[M+H]^+$), same as the calculated mass (540.0, $[M+H]^+$), as determined by electrospray ionization mass spectrometry (Scheme 3.3). The third amino acid was added following the same procedure as above; however, the test cleavage did not show the presence of any product or the starting material. The synthesis was discontinued at this stage.

3.5.3.2 Solid Phase Synthesis of 7 at Elevated Temperature

The synthesis of 7 was repeated at 60 °C following the same procedure as above (Section 3.5.5.1), except the side chain allyl deprotection and amine coupling were done at room temperature. During all the coupling steps at elevated temperatures, 0.8 M LiCl in NMP was added. A test cleavage after the dipeptide showed the presence of some starting material (allyl deprotected dipeptide of mass found to be (470.06, $[M+H]^+$), same as the calculated mass (470.0, $[M+H]^+$), as determined by electrospray ionization mass spectrometry. Therefore, coupling of the amine (trityl 1, 4 diaminobutane) was repeated three more times (4 hr x 3) with no success. At this point the synthesis was discontinued.

3.5.4 Synthesis of Homooligomeric β^3 -Peptide 8



8

3.5.4.1 Solid Phase Synthesis of **8** using Fmoc-Asp-OAll.

The synthesis of **8** was performed following the same procedure as for β^3 -peptide **6**. Briefly, Rink amide resin (172.7 mg, 0.1 mmol) was washed and swelled in DMF for 30 min. After deprotection of the Fmoc group with 20% piperidine, the resin was washed extensively and swelled in DMF. N- α -Fmoc-L-aspartic acid α -allyl ester or Fmoc-Asp-OAll (79 mg, 0.2 mmol) activated by BOP, HOBT, and NMM was added to the resin and the resin was stirred for 2.5 hr at room temperature. Following extensive washing of the resin, any remaining free amino groups on the resin were capped by addition of acetic anhydride (50 μ l, 0.5 mmol) and NMM (110 μ l, 1 mmol) in NMP (1 ml). The mixture was stirred for 15 minutes and this step was repeated. Following this, the Fmoc group was deprotected. The coupling, capping, and deprotection steps were repeated for the addition of next amino acids. The duration and the number of times the steps were repeated are listed in Table 3.3.

Table 3.3: Coupling, capping, and deprotection times for the synthesis of **8**.

Fmoc-Asp-OAll coupling		Capping	Fmoc-deprotection
aa	Time (hr)	Time (min)	Time (min)
First	2.5	15 x 2	15 x 2
Second	2.5	15 x 2	15 x 2
Third	3	15 x 2	15 x 2
Fourth	3 x 3	15 x 2	-

A test cleavage was performed after the addition of each amino acid to follow the progress of the synthesis. Test cleavage after the addition of fourth amino acid did not show the desired mass despite coupling of the fourth amino acid several times. At this stage the synthesis was discontinued.

3.5.4.2 Solid Phase Synthesis of **8** using Fmoc-Asp-OtBu.

A second attempt at the synthesis of **8** was made using *t*-Butyl protected L-aspartic acid. Rink amide resin (172.4mg, 1 mmol) was washed and deprotected as before. N- α -Fmoc-L-aspartic acid α -allyl or Fmoc-Asp-OtBu (82.3 mg, 0.2 mmol) was activated by addition of BOP (86 mg, 0.2 mmol), HOBT (27 mg, 0.2 mmol), NMM (50 μ l, 0.45 mmol) and 0.8 M LiCl in NMP (1 ml). The amino acid mixture was allowed to stand for 5 minutes and was then added to the resin. The amino acid was allowed to couple for 2.5 hr. After washing the resin, Fmoc group was deprotected. The coupling and deprotection steps were repeated till the addition of 6 amino acids. The duration and the number of times the steps were repeated are listed in Table 3.4.

Table 3.4: Coupling and deprotection times for the synthesis of β^3 -peptide **8**.

Fmoc-Asp-OtBu aa	Coupling Time (hr)	Fmoc-deprotection Time (min)
First	2.5	16 x 2
Second	2.5	16 x 2
Third	3	16 x 2
Fourth	3	15 x 3
Fifth	4	15 x 3
Sixth	3 x 2	15 x 3

Test cleavage after addition of all the six amino acids showed the presence of desired product along with three more peptides with uncompleted coupling as shown in (Scheme 3.5).

3.6 References

1. Jones RM, Boatman PD, Semple G, Shin YJ, Tamura SY. 2003. *Curr Opin Pharmacol* 3: 530-43
2. Hart M, Beeson C. 2001. *J Med Chem* 44: 3700-9
3. Simon RJ, Kania RS, Zuckermann RN, Huebner VD, Jewell DA, et al. 1992. *Proc Natl Acad Sci U S A* 89: 9367-71
4. Woll MG, Lai JR, Guzei IA, Taylor SJ, Smith ME, Gellman SH. 2001. *J Am Chem Soc* 123: 11077-8
5. Arndt HD, Ziemer B, Koert U. 2004. *Org Lett* 6: 3269-72
6. Cheng RP, Gellman SH, DeGrado WF. 2001. *Chem Rev* 101: 3219-32
7. Gademann K, Hintermann T, Schreiber JV. 1999. *Curr Med Chem* 6: 905-25
8. Lelais G, Seebach D. 2004. *Biopolymers* 76: 206-43
9. Seebach D, Overhand M, Kuhnle FNM, Martinoni B, Oberer L, et al. 1996. *Helv Chim Acta* 79: 913-41
10. Beke T, Somlai C, Perczel A. 2006. *J Comput Chem* 27: 20-38
11. Seebach D, Matthews JL. 1997. *Chem Commun* 2015-22
12. Appella DH, Christianson LA, Klein DA, Powell DR, Huang X, et al. 1997. *Nature* 387: 381-4
13. Kritzer JA, Tirado-Rives J, Hart SA, Lear JD, Jorgensen WL, Schepartz A. 2005. *J Am Chem Soc* 127: 167-78

14. Lee MR, Raguse TL, Schinnerl M, Pomerantz WC, Wang X, et al. 2007. *Org Lett* 9: 1801-4
15. Arvidsson PI, Rueping M, Seebach D. 2001. *Chem. Commun.*: 649-50
16. Cheng RP, DeGrado WF. 2001. *J Am Chem Soc* 123: 5162-3
17. Guarracino DA, Chiang HR, Banks TN, Lear JD, Hodsdon ME, Schepartz A. 2006. *Org Lett* 8: 807-10
18. Raguse TL, Lai JR, Gellman SH. 2003. *J Am Chem Soc* 125: 5592-3
19. Rueping M, Mahajan YR, Jaun B, Seebach D. 2004. *Chemistry* 10: 1607-15
20. Hart SA, Bahadoor AB, Matthews EE, Qiu XJ, Schepartz A. 2003. *J Am Chem Soc* 125: 4022-3
21. Marshall SA, Lazar GA, Chirino AJ, Desjarlais JR. 2003. *Drug Discov Today* 8: 212-21
22. Schreiber JV, Frackenpohl J, Moser F, Fleischmann T, Kohler HP, Seebach D. 2002. *Chembiochem* 3: 424-32
23. Wiegand H, Wirz B, Schweitzer A, Camenisch GP, Rodriguez Perez MI, et al. 2002. *Biopharm Drug Dispos* 23: 251-62
24. Hamuro Y, Schneider JP, DeGrado WF. 1999. *J Am Chem Soc* 121: 12200-1.
25. Porter EA, Weisblum B, Gellman SH. 2005. *J Am Chem Soc* 127: 11516-29.
26. LePlae PR, Fisk JD, Porter EA, Weisblum B, Gellman SH. 2002. *J Am Chem Soc* 124: 6820-1.
27. Gademann K, Kimmerlin T, Hoyer D, Seebach D. 2001. *J Med Chem* 44: 2460-8.

28. Kritzer JA, Lear JD, Hodsdon ME, Schepartz A. 2004. *J Am Chem Soc* 126: 9468-9.
29. English EP, Chumanov RS, Gellman SH, Compton T. 2006. *J Biol Chem* 281: 2661-7. Epub 005 Nov 7.
30. Gelman MA, Richter S, Cao H, Umezawa N, Gellman SH, Rana TM. 2003. *Org Lett* 5: 3563-5.
31. Ahmed S, Beleid R, Sprules T, Kaur K. 2007. *Org Lett* 9: 25-8
32. Abele S, Guichard G, Seebach D, . 1998. *Helv. Chim. Acta* 81: 2141-56
33. Fernandez-Santin JM, Aymami J, Rodriguez-Galan A, Munoz-Guerra S, Subirana JA. 1984. *Nature* 311: 53-4.
34. Raguse TL, Lai JR, LePlae PR, Gellman SH. 2001. *Org Lett* 3: 3963-6
35. Guntert P. 2004. *Methods Mol Biol* 278: 353-78
36. Seebach D, Beck AK, Bierbaum DJ. 2004. *Chem Biodivers* 1: 1111-239
37. Murray JK, Farooqi B, Sadowsky JD, Scalf M, Freund WA, et al. 2005. *J Am Chem Soc* 127: 13271-80
38. Wuthrich K. 1986. *Wiley, New York*

Chapter 4 General Conclusions and Future Directions

Our efforts toward the design, synthesis, and evaluation of α -peptides as HCV entry inhibitors, as well as, synthetic strategy for obtaining helical β -peptides were discussed in this thesis.

HCV infection is a major worldwide public health concern for which novel therapies are in urgent demand. Entry inhibitors offer a new class of anti-HCV agents. Chapter 2 describes the design and synthesis of five α -peptides, **1-5**, derived from the sequence of human lactoferrin that may act as HCV entry inhibitors. A 33-residue Nozaki peptide that has been shown to bind E2 and inhibit HCV entry into hepatocytes was truncated to obtain 27 (**2**) and 17 (**3**) residue peptides. Furthermore, binding enhancing mutations were introduced to obtain 33 and 27 residue peptides **4** and **5**, respectively. All five peptides were synthesized using Fmoc-solid phase synthesis, including the peptide **1**, which has same sequence as the Nozaki peptide but is covalently modified at the N-terminal with a biotin moiety like peptides **2-5**. Solution conformation of the peptides was determined using CD spectroscopy and peptide **5** displayed the presence of maximum helical secondary structure. An ELISA-based binding assay showed that all the peptides bound to E2 in a concentration-dependent manner. Two of the peptides, **3** and **5**, bound to E2 specifically at a single binding site with low micromolar affinity. Peptide **5** with the highest helical content was found to be the most potent binder with a K_d of 0.565 μ M. Further investigations of these peptides to confirm their ability to block HCV entry into the target cells and suppress viral infectivity are needed. A cell-based assay or an *in vivo* animal

model could be used to test these peptides. Upon confirmation of their anti-HCV activity, peptides **3** and **5** can serve as the lead molecules for the design of next generation anti-HCV peptides and peptidomimetics. The entry inhibitors studied here will bind to the virus and prevent its entry to the target cell. This protective mechanism against HCV provides a new strategy that would be useful in many situations including, preventing spread of the infection in case of an epidemic, preventing recurrent HCV infection in liver transplant patients, and protecting scientists and researchers working or subjected to the HCV. Furthermore, these entry inhibitors may be used in combination with other HCV medications enhancing anti-viral activity.

In Chapter 3, a solid phase synthesis method for the preparation of novel β^3 -peptides derived from L-aspartic acid monomers was developed. The methodology allows independent buildup of the β -peptide backbone and the introduction of sequential side chain substitutions. Attempts were made to synthesize three representative peptides, namely, **6**, **7**, and **8** using this methodology. β^3 -hexapeptide **6** was synthesized, purified, and fully characterized. The synthesis of **7** and **8** was completed only up to the dipeptide and tripeptide, respectively, due to the unsuccessful coupling of the subsequent amino acids.

β^3 -hexapeptide **6** contains an additional amide bond in the side chain that provides opportunities for additional hydrogen bonds and is speculated to give unprecedented secondary structures in this class of β -peptides. The solution conformation of **6** was studied using CD and NMR spectroscopy in TFE and

water, moreover, three dimensional NMR solution structure of **6** in TFE was obtained. The solution conformation of **6** suggested the presence of solvent-dependent secondary structure.

β^3 -hexpeptide **6** forms a right-handed helix in TFE, which may be due to the opposite stereochemistry at the β^3 carbon in the peptide backbone. β^3 -peptides from L-aspartic acid monomers seem to have an advantage over the β^3 -peptides obtained from the β^3 -amino acids derived from L-amino acids which form left-handed helices. The right-handed helical conformation makes them suitable for mimicking the structure of natural α -peptide such as peptide **5**. Finally, β^3 -peptides obtained L-aspartic acid monomers represent an interesting class of biomimetic oligomers that may find potential application not only in pharmaceutical sciences but also in the development of β -peptide arrays, β -peptides with enzymatic properties, and β -peptide based materials.

Bibliography

- Abe, K., A. Nozaki, K. Tamura, M. Ikeda, K. Naka, H. Dansako, H.O. Hoshino, K. Tanaka, and N. Kato. 2007. Tandem repeats of lactoferrin-derived anti-hepatitis C virus peptide enhance antiviral activity in cultured human hepatocytes. *Microbiol Immunol.* 51:117-25.
- Abele, S., G. Guichard, D. Seebach, and . 1998. *Helv. Chim. Acta.* 81:2141-2156.
- Agnello, V., G. Abel, M. Elfahal, G.B. Knight, and Q.X. Zhang. 1999. Hepatitis C virus and other flaviviridae viruses enter cells via low density lipoprotein receptor. *Proc Natl Acad Sci U S A.* 96:12766-71.
- Ahmed, S., R. Beleid, T. Sprules, and K. Kaur. 2007. Solid-phase synthesis and CD spectroscopic investigations of novel beta-peptides from L-aspartic acid and beta-amino-L-alanine. *Org Lett.* 9:25-8.
- Ammendolia, M.G., A. Pietrantonio, A. Tinari, P. Valenti, and F. Superti. 2007. Bovine lactoferrin inhibits echovirus endocytic pathway by interacting with viral structural polypeptides. *Antiviral Res.* 73:151-60.
- Appella, D.H., L.A. Christianson, D.A. Klein, D.R. Powell, X. Huang, J.J. Barchi, Jr., and S.H. Gellman. 1997. Residue-based control of helix shape in beta-peptide oligomers. *Nature.* 387:381-4.
- Arndt, H.D., B. Ziemer, and U. Koert. 2004. Folding propensity of cyclohexylether-delta-peptides. *Org Lett.* 6:3269-72.
- Arnold, D., A.M. Di Biase, M. Marchetti, A. Pietrantonio, P. Valenti, L. Seganti, and F. Superti. 2002. Antiadenovirus activity of milk proteins: lactoferrin prevents viral infection. *Antiviral Res.* 53:153-8.
- Arvidsson, P.I., M. Rueping, and D. Seebach. 2001. Design, machine synthesis, and NMR-solution structure of a β -heptapeptide forming a salt-bridge stabilised 3_{14} -helix in methanol and in water. *Chem. Commun.*:649-50.
- Baker, H.M., and E.N. Baker. 2004. Lactoferrin and iron: structural and dynamic aspects of binding and release. *Biometals.* 17:209-16.
- Barth, H., T.J. Liang, and T.F. Baumert. 2006. Hepatitis C virus entry: molecular biology and clinical implications. *Hepatology.* 44:527-35.
- Barth, H., C. Schafer, M.I. Adah, F. Zhang, R.J. Linhardt, H. Toyoda, A. Kinoshita-Toyoda, T. Toida, T.H. Van Kuppevelt, E. Depla, F. Von Weizsacker, H.E. Blum, and T.F. Baumert. 2003. Cellular binding of hepatitis C virus envelope glycoprotein E2 requires cell surface heparan sulfate. *J Biol Chem.* 278:41003-12.

- Beke, T., C. Somlai, and A. Perczel. 2006. Toward a rational design of beta-peptide structures. *J Comput Chem.* 27:20-38.
- Bellamy, W., M. Takase, K. Yamauchi, H. Wakabayashi, K. Kawase, and M. Tomita. 1992. Identification of the bactericidal domain of lactoferrin. *Biochim Biophys Acta.* 1121:130-6.
- Bertaux, C., D. Daelemans, L. Meertens, E.G. Cormier, J.F. Reinus, W.J. Peumans, E.J. Van Damme, Y. Igarashi, T. Oki, D. Schols, T. Dragic, and J. Balzarini. 2007. Entry of hepatitis C virus and human immunodeficiency virus is selectively inhibited by carbohydrate-binding agents but not by polyanions. *Virology.* 366:40-50.
- Cao, J., P. Zhao, X.H. Miao, L.J. Zhao, L.J. Xue, and Z. Qi. 2003. Phage display selection on whole cells yields a small peptide specific for HCV receptor human CD81. *Cell Res.* 13:473-9.
- Chan, W.C., P.D. White, and I. NetLibrary. 2000. Fmoc solid phase peptide synthesis a practical approach. Oxford University Press, New York.
- Cheng, R.P., and W.F. DeGrado. 2001. De novo design of a monomeric helical beta-peptide stabilized by electrostatic interactions. *J Am Chem Soc.* 123:5162-3.
- Cheng, R.P., S.H. Gellman, and W.F. DeGrado. 2001. beta-Peptides: from structure to function. *Chem Rev.* 101:3219-32.
- Chevaliez, S., and J.M. Pawlotsky. 2007. Hepatitis C virus: virology, diagnosis and management of antiviral therapy. *World J Gastroenterol.* 13:2461-6.
- De Clercq, E. 2007. The design of drugs for HIV and HCV. *Nat Rev Drug Discov.* 6:1001-18.
- Dimitrov, D.S. 2004. Virus entry: molecular mechanisms and biomedical applications. *Nat Rev Microbiol.* 2:109-22.
- English, E.P., R.S. Chumanov, S.H. Gellman, and T. Compton. 2006. Rational development of beta-peptide inhibitors of human cytomegalovirus entry. *J Biol Chem.* 281:2661-7.
- Ernst, J.T., O. Kutzki, A.K. Debnath, S. Jiang, H. Lu, and A.D. Hamilton. 2002. Design of a protein surface antagonist based on alpha - helix mimicry: inhibition of gp41 assembly and viral fusion. *Angew Chem Int Ed Engl.* 41:278 - 281.
- Este, J.A., and A. Telenti. 2007. HIV entry inhibitors. *Lancet.* 370:81-8.
- Falkowska, E., F. Kajumo, E. Garcia, J. Reinus, and T. Dragic. 2007. Hepatitis C

- virus envelope glycoprotein E2 glycans modulate entry, CD81 binding, and neutralization. *J Virol.* 81:8072-9.
- Fernandez-Santin, J.M., J. Aymami, A. Rodriguez-Galan, S. Munoz-Guerra, and J.A. Subirana. 1984. *Nature.* 311:53-54.
- Gademann, K., T. Hintermann, and J.V. Schreiber. 1999. Beta-peptides: twisting and turning. *Curr Med Chem.* 6:905-25.
- Gademann, K., T. Kimmerlin, D. Hoyer, and D. Seebach. 2001. Peptide folding induces high and selective affinity of a linear and small beta-peptide to the human somatostatin receptor 4. *J Med Chem.* 44:2460-8.
- Guarracino, D.A., H.R. Chiang, T.N. Banks, J.D. Lear, M.E. Hodsdon, and A. Schepartz. 2006. Relationship between salt-bridge identity and 14-helix stability of beta3-peptides in aqueous buffer. *Org Lett.* 8:807-10.
- Guntert, P. 2004. Automated NMR structure calculation with CYANA. *Methods Mol Biol.* 278:353-78.
- Hamuro, Y., J.P. Schneider, and W.F. DeGrado. 1999. De Novo Design of Antibacterial beta-Peptides. *J Am Chem Soc.* 121:12200-1.
- Hart, M., and C. Beeson. 2001. Utility of azapeptides as major histocompatibility complex class II protein ligands for T-cell activation. *J Med Chem.* 44:3700-9.
- Hart, S.A., A.B. Bahadoor, E.E. Matthews, X.J. Qiu, and A. Schepartz. 2003. Helix macrodipole control of beta 3 peptide 14-helix stability in water. *J Am Chem Soc.* 125:4022-3.
- Helle, F., and J. Dubuisson. 2007. Hepatitis C virus entry into host cells. *Cell Mol Life Sci.*
- Helle, F., C. Wychowski, N. Vu-Dac, K.R. Gustafson, C. Voisset, and J. Dubuisson. 2006. Cyanovirin-N inhibits hepatitis C virus entry by binding to envelope protein glycans. *J Biol Chem.* 281:25177-83.
- Huang, Z., M.G. Murray, and J.A. Secrist, 3rd. 2006. Recent development of therapeutics for chronic HCV infection. *Antiviral Res.* 71:351-62.
- Ikeda, M., A. Nozaki, K. Sugiyama, T. Tanaka, A. Naganuma, K. Tanaka, H. Sekihara, K. Shimotohno, M. Saito, and N. Kato. 2000. Characterization of antiviral activity of lactoferrin against hepatitis C virus infection in human cultured cells. *Virus Res.* 66:51-63.
- Ikeda, M., K. Sugiyama, T. Tanaka, K. Tanaka, H. Sekihara, K. Shimotohno, and N. Kato. 1998. Lactoferrin markedly inhibits hepatitis C virus infection in

- cultured human hepatocytes. *Biochem Biophys Res Commun.* 245:549-53.
- Iwasa, M., M. Kaito, J. Ikoma, M. Takeo, I. Imoto, Y. Adachi, K. Yamauchi, R. Koizumi, and S. Teraguchi. 2002. Lactoferrin inhibits hepatitis C virus viremia in chronic hepatitis C patients with high viral loads and HCV genotype 1b. *Am J Gastroenterol.* 97:766-7.
- Jameson, G.B., B.F. Anderson, G.E. Norris, D.H. Thomas, and E.N. Baker. 1998. Structure of human apolactoferrin at 2.0 Å resolution. Refinement and analysis of ligand-induced conformational change. *Acta Crystallogr D Biol Crystallogr.* 54:1319-35.
- Jones, R.M., P.D. Boatman, G. Semple, Y.J. Shin, and S.Y. Tamura. 2003. Clinically validated peptides as templates for de novo peptidomimetic drug design at G-protein-coupled receptors. *Curr Opin Pharmacol.* 3:530-43.
- Karlsson, A.J., W.C. Pomerantz, B. Weisblum, S.H. Gellman, and S.P. Palecek. 2006. Antifungal activity from 14-helical beta-peptides. *J Am Chem Soc.* 128:12630-1.
- Kaur, K., D. Das, and M. Suresh. 2008. Protein-protein interactions, in Preclinical Development of Protein Pharmaceuticals. in press.
- Kritzer, J.A., J.D. Lear, M.E. Hodsdon, and A. Schepartz. 2004. Helical beta-peptide inhibitors of the p53-hDM2 interaction. *J Am Chem Soc.* 126:9468-9.
- Kritzer, J.A., O.M. Stephens, D.A. Guarracino, S.K. Reznik, and A. Schepartz. 2005. beta-Peptides as inhibitors of protein-protein interactions. *Bioorg Med Chem.* 13:11-6.
- Kritzer, J.A., J. Tirado-Rives, S.A. Hart, J.D. Lear, W.L. Jorgensen, and A. Schepartz. 2005. Relationship between side chain structure and 14-helix stability of beta3-peptides in water. *J Am Chem Soc.* 127:167-78.
- Kuzmic, P. 1996. Program DYNAFIT for the analysis of enzyme kinetic data: application to HIV proteinase. *Anal Biochem.* 237:260-73.
- Lauer, G.M., and B.D. Walker. 2001. Hepatitis C virus infection. *N Engl J Med.* 345:41-52.
- Law, M., T. Maruyama, J. Lewis, E. Giang, A.W. Tarr, Z. Stamataki, P. Gastaminza, F.V. Chisari, I.M. Jones, R.I. Fox, J.K. Ball, J.A. McKeating, N.M. Kneteman, and D.R. Burton. 2008. Broadly neutralizing antibodies protect against hepatitis C virus quasispecies challenge. *Nat Med.* 14:25-7.
- Lee, M.R., T.L. Raguse, M. Schinnerl, W.C. Pomerantz, X. Wang, P. Wipf, and S.H. Gellman. 2007. Origins of the high 14-helix propensity of cyclohexyl-

- rigidified residues in beta-peptides. *Org Lett.* 9:1801-4.
- Lelais, G., and D. Seebach. 2004. Beta2-amino acids-syntheses, occurrence in natural products, and components of beta-peptides^{1,2}. *Biopolymers.* 76:206-43.
- LePlae, P.R., J.D. Fisk, E.A. Porter, B. Weisblum, and S.H. Gellman. 2002. Tolerance of acyclic residues in the beta-peptide 12-helix: access to diverse side-chain arrays for biological applications. *J Am Chem Soc.* 124:6820-1.
- Lozach, P.Y., H. Lortat-Jacob, A. de Lacroix de Lavalette, I. Staropoli, S. Foug, A. Amara, C. Houles, F. Fieschi, O. Schwartz, J.L. Virelizier, F. Arenzana-Seisdedos, and R. Altmeyer. 2003. DC-SIGN and L-SIGN are high affinity binding receptors for hepatitis C virus glycoprotein E2. *J Biol Chem.* 278:20358-66.
- Lyra, A.C., X. Fan, and A.M. Di Bisceglie. 2004. Molecular biology and clinical implication of hepatitis C virus. *Braz J Med Biol Res.* 37:691-5.
- Manns, M.P., H. Wedemeyer, and M. Cornberg. 2006. Treating viral hepatitis C: efficacy, side effects, and complications. *Gut.* 55:1350-9.
- Margraf, R.L., M. Erali, M. Liew, and C.T. Wittwer. 2004. Genotyping hepatitis C virus by heteroduplex mobility analysis using temperature gradient capillary electrophoresis. *J Clin Microbiol.* 42:4545-51.
- Marshall, S.A., G.A. Lazar, A.J. Chirino, and J.R. Desjarlais. 2003. Rational design and engineering of therapeutic proteins. *Drug Discov Today.* 8:212-21.
- Meanwell, N.A. 2006. Hepatitis C virus entry: an intriguing challenge for drug discovery. *Curr Opin Investig Drugs.* 7:727-32.
- Moore, G.J. 1994. Designing peptide mimetics. *Trends Pharmacol Sci.* 15:124-9.
- Murray, J.K., B. Farooqi, J.D. Sadowsky, M. Scalf, W.A. Freund, L.M. Smith, J. Chen, and S.H. Gellman. 2005. Efficient synthesis of a beta-peptide combinatorial library with microwave irradiation. *J Am Chem Soc.* 127:13271-80.
- Murray, J.K., and S.H. Gellman. 2006. Microwave-assisted parallel synthesis of a 14-helical beta-peptide library. *J Comb Chem.* 8:58-65.
- Nousbaum, J.B. 1998. [Genomic subtypes of hepatitis C virus: epidemiology, diagnosis and clinical consequences]. *Bull Soc Pathol Exot.* 91:29-33.
- Nozaki, A., M. Ikeda, A. Naganuma, T. Nakamura, M. Inudoh, K. Tanaka, and N. Kato. 2003. Identification of a lactoferrin-derived peptide possessing

- binding activity to hepatitis C virus E2 envelope protein. *J Biol Chem.* 278:10162-73.
- Organization WHO. <http://www.who.int/csr/disease/hepatitis/whocdscsrlyo2003/en/index.html>.
- Parfieniuk, A., J. Jaroszewicz, and R. Flisiak. 2007. Specifically targeted antiviral therapy for hepatitis C virus. *World J Gastroenterol.* 13:5673-81.
- Pawlotsky, J.M. 2007. Treatment of hepatitis C: don't put all your eggs in one basket! *Gastroenterology.* 132:1611-5.
- Pawlotsky, J.M. 2006. Therapy of hepatitis C: from empiricism to eradication. *Hepatology.* 43:S207-20.
- Pawlotsky, J.M., S. Chevaliez, and J.G. McHutchison. 2007. The hepatitis C virus life cycle as a target for new antiviral therapies. *Gastroenterology.* 132:1979-98.
- Pecheur, E.I., D. Lavillette, F. Alcaras, J. Molle, Y.S. Boriskin, M. Roberts, F.L. Cosset, and S.J. Polyak. 2007. Biochemical mechanism of hepatitis C virus inhibition by the broad-spectrum antiviral arbidol. *Biochemistry.* 46:6050-9.
- Petracca, R., F. Falugi, G. Galli, N. Norais, D. Rosa, S. Campagnoli, V. Burgio, E. Di Stasio, B. Giardina, M. Houghton, S. Abrignani, and G. Grandi. 2000. Structure-function analysis of hepatitis C virus envelope-CD81 binding. *J Virol.* 74:4824-30.
- Pileri, P., Y. Uematsu, S. Campagnoli, G. Galli, F. Falugi, R. Petracca, A.J. Weiner, M. Houghton, D. Rosa, G. Grandi, and S. Abrignani. 1998. Binding of hepatitis C virus to CD81. *Science.* 282:938-41.
- Purcell, R. 1997. The hepatitis C virus: overview. *Hepatology.* 26:11S-14S.
- Raguse, T., L.J. R., and S.H. Gellman. 2002. β -Peptide 14-Helix is Stabilized by β^3 -Residues with Side-Chain Branching Adjacent to the β -Carbon Atom. *Helv Chim Acta.* 85:4154-64.
- Raguse, T.L., J.R. Lai, and S.H. Gellman. 2003. Environment-independent 14-helix formation in short beta-peptides: striking a balance between shape control and functional diversity. *J Am Chem Soc.* 125:5592-3.
- Raguse, T.L., J.R. Lai, P.R. LePlae, and S.H. Gellman. 2001. Toward beta-peptide tertiary structure: self-association of an amphiphilic 14-helix in aqueous solution. *Org Lett.* 3:3963-6.
- Ralston, R., V. Bichko, R. Chase, M. LaColla, L. Lалlos, A. Skelton, M. Soubasakos, M. Tausek, X. Tong, and D. Standing. 2007. Combination of

two hepatitis C virus inhibitors, SCH 503034 and NM107, provides enhanced anti-replicon activity and suppresses emergence of resistant replicons. *J Hepatol.* 46:S298.

Redwan el, R.M., and A. Tabll. 2007. Camel lactoferrin markedly inhibits hepatitis C virus genotype 4 infection of human peripheral blood leukocytes. *J Immunoassay Immunochem.* 28:267-77.

Rey, M.W., S.L. Woloshuk, H.A. deBoer, and F.R. Pieper. 1990. Complete nucleotide sequence of human mammary gland lactoferrin. *Nucleic Acids Res.* 18:5288.

Roderiquez, G., T. Oravec, M. Yanagishita, D.C. Bou-Habib, H. Mostowski, and M.A. Norcross. 1995. Mediation of human immunodeficiency virus type 1 binding by interaction of cell surface heparan sulfate proteoglycans with the V3 region of envelope gp120-gp41. *J Virol.* 69:2233-9.

Rosa, D., S. Campagnoli, C. Moretto, E. Guenzi, L. Cousens, M. Chin, C. Dong, A.J. Weiner, J.Y. Lau, Q.L. Choo, D. Chien, P. Pileri, M. Houghton, and S. Abrignani. 1996. A quantitative test to estimate neutralizing antibodies to the hepatitis C virus: cytofluorimetric assessment of envelope glycoprotein 2 binding to target cells. *Proc Natl Acad Sci U S A.* 93:1759-63.

Rueping, M., Y.R. Mahajan, B. Jaun, and D. Seebach. 2004. Design, synthesis and structural investigations of a beta-peptide forming a 3_{14} -helix stabilized by electrostatic interactions. *Chemistry.* 10:1607-15.

Scarselli, E., H. Ansuini, R. Cerino, R.M. Roccasecca, S. Acali, G. Filocamo, C. Traboni, A. Nicosia, R. Cortese, and A. Vitelli. 2002. The human scavenger receptor class B type I is a novel candidate receptor for the hepatitis C virus. *Embo J.* 21:5017-25.

Schreiber, J.V., J. Frackenpohl, F. Moser, T. Fleischmann, H.P. Kohler, and D. Seebach. 2002. On the biodegradation of beta-peptides. *Chembiochem.* 3:424-32.

Seebach, D., A.K. Beck, and D.J. Bierbaum. 2004. The world of beta- and gamma-peptides comprised of homologated proteinogenic amino acids and other components. *Chem Biodivers.* 1:1111-239.

Seebach, D., M. Overhand, F.N.M. Kuhnle, B. Martinoni, L. Oberer, U. Hommel, and H. Widmer. 1996. β -Peptides: synthesis by Arndt-Eistert homologation with concomitant peptide coupling. Structure determination by NMR and CD spectroscopy and X-ray crystallography. Helical Secondary Structure of a α -Hexapeptide in Solution and Its Stability towards Pepsin. *Helv Chim Acta.* 79:913-41.

Siciliano, R., B. Rega, M. Marchetti, L. Seganti, G. Antonini, and P. Valenti.

1999. Bovine lactoferrin peptidic fragments involved in inhibition of herpes simplex virus type 1 infection. *Biochem Biophys Res Commun.* 264:19-23.
- Simon, R.J., R.S. Kania, R.N. Zuckermann, V.D. Huebner, D.A. Jewell, S. Banville, S. Ng, L. Wang, S. Rosenberg, C.K. Marlowe, and et al. 1992. Peptoids: a modular approach to drug discovery. *Proc Natl Acad Sci U S A.* 89:9367-71.
- Sreerama, N., S.Y. Venyaminov, and R.W. Woody. 2001. Analysis of protein circular dichroism spectra based on the tertiary structure classification. *Anal Biochem.* 299:271-4.
- Tanaka, K., M. Ikeda, A. Nozaki, N. Kato, H. Tsuda, S. Saito, and H. Sekihara. 1999. Lactoferrin inhibits hepatitis C virus viremia in patients with chronic hepatitis C: a pilot study. *Jpn J Cancer Res.* 90:367-71.
- Van Doorn, L.J., I. Capriles, G. Maertens, R. DeLeys, K. Murray, T. Kos, H. Schellekens, and W. Quint. 1995. Sequence evolution of the hypervariable region in the putative envelope region E2/NS1 of hepatitis C virus is correlated with specific humoral immune responses. *J Virol.* 69:773-8.
- Van Compernelle, S.E., A.V. Wiznycia, J.R. Rush, M. Dhanasekaran, P.W. Baures, and S.C. Todd. 2003. Small molecule inhibition of hepatitis C virus E2 binding to CD81. *Virology.* 314:371-80.
- Wagner, C.E., M.L. Mohler, G.S. Kang, D.D. Miller, E.E. Geisert, Y.A. Chang, E.B. Fleischer, and K.J. Shea. 2003. Synthesis of 1-boraadamantaneamine derivatives with selective astrocyte vs C6 glioma antiproliferative activity. A novel class of anti-hepatitis C agents with potential to bind CD81. *J Med Chem.* 46:2823-33.
- Wakabayashi, H., S. Abe, S. Teraguchi, H. Hayasawa, and H. Yamaguchi. 1998. Inhibition of hyphal growth of azole-resistant strains of *Candida albicans* by triazole antifungal agents in the presence of lactoferrin-related compounds. *Antimicrob Agents Chemother.* 42:1587-91.
- Wakita, T., C. Taya, A. Katsume, J. Kato, H. Yonekawa, Y. Kanegae, I. Saito, Y. Hayashi, M. Koike, and M. Kohara. 1998. Efficient conditional transgene expression in hepatitis C virus cDNA transgenic mice mediated by the Cre/loxP system. *J Biol Chem.* 273:9001-6.
- Wiegand, H., B. Wirz, A. Schweitzer, G.P. Camenisch, M.I. Rodriguez Perez, G. Gross, R. Woessner, R. Voges, P.I. Arvidsson, J. Frackenhohl, and D. Seebach. 2002. The outstanding metabolic stability of a ¹⁴C-labeled beta-nona peptide in rats--in vitro and in vivo pharmacokinetic studies. *Biopharm Drug Dispos.* 23:251-62.
- Woll, M.G., J.R. Lai, I.A. Guzei, S.J. Taylor, M.E. Smith, and S.H. Gellman.

2001. Parallel sheet secondary structure in gamma-peptides. *J Am Chem Soc.* 123:11077-8.

Wuthrich, K. 1986. *NMR of Proteins and Nucleic Acids.* Wiley, New York.

Yagnik, A.T., A. Lahm, A. Meola, R.M. Roccasecca, B.B. Ercole, A. Nicosia, and A. Tramontano. 2000. A model for the hepatitis C virus envelope glycoprotein E2. *Proteins.* 40:355-66.

Yi, M., S. Kaneko, D.Y. Yu, and S. Murakami. 1997. Hepatitis C virus envelope proteins bind lactoferrin. *J Virol.* 71:5997-6002.

Appendix A

Dynafit Files and Plasmid Map

Figure A.1 Dynafit input and output files for peptide 3.

INPUT

; Task: Fit of Complex Equilibria
; Data: ligand concentration (nM) vs. absorbance 650 nm (bound ligand)

[task]

data = equilibrium
task = fit
model = fixed ?

[mechanism]

$P + L \rightleftharpoons P.L$: Kd dissociation

[constants]

Kd = 20000.0 ? ; nM

[responses]

P.L = 0.08 ?

[concentrations]

P = 30 ; nM

[data]

variable L
file ./Kd/17-offset/data/d1.txt

[output]

directory ./Kd/17-offset/output

[end]

OUTPUT

LEAST-SQUARES FIT

mean square 0.000339946
standard deviation 0.0184376
log(determinant) -0.809
log(condition number) -2.19
Marquardt parameter 0.000488
execution time (sec) 0.040
datapoints 9
parameters 2
iterations 14
function evaluations 17

error status 0

PARAMETERS & STANDARD ERRORS

Set	Parameter	Initial	Fitted	Error	%Error
	Kd	20000	28780	2900	10
	r:L.R	0.08	0.07918	0.0047	6

Figure A.2 Dynafit input and output files for peptide 5.

INPUT

; Task: Fit of Complex Equilibria
; Data: ligand concentration (nM) vs. absorbance 650 nm (bound ligand)

[task]

data = equilibrium
task = fit
model = fixed ?

[mechanism]

$P + L \rightleftharpoons P.L$: Kd dissociation

[constants]

Kd = 500.0 ? ; nM

[responses]

P.L = 0.04 ?

[concentrations]

P = 40 ; nM

[data]

variable L
file ./Kd/27m-offset/data/d1.txt

[output]

directory ./Kd/27m-offset/output

[end]

OUTPUT

LEAST-SQUARES FIT

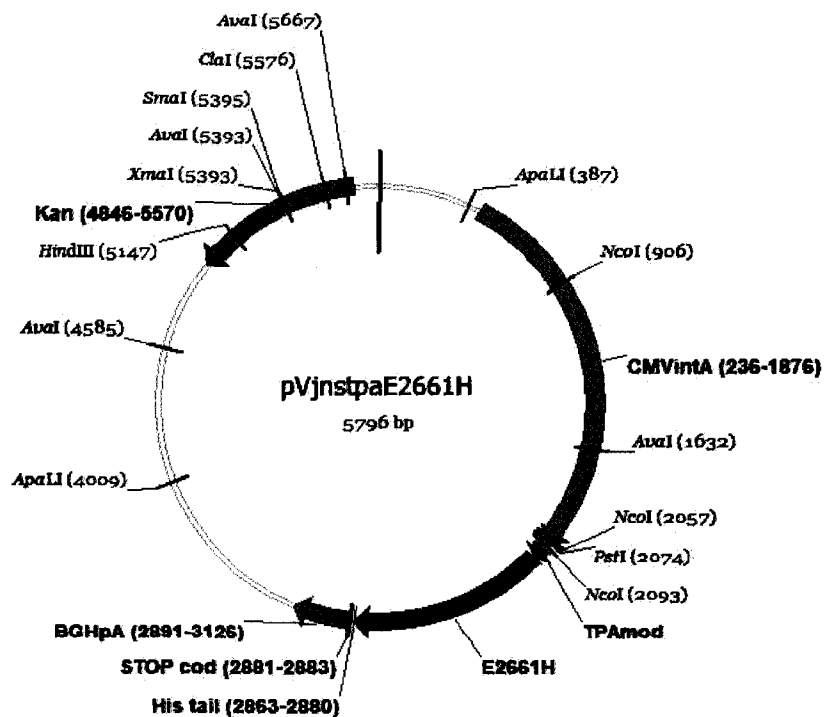
mean square 0.000662978
standard deviation 0.0257484

log(determinant) -0.348
 log(condition number) -1.2
 Marquardt parameter 0.00781
 execution time (sec) 0.050
 datapoints 10
 parameters 2
 iterations 10
 function evaluations 13
 error status 0

PARAMETERS & STANDARD ERRORS

Set	Parameter	Initial	Fitted	Error	%Error
	Kd	500	569.4	39	6.8
	r:L.R	0.04	0.039	0.0008	2.1

Figure A.3 Plasmid map of HCV strain E2 H77 (genotype 1a)



Appendix B

NMR Data for Structure Elucidation of 6

Table B.1: Chemical shift assignments for β^3 -hexapeptide 6.

Residue	Backbone shifts	Side chain shifts
1	7.84 (HN), 4.25 (HA), 2.84, 3.61 (HBs)	7.46 (HS), 4.03 (HG), 1.17, 1.22 (HDs)
2	8.78 (HN), 5.04 (HA), 2.61, 3.20 (HBs)	7.43 (HS), 3.22, 3.28 (HG), 1.61 (HDs), 1.70 (HEs), 3.01 (HEs), 7.32 (HR)
3	9.10 (HN), 4.86 (HA), 2.57, 3.08 (HBs)	6.90 (HS), 3.06 (HG), 1.76 (HD), 0.90 (HEs)
4	8.58 (HN), 5.03 (HA), 2.54, 2.73 (HBs)	8.24 (HS), 4.01 (HG), 1.20 (HDs)
5	7.32 (HN), 5.22 (HA), 2.64, 2.73 (HBs)	8.26 (HS), 3.20, 3.28 (HG), 1.61 (HDs), 1.70 (HEs), 3.01 (HEs), 7.20 (HR)
6	7.24 (HN), 5.22 (HA), 2.71 (HBs)	8.28 (HS), 2.98, 3.08 (HG), 1.81 (HD), 0.90 (HEs)
C-terminus	6.73, 6.92 (NH ₂)	

The final concentration of 1 in TFE was 1.5 mM. The chemical shifts were referenced to the TFE methylene protons at 2.88 ppm

Table B.2: Structure calculation statistics for β^3 -hexapeptide 6.

NOE upper distance limits ^a	153
Intra-residue	102
Sequential	21
Medium range (<i>i</i> to <i>i</i> +2 or <i>i</i> +3)	30
Final CYANA structures ^b	
CYANA target function	0.17 ± 0.002 Å ²
Average backbone RMSD to mean	0.47 ± 0.11 Å
Average heavy atom RMSD to mean	1.31 ± 0.23 Å
Distance restraint violations	0

^a148 unambiguous NOEs and 5 ambiguous NOEs used for the structure calculation. ^b10 lowest energy structures of the 200 calculated.

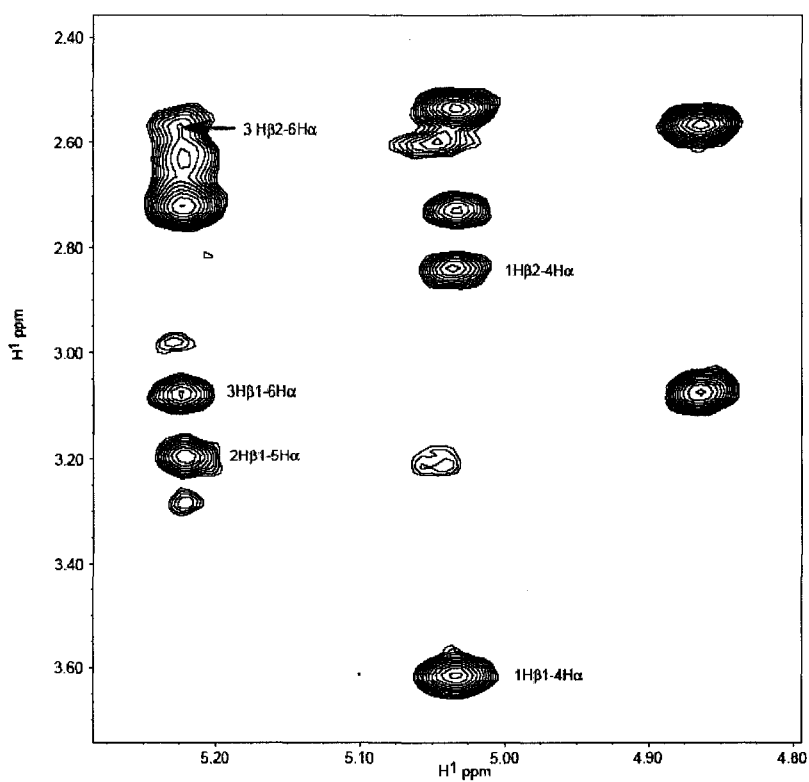
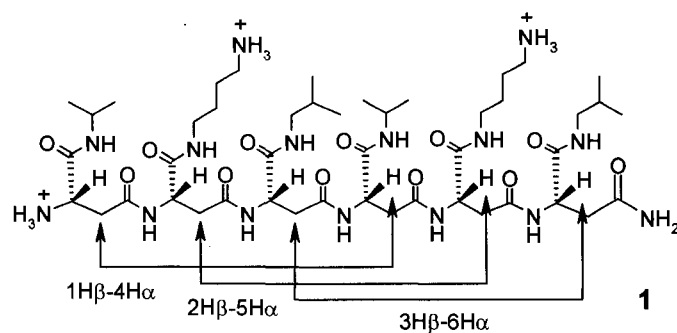


Figure B.1 2D NOESY of β^3 -peptide 6 in TFE showing the long range NOEs, $\text{C}_\beta\text{H}(i)-\text{C}_\alpha\text{H}(i+3)$ characteristic of 14-helix conformation.

Table B.3: NOE upper limit constraints (153) for β^3 -hexapeptide **6** used for structure calculation.

6	BGLN	H	6	BGLN	QQZ	6.000	#	Bpep1_800_300ms_noe_a.82
6	BGLN	H	3	BLEU	QQZ	0.000	#	Bpep1_800_300ms_noe_a.82
6	BGLN	QB	6	BGLN	QQZ	6.000	#	Bpep1_800_300ms_noe_a.125
6	BGLN	QB	3	BLEU	QQZ	0.000	#	Bpep1_800_300ms_noe_a.125
4	BVAL	HB21	6	BGLN	QQZ	6.000	#	Bpep1_800_300ms_noe_a.127
4	BVAL	HB21	3	BLEU	QQZ	0.000	#	Bpep1_800_300ms_noe_a.127
3	BLEU	H	4	BVAL	HB21	6.000	#	Bpep1_800_300ms_noe_a.27
3	BLEU	H	5	BLYS	HB21	0.000	#	Bpep1_800_300ms_noe_a.27
5	BLYS	H	4	BVAL	HB21	6.000	#	Bpep1_800_300ms_noe_a.49
5	BLYS	H	5	BLYS	HB21	0.000	#	Bpep1_800_300ms_noe_a.49
4	BVAL	H	4	BVAL	QQE	6.000	#	Bpep1_800_300ms_noe_a.76
4	BVAL	HG2	4	BVAL	QQE	3.400	#	Bpep1_800_300ms_noe_a.77
6	BGLN	HG2	6	BGLN	QQZ	6.000	#	Bpep1_800_300ms_noe_a.78
3	BLEU	HG2	3	BLEU	QQZ	6.000	#	Bpep1_800_300ms_noe_a.83
4	BVAL	HA	4	BVAL	QQE	3.400	#	Bpep1_800_300ms_noe_a.101
6	BGLN	HD2	6	BGLN	QQZ	6.000	#	Bpep1_800_300ms_noe_a.126
4	BVAL	HB22	4	BVAL	QQE	6.000	#	Bpep1_800_300ms_noe_a.128
3	BLEU	QD	3	BLEU	QQZ	6.000	#	Bpep1_800_300ms_noe_a.178
4	BVAL	HB21	4	BVAL	QQE	6.000	#	Bpep1_800_300ms_noe_a.179
1	BVAL	HA	1	BVAL	HB21	3.400	#	Bpep1_800_300ms_noe_a.85
1	BVAL	HA	1	BVAL	HB22	2.800	#	Bpep1_800_300ms_noe_a.96
1	BVAL	HA	1	BVAL	QE1	6.000	#	Bpep1_800_300ms_noe_a.102
1	BVAL	HB22	1	BVAL	QE1	6.000	#	Bpep1_800_300ms_noe_a.123
1	BVAL	HA	1	BVAL	QE2	6.000	#	Bpep1_800_300ms_noe_a.103
1	BVAL	HB21	1	BVAL	QE2	6.000	#	Bpep1_800_300ms_noe_a.120
1	BVAL	HB22	1	BVAL	QE2	6.000	#	Bpep1_800_300ms_noe_a.124
1	BVAL	HA	1	BVAL	HD	6.000	#	Bpep1_800_300ms_noe_a.107
1	BVAL	HG2	1	BVAL	HA	2.800	#	Bpep1_800_300ms_noe_a.17
1	BVAL	HG2	1	BVAL	HB21	6.000	#	Bpep1_800_300ms_noe_a.24
1	BVAL	HG2	1	BVAL	HB22	3.400	#	Bpep1_800_300ms_noe_a.48
1	BVAL	HG2	1	BVAL	QE1	2.800	#	Bpep1_800_300ms_noe_a.80
1	BVAL	HG2	1	BVAL	QE2	2.800	#	Bpep1_800_300ms_noe_a.81
1	BVAL	HG2	1	BVAL	HD	3.400	#	Bpep1_800_300ms_noe_a.23
1	BVAL	H	1	BVAL	HA	3.400	#	Bpep1_800_300ms_noe_a.16
1	BVAL	H	1	BVAL	HB21	6.000	#	Bpep1_800_300ms_noe_a.22
1	BVAL	H	1	BVAL	HB22	6.000	#	Bpep1_800_300ms_noe_a.39
1	BVAL	H	1	BVAL	QE1	6.000	#	Bpep1_800_300ms_noe_a.79
1	BVAL	H	1	BVAL	HD	6.000	#	Bpep1_800_300ms_noe_a.21
1	BVAL	HG2	1	BVAL	H	6.000	#	Bpep1_800_300ms_noe_a.168
2	BLYS	H	1	BVAL	HA	6.000	#	Bpep1_800_300ms_noe_a.15
2	BLYS	H	1	BVAL	HB21	2.800	#	Bpep1_800_300ms_noe_a.18
2	BLYS	H	1	BVAL	HB22	2.800	#	Bpep1_800_300ms_noe_a.30
1	BVAL	HG2	2	BLYS	H	6.000	#	Bpep1_800_300ms_noe_a.173
2	BLYS	H	1	BVAL	H	6.000	#	Bpep1_800_300ms_noe_a.155
2	BLYS	HG2	1	BVAL	H	6.000	#	Bpep1_800_300ms_noe_a.169
2	BLYS	HA	2	BLYS	HB22	6.000	#	Bpep1_800_300ms_noe_a.92
2	BLYS	HA	2	BLYS	HB21	6.000	#	Bpep1_800_300ms_noe_a.98
2	BLYS	HB21	2	BLYS	QE	6.000	#	Bpep1_800_300ms_noe_a.180
2	BLYS	HB21	2	BLYS	QZ	6.000	#	Bpep1_800_300ms_noe_a.181
2	BLYS	HD3	2	BLYS	QZ	2.800	#	Bpep1_800_300ms_noe_a.112
2	BLYS	HD2	2	BLYS	QE	2.800	#	Bpep1_800_300ms_noe_a.116
2	BLYS	HD2	2	BLYS	QZ	3.400	#	Bpep1_800_300ms_noe_a.183

2	BLYS H	2	BLYS HA	6.000	# Bpepl_800_300ms_noe_a.4
2	BLYS H	2	BLYS HB22	3.400	# Bpepl_800_300ms_noe_a.28
2	BLYS H	2	BLYS HB21	3.400	# Bpepl_800_300ms_noe_a.55
2	BLYS HG2	2	BLYS HA	6.000	# Bpepl_800_300ms_noe_a.13
2	BLYS HG2	2	BLYS HB21	6.000	# Bpepl_800_300ms_noe_a.62
2	BLYS HG2	2	BLYS QE	3.400	# Bpepl_800_300ms_noe_a.73
2	BLYS HG2	2	BLYS QZ	6.000	# Bpepl_800_300ms_noe_a.68
2	BLYS HG2	2	BLYS HD3	3.400	# Bpepl_800_300ms_noe_a.40
2	BLYS HG2	2	BLYS HD2	3.400	# Bpepl_800_300ms_noe_a.42
2	BLYS HG2	2	BLYS H	6.000	# Bpepl_800_300ms_noe_a.174
2	BLYS QT	2	BLYS QZ	2.800	# Bpepl_800_300ms_noe_a.118
1	BVAL H	3	BLEU HA	6.000	# Bpepl_800_300ms_noe_a.10
3	BLEU H	2	BLYS HB22	2.800	# Bpepl_800_300ms_noe_a.25
3	BLEU H	2	BLYS HB21	2.800	# Bpepl_800_300ms_noe_a.54
3	BLEU H	2	BLYS H	6.000	# Bpepl_800_300ms_noe_a.153
3	BLEU HA	3	BLEU HB21	3.400	# Bpepl_800_300ms_noe_a.93
3	BLEU HA	3	BLEU HB22	3.400	# Bpepl_800_300ms_noe_a.99
3	BLEU QD	3	BLEU HE	3.400	# Bpepl_800_300ms_noe_a.111
3	BLEU H	3	BLEU HA	3.400	# Bpepl_800_300ms_noe_a.1
3	BLEU H	3	BLEU HB21	3.400	# Bpepl_800_300ms_noe_a.26
3	BLEU H	3	BLEU HB22	2.800	# Bpepl_800_300ms_noe_a.134
3	BLEU HG2	3	BLEU HA	2.800	# Bpepl_800_300ms_noe_a.14
3	BLEU HG2	3	BLEU HB22	6.000	# Bpepl_800_300ms_noe_a.64
3	BLEU HG2	3	BLEU HE	6.000	# Bpepl_800_300ms_noe_a.75
3	BLEU HG2	3	BLEU QD	2.800	# Bpepl_800_300ms_noe_a.51
3	BLEU H	3	BLEU HG2	6.000	# Bpepl_800_300ms_noe_a.150
4	BVAL HA	1	BVAL HB21	3.400	# Bpepl_800_300ms_noe_a.84
4	BVAL HA	1	BVAL HB22	3.400	# Bpepl_800_300ms_noe_a.94
1	BVAL H	4	BVAL HA	6.000	# Bpepl_800_300ms_noe_a.9
1	BVAL HB21	4	BVAL HB22	6.000	# Bpepl_800_300ms_noe_a.177
4	BVAL HG2	1	BVAL HB21	6.000	# Bpepl_800_300ms_noe_a.20
4	BVAL HG2	1	BVAL HB22	6.000	# Bpepl_800_300ms_noe_a.36
4	BVAL HG2	1	BVAL HG2	6.000	# Bpepl_800_300ms_noe_a.167
4	BVAL HG2	1	BVAL H	6.000	# Bpepl_800_300ms_noe_a.164
4	BVAL HG2	2	BLYS H	6.000	# Bpepl_800_300ms_noe_a.163
4	BVAL H	3	BLEU HA	6.000	# Bpepl_800_300ms_noe_a.6
4	BVAL H	3	BLEU HB21	2.800	# Bpepl_800_300ms_noe_a.29
4	BVAL H	3	BLEU HB22	2.800	# Bpepl_800_300ms_noe_a.135
3	BLEU H	4	BVAL H	6.000	# Bpepl_800_300ms_noe_a.152
4	BVAL HG2	3	BLEU HB21	6.000	# Bpepl_800_300ms_noe_a.139
4	BVAL HA	4	BVAL HB21	3.400	# Bpepl_800_300ms_noe_a.95
4	BVAL HA	4	BVAL HB22	3.400	# Bpepl_800_300ms_noe_a.100
4	BVAL HA	4	BVAL HD	6.000	# Bpepl_800_300ms_noe_a.106
4	BVAL H	4	BVAL HA	6.000	# Bpepl_800_300ms_noe_a.5
4	BVAL H	4	BVAL HB21	3.400	# Bpepl_800_300ms_noe_a.31
4	BVAL H	4	BVAL HB22	2.800	# Bpepl_800_300ms_noe_a.56
4	BVAL HG2	4	BVAL HA	2.800	# Bpepl_800_300ms_noe_a.8
4	BVAL HG2	4	BVAL HB21	3.400	# Bpepl_800_300ms_noe_a.138
4	BVAL HG2	4	BVAL HB22	3.400	# Bpepl_800_300ms_noe_a.59
4	BVAL HG2	4	BVAL HD	3.400	# Bpepl_800_300ms_noe_a.19
4	BVAL HG2	4	BVAL H	6.000	# Bpepl_800_300ms_noe_a.160
5	BLYS H	1	BVAL H	6.000	# Bpepl_800_300ms_noe_a.170
5	BLYS HA	2	BLYS HB22	3.400	# Bpepl_800_300ms_noe_a.87
2	BLYS H	5	BLYS HA	6.000	# Bpepl_800_300ms_noe_a.2
5	BLYS H	2	BLYS HA	6.000	# Bpepl_800_300ms_noe_a.136
2	BLYS H	5	BLYS H	6.000	# Bpepl_800_300ms_noe_a.156

5	BLYS	HG2	2	BLYS	H	6.000	#	Bpepl_800_300ms_noe_a.162
5	BLYS	H	4	BVAL	HB22	2.800	#	Bpepl_800_300ms_noe_a.63
4	BVAL	H	5	BLYS	H	6.000	#	Bpepl_800_300ms_noe_a.159
5	BLYS	HA	5	BLYS	HB21	3.400	#	Bpepl_800_300ms_noe_a.90
5	BLYS	HA	5	BLYS	HB22	6.000	#	Bpepl_800_300ms_noe_a.105
5	BLYS	HA	5	BLYS	QE	6.000	#	Bpepl_800_300ms_noe_a.149
5	BLYS	HA	5	BLYS	HD3	6.000	#	Bpepl_800_300ms_noe_a.86
5	BLYS	HD3	5	BLYS	HB21	6.000	#	Bpepl_800_300ms_noe_a.143
5	BLYS	HD2	5	BLYS	QE	2.800	#	Bpepl_800_300ms_noe_a.115
5	BLYS	HD2	5	BLYS	QZ	3.400	#	Bpepl_800_300ms_noe_a.113
5	BLYS	H	5	BLYS	HA	6.000	#	Bpepl_800_300ms_noe_a.11
5	BLYS	H	5	BLYS	HB22	2.800	#	Bpepl_800_300ms_noe_a.61
5	BLYS	H	5	BLYS	HD3	6.000	#	Bpepl_800_300ms_noe_a.41
5	BLYS	H	5	BLYS	HD2	6.000	#	Bpepl_800_300ms_noe_a.43
5	BLYS	HG2	5	BLYS	HA	3.400	#	Bpepl_800_300ms_noe_a.7
5	BLYS	HG2	5	BLYS	HB21	3.400	#	Bpepl_800_300ms_noe_a.37
5	BLYS	HG2	5	BLYS	HB22	6.000	#	Bpepl_800_300ms_noe_a.57
5	BLYS	HG2	5	BLYS	QE	3.400	#	Bpepl_800_300ms_noe_a.67
5	BLYS	HG2	5	BLYS	QZ	6.000	#	Bpepl_800_300ms_noe_a.66
5	BLYS	HG2	5	BLYS	HD3	2.800	#	Bpepl_800_300ms_noe_a.32
5	BLYS	HG2	5	BLYS	HD2	2.800	#	Bpepl_800_300ms_noe_a.33
5	BLYS	HG2	5	BLYS	H	3.400	#	Bpepl_800_300ms_noe_a.165
5	BLYS	QT	5	BLYS	QE	2.800	#	Bpepl_800_300ms_noe_a.119
5	BLYS	HD3	5	BLYS	QT	3.400	#	Bpepl_800_300ms_noe_a.142
6	BGLN	HA	3	BLEU	HB21	3.400	#	Bpepl_800_300ms_noe_a.88
6	BGLN	HA	3	BLEU	HB22	6.000	#	Bpepl_800_300ms_noe_a.97
3	BLEU	H	6	BGLN	HA	6.000	#	Bpepl_800_300ms_noe_a.0
6	BGLN	H	3	BLEU	H	6.000	#	Bpepl_800_300ms_noe_a.176
6	BGLN	HG2	3	BLEU	HB22	6.000	#	Bpepl_800_300ms_noe_a.58
3	BLEU	H	6	BGLN	HG2	6.000	#	Bpepl_800_300ms_noe_a.151
4	BVAL	H	6	BGLN	HA	6.000	#	Bpepl_800_300ms_noe_a.3
6	BGLN	H	4	BVAL	H	6.000	#	Bpepl_800_300ms_noe_a.175
6	BGLN	HG2	4	BVAL	H	6.000	#	Bpepl_800_300ms_noe_a.161
6	BGLN	H	5	BLYS	HB21	2.800	#	Bpepl_800_300ms_noe_a.50
6	BGLN	H	5	BLYS	HB22	2.800	#	Bpepl_800_300ms_noe_a.60
6	BGLN	HD3	6	BGLN	HE	3.400	#	Bpepl_800_300ms_noe_a.110
6	BGLN	HD3	6	BGLN	HE	3.400	#	Bpepl_800_300ms_noe_a.122
6	BGLN	HA	6	BGLN	HD2	6.000	#	Bpepl_800_300ms_noe_a.89
6	BGLN	HD2	6	BGLN	HE	6.000	#	Bpepl_800_300ms_noe_a.117
6	BGLN	H	6	BGLN	HA	6.000	#	Bpepl_800_300ms_noe_a.12
6	BGLN	H	6	BGLN	QB	6.000	#	Bpepl_800_300ms_noe_a.182
6	BGLN	HG2	6	BGLN	HA	3.400	#	Bpepl_800_300ms_noe_a.137
6	BGLN	HG2	6	BGLN	QB	3.400	#	Bpepl_800_300ms_noe_a.38
6	BGLN	HG2	6	BGLN	HE	6.000	#	Bpepl_800_300ms_noe_a.65
6	BGLN	HG2	6	BGLN	HD3	2.800	#	Bpepl_800_300ms_noe_a.34
6	BGLN	HG2	6	BGLN	HD2	2.800	#	Bpepl_800_300ms_noe_a.35
6	BGLN	HG2	6	BGLN	H	6.000	#	Bpepl_800_300ms_noe_a.166
4	BVAL	H	6	BGLN	HT2	6.000	#	Bpepl_800_300ms_noe_a.158
6	BGLN	HT2	6	BGLN	QB	3.400	#	Bpepl_800_300ms_noe_a.52
6	BGLN	H	6	BGLN	HT2	6.000	#	Bpepl_800_300ms_noe_a.171